ALDOSTERONE AND THE CARDIOVASCULAR COMPLICATIONS OF CHRONIC KIDNEY DISEASE

By

DR JOANNA RUTH POWELL MBBS, MRCP (UK)

Thesis submitted for the degree of Masters of Science to the Faculty of Medicine at the University of Glasgow

Cardiovascular Research Centre
British Heart Foundation Building
University of Glasgow
126 University Place
Glasgow

DEC 2010

Declaration

I declare that the research design for this thesis was the combined work of my Supervisors (Professor Alan Jardine and Dr Patrick Mark) and the author of this thesis. I also declare that this work has not previously been submitted for a higher degree.

All the laboratory work was carried out personally with the aid of William Sands, Dianne Hilliard and Mary Ingram. However as part of the Aldosterone study, the Cardiac MR acquisition by performed in part by myself and in part by Tracey Steedman (Glasgow Magnetic Resonance Imaging Unit, University of Glasgow) and Rajan Patel (Clinical Research Fellow, University of Glasgow). All CMR image analysis, exercise tolerance tests, QT dispersal measurements and venepuncture were performed by Rajan Patel. Echocardiography was performed and analysed by Tony Cunningham (Clinical Research Initiative, University of Glasgow).

The initial data for the West of Scotland Kidney Disease study was collated by Dr G.A. Stewart as part of his research project and the results were published in Kidney International in 2005. However the follow-up data was collated from the electronic renal patient record at the Western Infirmary and analysed personally.

The research took place in the British Heart Foundation Building and NHS Clinical Research facility located at the University of Glasgow and Western Infirmary, Glasgow.

Joanna Powell, Dec 2010

Acknowledgements

I would like to thank my Supervisors Prof. Alan Jardine and Dr Patrick Mark who have supported and guided me through the past few years. Billy Sands also deserves particular thanks for putting up with my constant questions and teaching me most of the laboratory techniques used in this project, from scratch.

Thanks should also go to my fellow research team colleagues; Emily McQuarrie, Rajan Patel and Dianne Hilliard.

Other important advisory and teaching contributions were gratefully received from Mary Ingram, Stuart Nicklin, Andy Carswell, Tony Workman, Tracey Steedman and John Foster.

Table of Contents:

Chapter 1: Introduction

Chapter 2: Generic Methods

Index of Tables and Figures

Abbreviation Key

2,3 DPG	2,3 Diphosphoglycerate
3βHSD	3β- Hydroxysteroid Dehydrogenase 2
17βHSD	17β- Hydroxysteroid Dehydrogenase
^{31}P	Phosphorus - 31
ACE	Angiotensin Converting Enzyme
ACEI	Angiotensin Converting Enzyme Inhibitor
ACTH	Adrenocorticotrophic Hormone
ADP	Adenosine Diphosphate
AIPs	Aldosterone Induced Proteins
Alb	Albumin
Aldo	Aldosterone
Aldo synthase	Aldosterone Synthase
APES	3-Aminopropyltriethoxysilane
PCKD	Polycystic Kidney Disease
ARB	Angiotensin II Receptor Blocker
ARR	Aldosterone: Renin Ratio
ATP	Adenosine Triphosphate
ATPase	ATP hydrolysis
BB	Beta Blocker
BSA	Body Surface Area
BMI	Body Mass Index
BMP	Bone Morphogenetic Proteins
BNP	Brain Natriuretic Peptide
Bp	Base Pairs
Ca^{2+}	Calcium Ions
Ca x PO_4	Calcium Phosphate Product
CCA	Calcium Channel Antagonists
CFB	Calcium Free Buffer
CHF	Chronic Heart Failure
CHIF	Corticosteroid Hormone-induced factor
CKD	Chronic Kidney Disease
CMR	Cardiac Magnetic Resonance
Cr	Creatinine
CRP	C-Reactive Protein
CVA	Cerebrovascular Disease
CVD	Cardiovascular Disease
CYP11B1	Gene encoding 11β-Hydroxylase
CYP11B2	Gene encoding Aldosterone Synthase
DBP	Diastolic Blood Pressure
DHEA	Dehydroepiandrosterone Sulphates
DOC	Deoxycorticosterone
DMEM	Dulbecco's Modified Eagle Medium
DMSO	Dimethyl Sulfoxide

ECG	Electrocardiogram
EDV	End Diastolic Volume
EF	Ejection Fraction
ELISA	Enzyme-linked Immunosorbent Assay
ENaC	Epithelial Sodium Channel
ESV	End Systolic Volume
GAPDH	Glyceraldehyde 3-phosphate dehydrogenase
GFR	Glomerular filtration rate
GILZ	Glucocorticoid-induced Leucine Zipper
Hb	Haemoglobin
HD	Dialysis
HLA	Horizontal Long Axis
HRE	Hormone-Response Elements
IHD	Ischaemic Heart Disease
$IVST_d$	Interventricular Septal Thickness in Diastole
K^+	Potassium Ions
Ki-RasA	Kirsten-RasA
LAP	Latent Associated Protein
LDH	Lactate Dehydrogenase
LV	Left ventricular
LVH	Left Ventricular Hypertrophy
LVEF	Left Ventricular Ejection Fraction
$LVID_d$	Left Ventricular Internal Diameter in Diastole
LVMI	Left Ventricular Mass Index
MDRD-6	Modification of Diet in Renal Disease GFR - 6
MiCK	Mitochondrial Kinases
MMCK	Myofibrillar Kinases
MMP	Matrix Metalloproteinases
MR	Mineralocorticoid Receptor
MRI	Magnetic Resonance Imaging
MTT	3-(4,5-dimethylthiazol-2-yl)-2,5-diphenyl tetrazolium bromide
MVO	Microvascular Obstruction
Na^+	Sodium ions
Nedd4-2	Neuronal Developmentally Down-regulated Protein 4
NMV	Net Magnetic Vector
Ox-phos	Oxidative phosphorylation
P450scc	P450 Side Chain Cleavage
P450c21	21-Hydroxylase
P450 arom	Aromatase
P45017α	17α- Hydroxylase
P450c11	11- Hydroxylase
PA-1	Plasminogen Activator -1
Pi	Inorganic Phosphate
PCR	Phosphocreatine
PVD	Peripheral Vascular Disease
PTH	Parathyroid Hormone

PWT_d	Posterior Wall Thickness in Diastole
QTD	QT Dispersal
RF	Radiofrequency Pulse
RNA	Ribonucleic Acid
RWT	Relative Wall Thickness
SA	Short Axis
SBP	Systolic Blood Pressure
SGK1	Serine-Threonine Kinase
StAR	Steroidogenic acute regulatory protein
TGF	Transforming Growth Factor
tPA	Tissue – Plasminogen Activator
Tx	Renal Transplant
uPA	Urokinase Plasminogen Activator
UrProtein	Urinary Protein
VCL	Viable Cell Luminescence
VLA	Vertical Long Axis
WKC	Wistar-Kyoto Control

Abstract

Cardiac mortality and morbidity is a significant problem in the renal failure population. For some, their renal dysfunction is a consequence of their cardiac failure or general vascular disease; for others it develops and progresses over the course of their renal disease.

Uraemic Cardiomyopathy is a group of particular cardiac abnormalities that are found in renal failure; left ventricular hypertrophy, ventricular dilatation and left ventricular systolic dysfunction. Left ventricular hypertrophy is the commonest of these and occurs in 75% of those starting dialysis. Pathological examination of these hearts reveals prominent cardiac fibrosis and expansion of the ventricular muscular wall.

Uraemic cardiomyopathy is more common as renal function deteriorates but doesn't occur in all patients requiring renal replacement therapy. Therefore it has been proposed that factors other than uraemia and uraemic toxins probably contribute to this pathological process.

The renin-angiotensin-aldosterone system is one of the possible contributing factors. Animal studies and more recently clinical studies have added weight to this theory. Brilla and Weber published a set of landmark papers in 1992, demonstrating an increase in cardiac fibrosis in rats treated with an aldosterone infusion. However, these finding were only present in rats fed a high sodium diet. They also appear to be independent of hypertension; another known cause of left ventricular hypertrophy.

Evidence in humans is more difficult to prove and remains varied in outcome. A recent study in a hypertensive population found a positive correlation between aldosterone serum levels and left ventricular mass. Evidence in renal failure is even more limited and it is this situation that we have focused on in our study.

Transforming growth factor beta is a proposed down-stream signalling molecule of the renin-angiotensin-aldosterone system in cardiac fibrosis/left ventricular hypertrophy. However this is not the only signalling pathway that is under investigation and at present the evidence is equivocal.

This Thesis incorporates three separate but related studies. The West of Scotland Kidney Disease Study was a 10 year follow-up analysis of patients initially enrolled in 2005, with a range of renal failure from mild to end-stage, those on dialysis and transplanted patients. As expected survival decreased as renal function declined and survival rates were better in the transplanted group than those on dialysis. However, survival rates in this group of patients were not determined by aldosterone, total renin, aldosterone:renin ratio, left ventricular mass or ejection fraction. Our study did confirm previous evidence that urinary protein excretion greater than 1 g/day was associated with a significant increase in mortality over the 10 year follow-up.

The Aldosterone Study, aimed to identify factors affecting left ventricular mass and aldosterone levels in a renal failure population. Unfortunately no link was identified between aldosterone and left ventricular mass, or surrogate

markers of cardiac disease. Also no significant factors affecting the aldosterone levels of these patients were identified.

The Rat Slice Study was an experimental model developed in an attempt to replicate ventricular cell interactions and structure that occurs within the body. Rat ventricle tissue slices were used and incubated in media for 48hours. The media was supplemented with different concentrations of aldosterone, water or both to determine the effects of aldosterone and sodium concentration on TGF-β_1 production and cardiac fibrosis.

Viability of the slices was evident at 48hours although at a much lower level than at the start of the experiment. No increase in cardiac fibrosis or TGF-β_1 production was found in any of the groups of tissue slices.

In Conclusion, the three studies undertaken found no definitive evidence for the role of aldosterone or TGF-β_1 in cardiac fibrosis/left ventricular hypertrophy. This was true of both the uraemic and non-uraemic states.

Chapter 1: Introduction

1.1 Cardiovascular Disease in Renal Failure

1.1.1 Epidemiology and Cardiovascular Risk

End stage renal failure carries an increased risk of premature death (from any cause) compared to the general population. However, it is the increased risk of cardiovascular death that is the most pronounced; up to 100 times that of the general population by the time end stage renal failure is reached [1, 2]. This equates to a risk of cardiac death that is 20 times that of progression to renal replacement therapy [1].

Recently the UK renal registry calculated the prevalence of patients needing renal replacement therapy as 725 per million population [3]. Unfortunately the incidence and prevalence of chronic kidney disease is not so easily defined. Not all patients are aware that they have renal impairment and most are followed up solely in the community. Despite this, renal dysfunction, and it's associated cardiovascular morbidity and mortality provide a major target group for research and intervention.

1.2 Risk Factors for Cardiovascular Disease

1.2.1 Traditional Risk Factors

Determination of the exact cause of increased cardiovascular risk in renal patients is difficult to determine. Renal failure often co-exists with "traditional" risk

factors for cardiovascular disease, for example hypertension, diabetes and hyperlipidaemia. However, these “traditional” risk factors appear to have their effects reversed or altered in renal failure e.g. the “U-shaped curve” effect for blood pressure on mortality risk and the lack of evidence for statins in this population [4, 5].

1.2.2 Non-Traditional Risk Factors

Non-traditional risk factors include anaemia, volume overload, raised C-reactive protein (CRP) and increased calcium/phosphate [1]. Despite progressive renal failure causing or being associated with many of the risk factors mentioned above, chronic renal failure itself is independently associated with increased cardiovascular risk [6]. The mechanisms for this are not yet clearly defined but the paragraphs below detail some of the advances and possible mechanisms involved.

1.3 Types of Cardiac Disease in Renal Failure

1.3.1 Atherosclerotic

As would be expected for a population with a high proportion of traditional risk factors; atherosclerosis is common. Data from the HEMO study in 2000 demonstrated that 40% of enrolled chronic haemodialysis patients had evidence of coronary heart disease; patients with known unstable angina and severe heart failure were excluded [7].

Recent evidence suggests that the atheromatous plaques developing in uraemic patients are highly calcified compared with age matched controls [8]. Other non-traditional risk factors have been assessed to identify uraemia specific conditions necessary for this calcification and increased disease prevalence e.g. phosphate and CRP.

1.3.2 Uraemic Cardiomyopathy

Uraemic cardiomyopathy is a term that amalgamates the common cardiac abnormalities found in renal failure patients; left ventricular hypertrophy, left ventricular systolic dysfunction and left ventricular dilatation.

Left ventricular hypertrophy (LVH) has been identified in approximately 75% of patients reaching dialysis [9] and is considered an independent risk factor for cardiovascular mortality [10] [11].

Therefore, there has been a large emphasis in renal and cardiac research aimed at determining the causative factors and potential interventions to reverse this pathological process. Systolic blood pressure is known to be one of the determinants of left ventricular mass [12] and has been shown in many studies to regress with antihypertensive treatment [13, 14]. However, LVH has also been shown in some animal and human models to develop independently of blood pressure [15, 16].

1.3.3 Sudden Cardiac Death

Sudden cardiac death is the most common cause of death in end-stage renal failure patients and forms 62% of all cardiac deaths in this group [17]. It is

thought that these patients develop fatal cardiac arrhythmia e.g. ventricular tachycardia or fibrillation. However, our knowledge of the exact pathological/biochemical processes underlying the final event is incomplete.

Several theories exist to explain the high levels of sudden cardiac death in dialysis patients. These include existing myocardial damage predisposing to an increased risk of myocardial ischaemia, rapid electrolyte shifts during dialysis, and coronary heart disease. Other potential factors include chronic anaemia, disturbance of calcium/phosphate equilibrium, chronic fluid overload and inflammation i.e. high CRP [17].

Some of the most convincing evidence that coronary artery disease isn't the only contributing factor comes from the evidence that coronary artery stenting and coronary artery bypass grafting in patients with significant stenoses did not prevent sudden cardiac death [18].

The fact that most dialysis patients have evidence of at least one form of uraemic cardiomyopathy is probably one of the reasons why they are at such high risk of sudden cardiac death.

1.4 Aldosterone

Aldosterone (Figure 1.1a) is the primary mineralocorticoid hormone in humans; defined as a hormone that "promotes unidirectional transepithelial sodium transport" [19].

It was first discovered by Sylvia Simpson and Graham Tait in adrenal extract and the term aldosterone was coined in 1954 [19]. Following this

discovery, Jerome Conn went on to describe Conn's syndrome linking aldosterone secreting tumours with hypertension and hypokalaemia [20]. Since then interest in this hormone has grown particularly in terms of its effects on blood pressure and the cardiovascular system. These effects will be discussed in more detail, later on in this chapter.

1.4.1 The Adrenal Glands

Aldosterone is produced in the adrenal glands; two small endocrine glands that lie superior and adjacent to both kidneys. Each adrenal gland is divided histologically into the adrenal cortex and medulla. The cortex is then sub-divided into three zones; the outermost zona glomerulosa, beneath which lies the fasciculata and then the reticularis. (Figure 1.2) The adrenal medulla forms the core of the adrenal gland and produces catecholamines rather than steroid hormones.

Aldosterone is produced in relatively small amounts (10-150µg/day) [21] exclusively by the zona glomerulosa . Whereas, the zona fasciculata is concerned primarily with the synthesis of cortisol (10 - 20mg/day) [21] and the zona reticularis with androgens called Dehydroepiandrosterone sulphates (DHEAs).

1.4.2 Synthesis

Aldosterone and the other adrenal steroid hormones share the first part of their biosynthetic pathway and have a similar basic chemical structure (figure 1.1a and 1.1b).

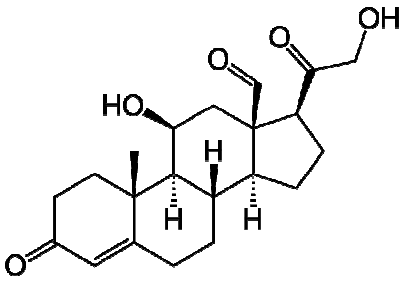

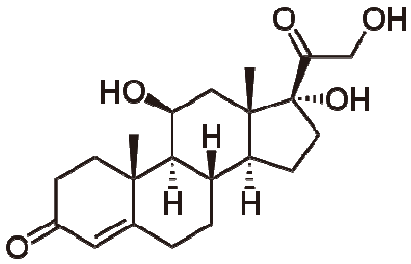

Figure 1.1a **Aldosterone** [22] ***Figure 1.1b*** **Cortisol** [23]

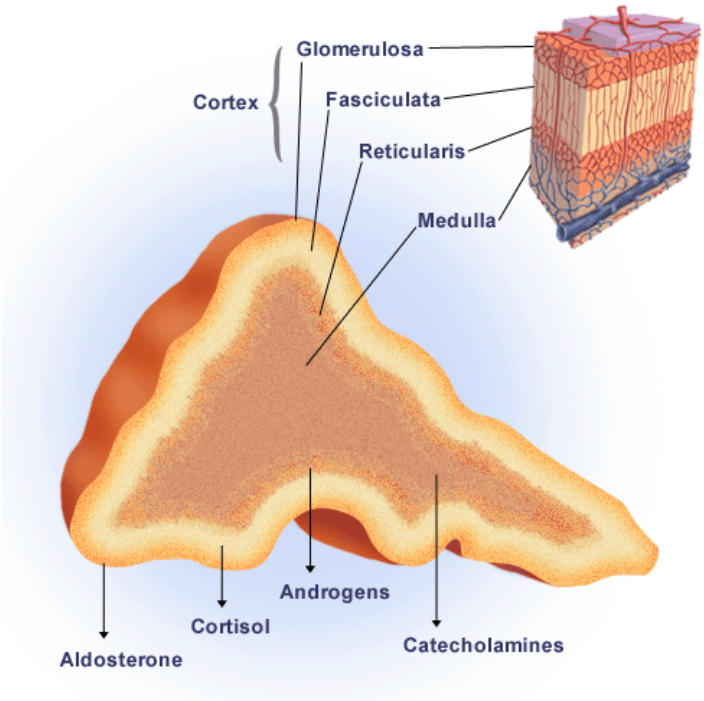

Figure 1.2 **The Adrenal Gland Anatomy and Hormone Production** [24]

The first step in this pathway is cholesterol. This is taken up from the blood (where it is bound to low-density lipoproteins) by a protein called steroidogenic acute regulatory protein (StAR). StAR allows transport of cholesterol into mitochondria where it is converted to pregnenolone by cytochrome p450 side-chain cleavage enzyme (p450scc), located on the inner mitochondrial membrane. The pregnenolone is then transported into the cytosol where it is converted to progesterone by 3β-hydroxysteroid dehydrogenase 2 on the membrane of the endoplasmic reticulum. Progesterone is then converted to deoxycorticosterone (DOC) by 21-hydroxylase enzyme also located in the endoplasmic reticulum [25]. (Figure1.3)

However, differentiation of the final hormone produced by the different zones of the cortex is determined by the expression of specific enzymes present at the end of the biosynthesis pathway. The zona glomerulosa uniquely contains an enzyme called aldosterone synthase, present on the inner mitochondrial membrane. This converts DOC via 3 steps of hydroxylation (one of which is 11β-hydroxylation) and oxidation to aldosterone [26]. In contrast, in the zona fasciculate, progesterone is 17α-hydroxylated to deoxycortisol before being hydroxlated by 11β- hydroxylase enzyme to cortisol. A small amount of corticosterone is also produced in the zona fasciculate from DOC by the 11β-hydroxylase enzyme.

Aldosterone synthase is present in the zona glomerulosa because of the local presence of the gene CYP11B2. This is not present in the zona fasciculata;

instead CYP11B1 is present leading to the production of 11β- hydroxylase enzyme.

1.5 Control of Aldosterone Production and Release

1.5.1 ACTH

ACTH is the pituitary hormone primarily responsible for glucocorticoid release and as such is known to regulate CYP11B1 expression. However it has also been shown to affect aldosterone synthesis and expression of CYP11B2, athough the mechanism remains unclear.

ACTH's effects on aldosterone release can be separated into two parts. Acutely, ACTH increases aldosterone release via an increase in the Steroidogenic acute regulatory (STAR) protein [27]. This enables more cholesterol to be taken into the mitochondria in order to start the process of steroidogenesis.

However chronic infusion and 24 – 48 hours post acute administration causes a fall in aldosterone levels to pre-infusion or sub pre-infusion levels [28-30]. This negative effect has also been demonstrated on aldosterone synthase mRNA expression in rats over a similar time course [31] and appears to be dose related [28].

Nevertheless, CYP11B2 but not CYP11B1 expression has been shown to persist where ACTH has been suppressed indicating that ACTH is not vital for its existence [32, 33]. Despite the previous evidence, ACTH is still considered an

Figure 1.3 Adrenal Steroid Synthesis Pathway [34]

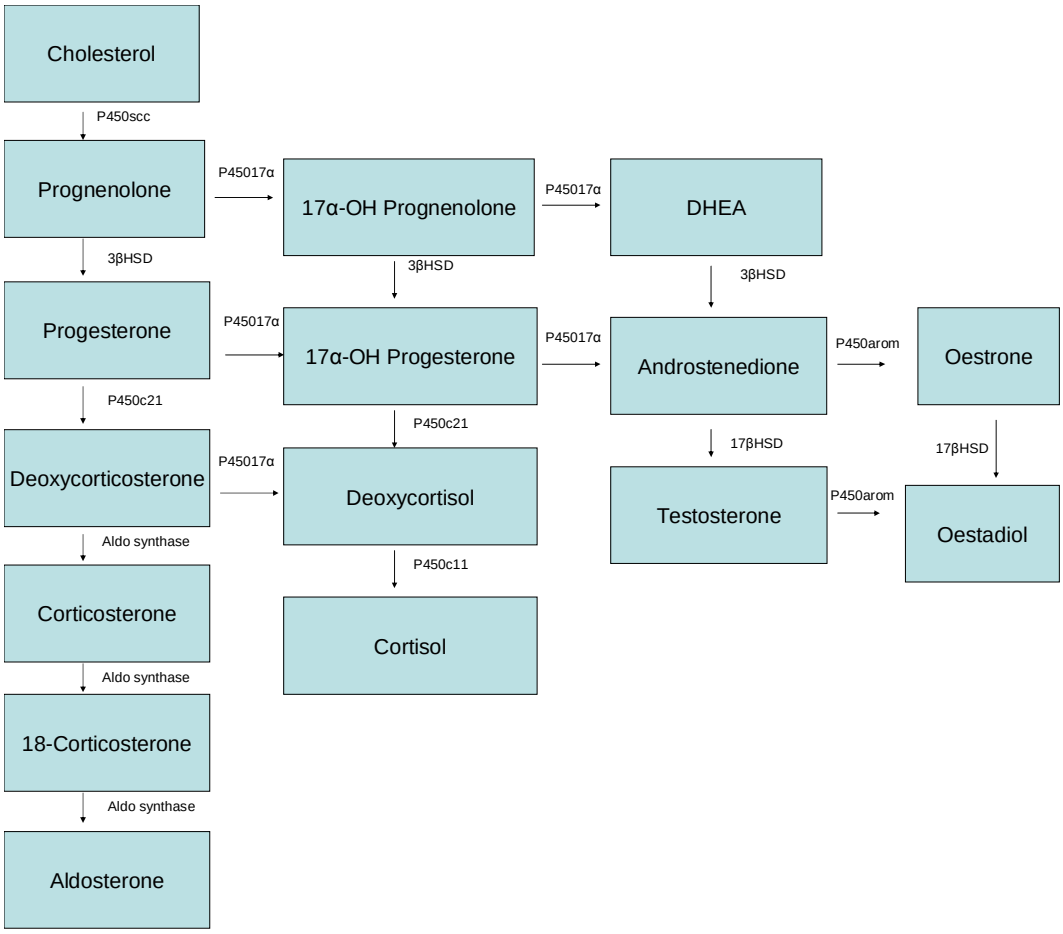

Enzyme Key:

P450scc – P450 side chain cleavage

3βHSD - 3β-hydroxysteroid dehydrogenase 2

P450c21 – 21-hydroxylase

Aldo synthase – aldosterone synthetase

17βHSD - 17β- hydroxysteroid dehydrogenase

P450 arom – aromatase

P45017α – 17α- hydroxylase

P450c11 – 11-hydroxylase

important physiological trigger of aldosterone production, evidenced by the diurnal secretion pattern of aldosterone following that of cortisol. However, no feedback loop has been identified as yet [35].

In addition, sodium repletion, potassium loading and increased angiotensin II levels have been shown to alter this relationship and increase the production of aldosterone in response to ACTH [30, 36]. In fact one small study showed that blocking angiotensin II production (with captopril) associated with ACTH infusion, dampened the aldosterone response [35].

1.5.2 Angiotensin II and the Renin-Angiotensin System

In response to low circulating intravascular volume (detected by the baroreceptors) and reduced plasma sodium concentration (detected in the macula densa) renin is produced and then secreted from the juxta-glomerular apparatus. This forms the starting point of the renin-angiotensin system. Renin then catalyses the conversion of angiotensinogen, produced in the liver, into biologically inactive angiotensin I. Angiotensin I is subsequently converted into active angiotensin II by angiotensin converting enzyme (ACE) (Figure 1.4). ACE has gained clinical importance with the development of a class of medication called ACE inhibitors (ACEI). ACEI have been shown to have beneficial effects e.g. post myocardial infarction, in heart failure and proteinuric states. ACE is found primarily in the lungs but also in the vascular endothelium and has recently been demonstrated in other tissues e.g. myocardium. Angiotensin II is a potent vasoconstrictor and also acts within minutes to stimulate the glomerulosa cells to secrete aldosterone.

Figure 1.4 **Basic Schematic Diagram of the Renin Angiotensin System**

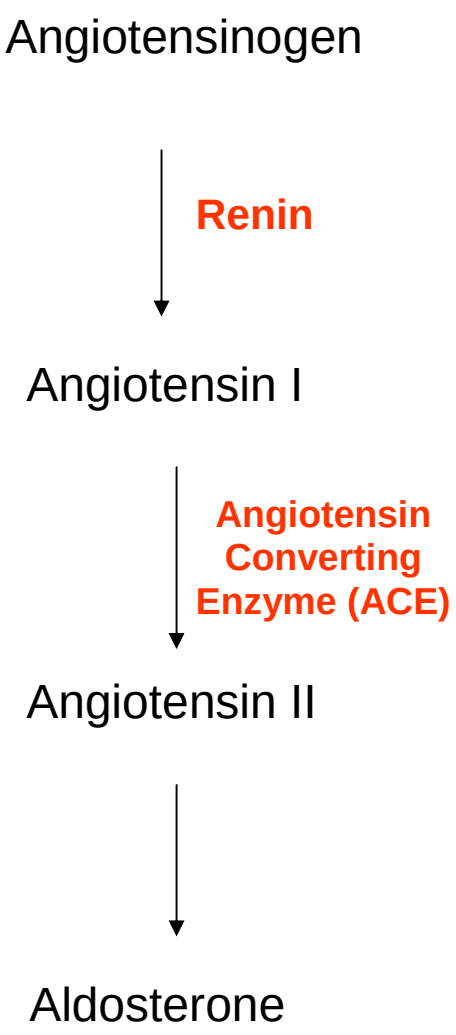

Renin catalyses the conversion of angiotensinogen to angiotensin I and ACE catalyses the conversion of Angiotensin I to Angiotensin II

1.5.3 Potassium

As mentioned previously, potassium influences the interaction of ACTH and angiotensin II with glomerulosa cells. However it also has independent effects on aldosterone production. This has been shown with the use of the angiotensin converting enzyme inhibitor captopril. Captopril was unable to block the actions of K^+ allowing the increase of aldosterone synthase mRNA expression in rats [37]. Figure 1.5 demonstrates the positive correlation between potassium levels and aldosterone.

Studies examining these effects have also examined the levels of ACTH and cortisol during K^+ loading; finding that the levels of ACTH and cortisol remained unchanged. These data indicate that neither the renin-angiotensin sytem nor ACTH are needed for aldosterone production to be induced by K^+ loading [33]

Figure 1.5 **The Effect of Potassium on Aldosterone Production in Humans** [33]

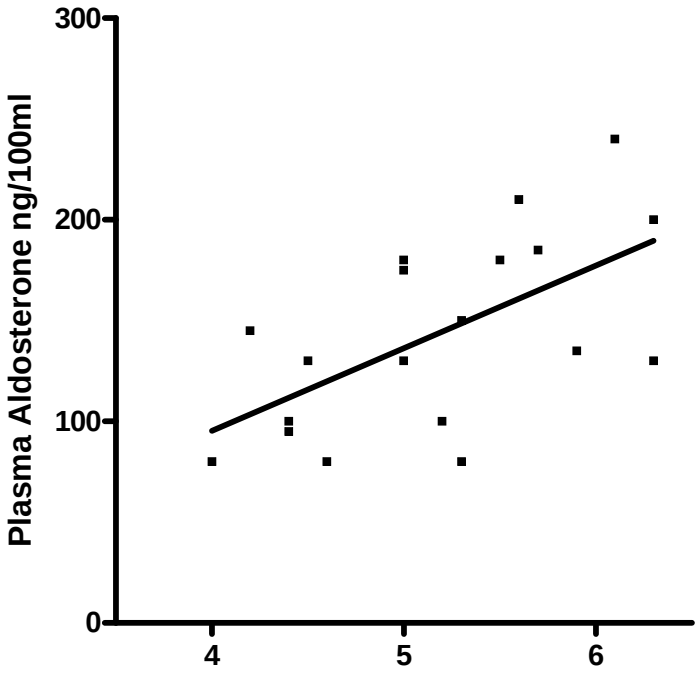

"The relation of plasma aldosterone and serum potassium response to an infusion of potassium chloride in live normal subjects (correlation coefficient 0.62, $p<0.01$). The potassium chloride was infused at a constant rate of 37.5mEq/hr for two hours. The subjects were in balance on a 10mEq sodium/200mEq potassium diet and were studied supine." [33]

In fact, glomerulosa cells are very sensitive to even small increases in potassium (K^+) consequently causing large increases aldosterone synthase production and aldosterone secretion [33, 38, 39]. In order to increase aldosterone production, K^+ acts by depolarising the cell membrane causing voltage gated Ca^{2+} channels to open [40]. Successful use of the calcium channel blocker, nifedipine to block K^+ effects on Ca^{2+} influx and CYP11B2 mRNA production confirms this mechanism of action [41, 42]. It is then thought that this Ca^{2+} influx activates calmodulin dependent kinases and in particular Calmodulin protein kinase I. CMKI is concentrated in the zona glomerulosa cells of the adrenal and using antagonists (e.g.KN93 and calmidazolium) the effects mediated by K^+ on CYP11B2 expressioncan be ameliorated [43, 44].

1.6 Mechanisms of Action

1.6.1 The MR Receptor

Classically aldosterone is described as a hormone that acts on the distal nephron to increase sodium reabsorbtion. It does so by diffusing into the cell and binding to an intracellular mineralocorticoid receptor (MR).

The MR belongs to a group of proteins called the nuclear receptor subfamily; other members of which include sex-hormone and cortisol binding receptors. It is the MR that is considered the mediator of aldosterone's genomic effects. However MR binding is not specific to aldosterone; in fact it has an equal affinity for cortisol. Circulating levels of cortisol are at least 100 times that of

aldosterone and therefore in theory it should occupy more MR than aldosterone. Since this is not the case, it is reasonable to assume that other mechanisms exist to regulate cortisol occupation of the MR [45]. In epithelial tissues the expression of a type 2 isoform of 11-hydroxysteroid dehydrogenase enzyme (11β-HSD2) deactivates cortisol to form 11-cortisone. 11-cortisone cannot bind to the MR and so in these cells the MR is thought to preferentially bind aldosterone [26, 46]. The best characterised action of aldosterone is increased sodium reabsorbtion in the kidney. An electrochemical gradient allows diffusion of sodium into the distal nephron epithelial cells via amiloride-sensitive epithelial sodium channels (ENaC) present on the apical cell membrane of the kidneys. The Na^+/K^+ -ATPase located on the baso-lateral cell membrane then actively transports Na^+ into the bloodstream. This increases Na^+ reabsorbtion whilst simultaneously causing excretion of potassium into the urine. Water accompanies the movement of sodium and therefore an increase in plasma volume also results [25].

Only a small proportion of ENaC channel synthesised by the cell are expressed on the cell surface [47]. Therefore this provides potential for a quicker response to aldosterone than by an increase in ENaC protein production.

In the presence of aldosterone, MR dependent effects appear to occur in two stages; an early (i.e. before 3 hours) and a late stage (i.e. after 3 hours). In the early stage of aldosterone administration there is an increase in the mean opening time and number of ENaC channels at the apical cell membrane [48], thereby increasing sodium reabsortion in these tissues. However 3-6 hours after

exposure increased biosynthesis of ENaC and Na^+/K^+ ATPase results [49, 50]. This is believed to be responsible for the sustained Na^+ response.

The MR receptor consists of an N-terminal domain, DNA-binding domain and a C-terminal ligand binding domain. It is the latter of these to which aldosterone binds causing a conformational change, followed by dimerisation. The complex then translocates to the nucleus [25]. Here the DNA-binding domain of the MR receptor binds to the hormone-response elements (HRE) and causes up-regulation of aldosterone induced proteins (AIPs). Of the AIPs produced the serine-threonine kinase SGK1 is most described. SGK1 is phosphorylated and activated within 30 minutes of aldosterone administration [51]. It is now thought that SGK1 increases ENaC surface expression via phosphorylation of the ubiquitin protein ligase; Neuronal developmentally down-regulated protein 4 (Nedd4-2) [52]. (Figure 1.6)

Nedd4-2 is an inhibitory protein that binds to the β and γ subunits of ENaC causing its internalisation and breakdown [53]. Therefore it's inhibition by SGK1 increases expression of ENaC at the cell surface and hence increases Na+ reabsorbtion.

Other AIPs include Kirsten-RasA (Ki-RasA), Corticosteroid Hormone-induced factor (CHIF), Glucocorticoid-induced leucine zipper (GILZ) and PI3K. Ki-RasA is a GTP- binding protein that regulates G-proteins and is a known activator of the MAPK1/2 cascade (involved in cell proliferation). Evidence in both renal A6 epithelial cells and rat cardiac myofibroblasts demonstrate an increase in active GTP-bound Ki-RasA [54, 55] following aldosterone infusion.

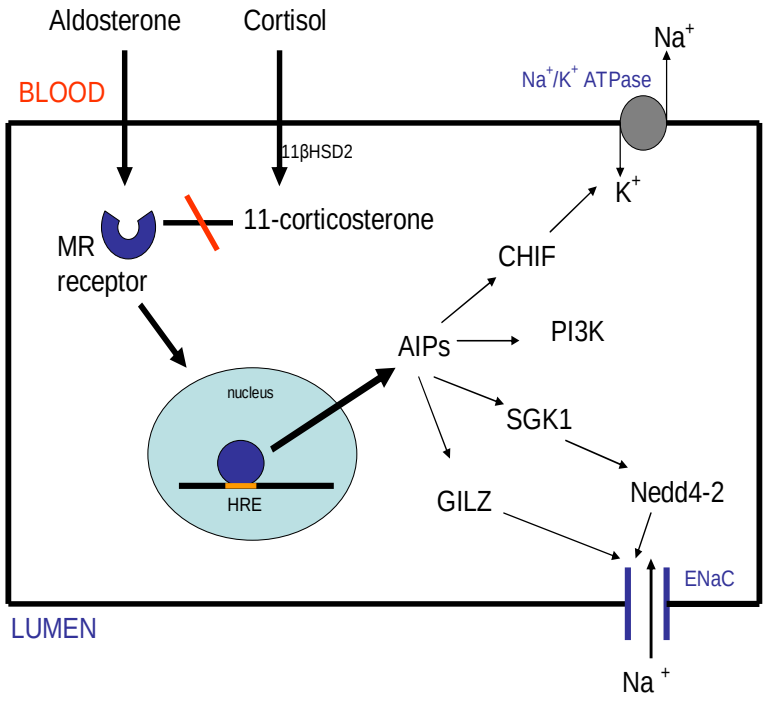

Figure 1.6 **The Classical Mechanism of Aldosterone's Action in Epithelial Cells.**

The occupied Mineralocorticoid complex binds to the HRE of Target Genes to Influence Gene Transcription

Key: Aldosterone-induced proteins (AIPs)

Corticosteroid Hormone-induced factor (CHIF)

P13K

Serine-theonine kinase 1 (SGK1)

Glucocorticoid-induced leucine zipper(GILZ)

Epithelial sodium channel (ENaC)

However the exact functions of Ki-RasA during aldosterone administration are not yet clear.

CHIF is a member of the one-transmembrane segment protein family named FXYD. It is found mainly in the renal collecting duct and distal colon and increases the sensitivity and work rate of the Na/KATPase pump to sodium [56].

As explained above MR receptors are classically described in the distal nephron however increasing evidence reports findings in other epithelial (colon, salivary glands and sweat glands) and non-epithelial cells (mesangial cells, fibroblasts, vascular smooth muscle cells, cardiomyocytes, brain, liver and leukocytes) [26, 46].

This classical view of aldosterone's mechanism of action is either termed "Genomic" or "MR-dependent". However there is now evidence that aldosterone's effects spread beyond the distal nephron and the MR receptor. These non-genomic effects are discussed below.

1.6.2 Non-Genomic Effects of Aldosterone

Classical MR activation requires time to take effect because it involves gene transcription and protein production. However, aldosterone's actions are not all thought to occur from this classical genomic pathway. Effects of Aldosterone have been noted within minutes of injection and are therefore considered too rapid to be from genomic effects alone. Some but not all of these non-genomic effects appear MR mediated.

The first description of these rapid non-genomic effects was reported by Spach and Streeten more than 40years ago. They found that aldosterone

caused effects on sodium exchange in dog erythrocytes at physiological concentrations of aldosterone [57]. Since erythrocytes have no nucleus these effects could not have been genomic. Another convincing discovery was made from experiments conducted on cutaneous fibroblasts of MR knockout mice. In these mice aldosterone caused a rapid increase in the levels of intracellular calcium and cAMP [58]. Despite the early discoveries by Spach and Streeten further research in this area only really started in the late 1980s. It was then that Human Mononuclear Leukocytes (HMLs) were used to investigate ion transfer in response to aldosterone. Wehling described a significant increase in intracellular K^+, Na^+, Ca^{2+} and volume within one hour of treatment with aldosterone at 0.1nmol/l concentration. This effect was not inhibited by canrenone (an MR antagonist) [59]. A hypothesis exists that these effects are brought about through interaction with a membrane bound receptor however this is yet to be identified and sequenced [60].

Other evidence suggests that the MR might have a role in these rapid non-genomic effects. Indeed, Eplenerone (a new MR antagonist) has been found to block the rapid vasoconstricting effects of aldosterone on mesenteric vessels in animal models [61]. So perhaps a combination of the two pathways, with cross talk between them, might actually be the true situation.

1.7 Cardio-Renal Effects of RAS

Animal studies (mainly in rats) have shown deleterious cardio renal effects of increased aldosterone levels. These cardio renal effects include inflammation, endothelial dysfunction, increased blood pressure, oxidative stress, fibrosis and

increased proteinuria. However these effects have been demonstrated to be salt dependent in animals [46, 62-65] but not conclusively in humans.

Some of these deleterious effects seem to be due to activation of the mineralocorticoid receptor (MR) or production of angiotensin II whilst others are due to direct effect of aldosterone.

1.7.1 Myocardial Fibrosis

MR activation in the heart has been shown to regulate collagen formation, activate smooth muscle cells and alter the effects of the adrenergic system [26]. There is still controversy over the presence of the 11β-hydroxydehydrogenase enzyme in addition to the MR, in human hearts but it is known to be present in vascular tissue. Without this enzyme we could conclude that cortisol was driving the MR effects rather than aldosterone. But the evidence for aldosterone acting via MR's as cause for cardiac fibrosis in vivo is well recognized [66].

Recent studies examining left ventricular hypertrophy have found an abnormal accumulation of fibrillar collagen in the interstitium, perivascular tissue, as well as increasing myocardial cell growth. The presence of this fibrosis is now thought to be a consequence of hormone activation rather than haemodynamic effects. This has been demonstrated in vivo where infra-renal aortic banding was used to precipitate hypertension and left ventricular hypertrophy but myocardial fibrosis was not found histologically [67]. In other studies, rats have been given intracerebral mineralocorticoid receptor blockers to prevent hypertension whilst concurrently being given a peripheral aldosterone infusion. In these rats cardiac hypertrophy and fibrosis did develop [68].

These effects of aldosterone are, in most cases, salt sensitive, with fibrosis only occurring in the presence of increased salt intake [46, 62, 63, 69]. Unfortunately the mechanisms for this interaction are not yet fully understood. One hypothesis is that the high salt levels activate the renin-angiotensin system in the myocardium. To support this; increased mRNA levels for angiotensin converting enzyme have been reported in vivo and in patients with dilated cardiomyopathy [70].

Other researchers have attempted to determine the mechanism of aldosterone induced cardiac fibrosis. Some in vivo studies using spironalactone (an MR antagonist) demonstrated that it could be used to inhibit aldosterone induced fibrosis [66]. However in rat cardiac fibroblasts spironalactone failed to inhibit fibrosis suggesting that at least some of aldosterone's effects were due to non-MR effects[71].

The time course of these effects in the heart has also been estimated. By 8 weeks of aldosterone and salt infusion, marked fibrosis has developed in uninephrectomised rat models [67, 68]. But prior to this vascular inflammation and oxidative stress have been demonstrated and are thought to precede the fibrosis [65, 72, 73].

1.8 Epidemiology of Primary Hyperaldosteronism

Functional primary hyperaldosteronism might account for approximately 5-10% of hypertension in general population and 20% of those with resistant hypertension [63, 74]. This is a higher incidence than previously thought and follows the introduction of the aldosterone:renin ratio (ARR) as a more sensitive

screening measure. In addition, wider screening to include those patients who are normokalaemic “essential” hypertensive patients has revealed previously unidentified hyperaldosteronism [74].

1.9 Aldosterone to Renin Ratio

Recently it has been recognised that the proportion of hypertensive patients with excess aldosterone is larger than originally thought. This increased estimation might be due in part to the initiation of aldosterone:renin ratio as a screening and diagnostic test for hypertension. In theory the ratio between these hormones is a more accurate assessment of the status of aldosterone and the renin-angiotensin system than aldosterone alone. This is because the ratio takes into account the sodium and postural effects on levels in the blood. However the ratio is affected by medication in particular angiotensin converting enzyme inhibitors (ACEI) and beta-blockers (BB). ACEI increase renin levels via feedback mechanisms therefore reducing the ratio whereas BB reduce renin and therefore increase the ratio.

1.10 Mortality

The Consensus study, investigating patients with heart failure, found that baseline aldosterone concentrations above the median had a significantly higher mortality compared to those below (55% vs. 32%, $p<0.001$) [75] . It also demonstrated a reduction in mortality, due to worsening heart failure, in patients

treated with enalapril. This was the first large randomized controlled trial to demonstrate a potential link in humans between aldosterone and mortality.

Subsequently, human studies have demonstrated a benefit from aldosterone antagonists. The RALES study demonstrated a 30% reduction in mortality of severe chronic heart failure patients with the use of spironalactone [76]. Another large human study was the EPHESUS study, this enrolled patients with heart failure post myocardial infarction. They demonstrated a reduction in all cause mortality but this time with eplenerone (a new selective Aldosterone blocker) [77].

1.11 Magnetic Resonance Imaging (MRI)

1.11.1 Physics

Conventional MRI uses excitation of hydrogen atoms to form images. Hydrogen is used predominantly due to its abundance within our bodies (80% water) and due to the fact that it has the largest magnetic moment. However any atom with an odd number of protons can be utilised [78]. With only 1 proton in a hydrogen nucleus, it is unbalanced and a net charge and spin is produced. This in turn produces a magnetic charge the strength and direction of which is called magnetic moment [79]. These charged nuclei repel or attract each other depending on their orientation. At rest the hydrogen atoms and protons are aligned in different directions however when the human body is put into a strong

magnetic field the protons line up. They can line up parallel or anti-parallel to the main magnetic field depending on their energy state (Figure 1.7).

The protons also precess or “wobble” under the influence of an external magnetic field. This precession causes the nucleus to orbit around the direction of the external field (B_0) The frequency of the precession can be calculated from the equation below called the Larmor frequency [78].

$$\omega_0 = \gamma B_0$$

Where: ω_0 = Precessional or Larmor frequency. (MHz)

γ = Gyro Magnetic Ratio. (MHz/T) or magnetic moment

B_0 = Magnetic field strength. (T)

The majority of protons align parallel with the magnetic field and this is called net magnetisation vector (NMV). As the magnetic strength increases so does the percentage of protons parallel to B_0, therefore increasing the NMV [79].

1.11.2 Excitation

For a 1.5 Tesla machine the Larmor frequency is 63 MHz for Hydrogen ions. A radio frequency (RF) pulse at that frequency is provided to excite the protons. This causes the targeted particles to resonate and increases the number of high energy particles. The increase in energy state allows more protons to oppose B_0 therefore changing the net vector.

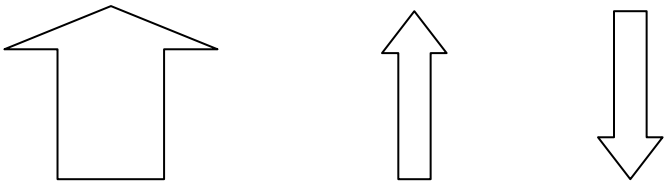

Main Magnetic field (B_0)	Parallel (low energy)	Anti-parallel (high energy)

Figure 1.7 **Magnetic Field Effects on individual protons within the MRI scanner**

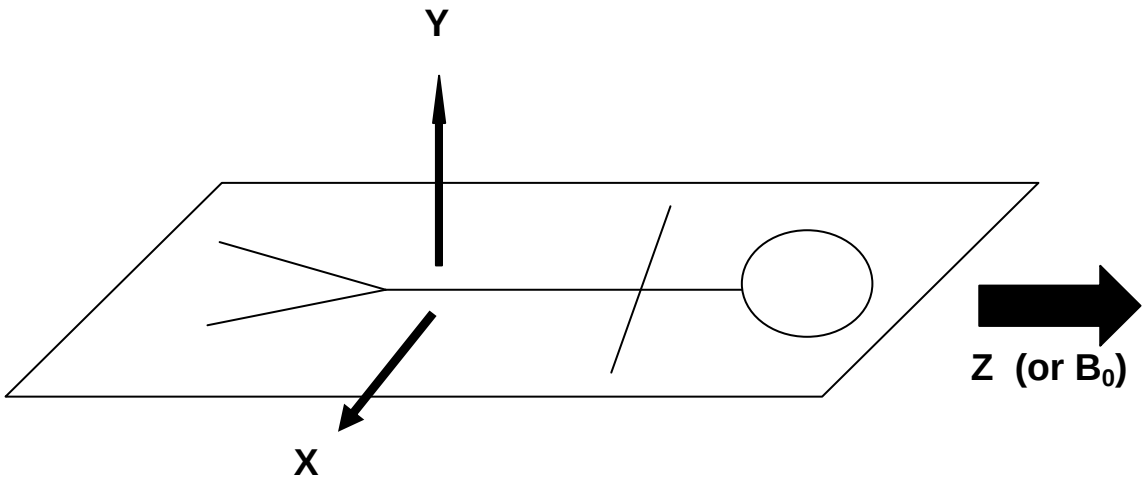

Figure 1.8 **Schematic diagram to demonstrate the directionof main MR axis (B_0), and x and y axis with respect to the patient in the MR scanner.**

1.11.3 T1 Relaxation

This process occurs after the RF pulse has been given and the protons excited to 90° i.e. moved into the x-y plane. The protons then lose the energy received by the RF pulse over time and return to their original position (i.e. parallel to B_0/the z plane) (Figure 1.9). The energy released takes the form of radio waves and a small amount of heat. The time for 63% of the nuclei to return to their longitudinal magnetisation is called the T1 recovery time. This time is constant for a particular tissue e.g. fat or water[79].

1.11.4 T2 Decay

T2 Decay is caused by the interaction of the magnetic fields around each atom. To understand T2 decay, it is important to understand phase coherence. Once the RF pulse has been given the particles not only gain enough energy to move into the x-y plane, the magnetic moments also move into phase. That is to say that if you looked at the nuclei from above, the protons would be spinning in a circle, all at the same point on the circle (Figure 1.10 A).

After the RF pulse is given you would see that the protons were all at the same place on the circle at a given time. Over time the nuclei will interact so that in the end the protons would be seen in all different places on the circle. Therefore the net magnetisation vector in x-y plane would cancel out. (Figure 1.10E)

The T2 decay time is the time it takes for 63% of the transverse magnetisation to be lost, due to de-phasing.

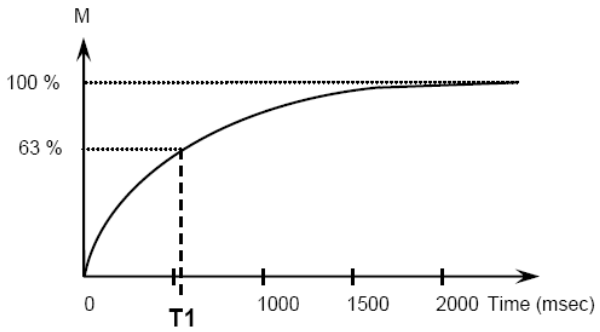

Figure 19

The curve shows at time = 0 that there is no magnetization in the Z-direction right after the RF-pulse. But immediately the M_z starts to recover along the Z-axis. T1 relaxation is a time constant. T1 is defined as the time it takes for the longitudinal magnetization (M_z) to reach 63 % of the original magnetization.
A similar curve can be drawn for each tissue. That's what **Damadian** and **Lauterbur** discovered many moons ago. Each tissue will release energy (relax) at a different rate and that's why MRI has such good contrast resolution.

Figure 1.9 **T1 relaxation [78]**

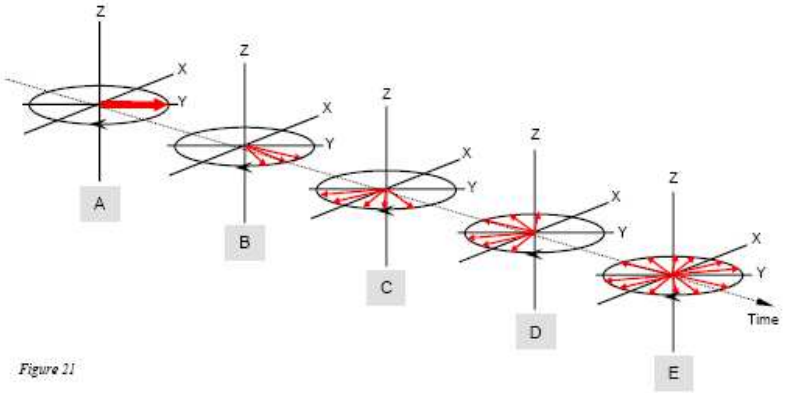

Figure 21

Figure 1.10 **T2 Decay [78]**

The T2 decay time is intrinsic and constant for a particular tissue.

The processes of T1 relaxation and T2 decay occur in different planes but at the same time. Once both processes of relaxation have occurred the NMV is back at B_0 and the protons are spinning out-of-phase.

1.11.5 Image Acquisition

Faraday's law states that "a change in magnetic flux through a closed circuit induces an electromotive force" and consequently a current [79]. It is this current that is picked up by a receiver coil and interpreted into the MRI image. A receiver coil is placed on the patient over the part of the body that is being imaged prior to them entering the scanner. This receiver coil must be at 90° to B_0 in order to generate the current in the coil and one that is not overpowered by the signal from the main magnetic field.

Cardiac function is evaluated using cine gradient echo sequences. Steady-state free precession (SSFP) gradient echo sequences have largely replaced spoiled gradient echo sequences for this purpose. Different trade names for these SSFP sequences are used by different manufacturers. Siemens have called theirs TrueFISP (True Fast Imaging with Steady-state Precession).

1.11.6 Gadolinium

Gadolinium is a chemical that is used in cardiac MRI scanning to identify areas of ishaemia and fibrosis. It reduces the T1 time of the tissues that absorb it. Therefore early Gadolinium scans can identify areas that are slow to take up

Gadolinium (so called microvascular obstruction or MVO) and late Gadolinium enhancement identifies areas of fibrosis.

1.11.7 Advantages of MRI Compared with Echocardiography

Echocardiography has been used for many years with the accompanying confidence and ease of use that experience brings. However echocardiography is affected by intravascular fluid status and adiposity, and can over-estimate left ventricular mass; whereas MR is volume independent and clear images are available in a greater proportion of patients (including those with a large body surface mass index).

1.12 Spectroscopy

Conventional MRI is based on the magnetic fields generated by the Hydrogen atoms within body. However, as indicated above, any nuclei with an odd number of protons can be studied (Figure 1.11). Spectroscopy is used to non-invasively quantify phosphate containing molecules found within regions of the heart in vivo [80].

In our study ^{31}P Spectroscopy was used to study high energy phosphate groups within the cardiac ventricular wall (e.g. phosphocreatinine (PCr) and adenosine tri-phosphate (ATP)) that are responsible for providing immediate energy for cardiac myocytes. The metabolic reaction used to generate these high energy phosphate groups is called the creatine kinase reaction (Figure 1.12).

Isotope	Symbol	Spin Quantum number	Gyro Magnetic Ratio (MHz/T)
Hydrogen	^{1}H	1/2	42.6
Carbon	^{13}C	1/2	10.7
Oxygen	^{17}O	5/2	5.8
Fluorine	^{19}F	1/2	40.0
Sodium	^{23}Na	3/2	11.3
Magnesium	^{25}Mg	5/2	2.6
Phosphorus	^{31}P	1/2	17.2
Sulphur	^{33}S	3/2	3.3
Iron	^{57}Fe	1/2	1.4

Figure 1.11 **MRI "Friendly" Elements [78]**

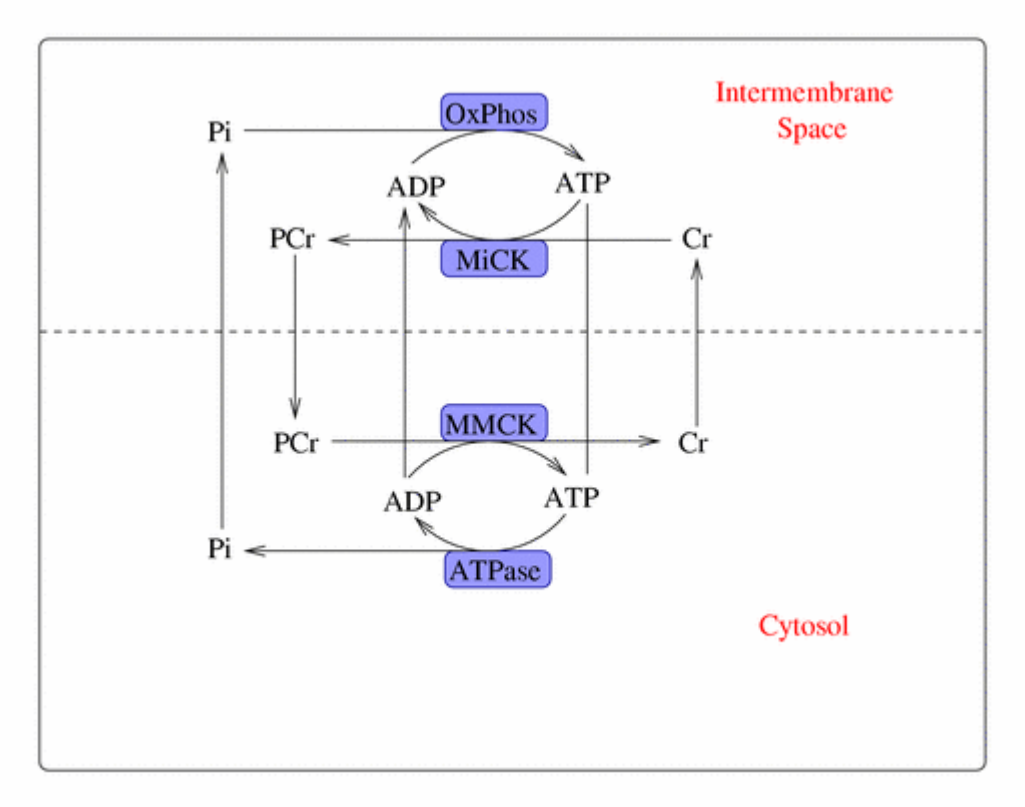

Figure 1.12 **The Creatinine Kinase Reaction** [81]

Key: ATP = Adenosine triphosphate

ADP = Adenosine diphosphate

Pi = inorganic phosphate

PCr = Phosphocreatinine

Ox-phos = oxidative phosphorylation

MiCK = mitochondrial kinases

MMCK = myofibrillar kinases

ATPase = ATP hydrolysis

The chemical bonds and structure of the tissues under examination affects the magnetic shielding of the nucleus and consequently its magnetic frequency. Therefore different chemicals resonate at slightly different frequencies despite all containing the ^{31}P ion. This array of magnetic frequencies provides us with a spectrum of results allowing differentiation of ATP, PCr etc. Unfortunately ^{31}P has a lower intrinsic MR sensitivity than ^{1}H and the low concentrations of substances examined in ^{31}P spectroscopy limits the depth to which ^{31}P signals can be accurately interpreted. In the heart this restricts us to spectrum received from the anterior ventricular wall or septum [80].

Phosphocreatinine is stored in muscle cells and provides a store of immediate energy for the myocytes. The cycle above is controlled by the enzyme creatinine kinase that phosphorylates ADP and dephosphorylates ATP to provide the energy.

Unfortunately when acquiring the spectra our voxels often included blood as well as the ventricular wall. Blood contains high levels of ATP so it was important to subtract the contribution of blood ATP from the total ATP results. We were able to do this by applying the equation below:

$$\beta\text{-ATP correction for blood} = \beta\text{-ATP}_{heart} - (0.15 \times 2{,}3\ DPG_{blood}) \quad [82]$$

1.12.1 Method

Using the MRI scanner, a ^{31}P transmitter coil is used to provide a uniform excitation field. A ^{31}P surface coil is positioned over the heart on the anterior chest wall. Once the patient is returned to the scanner, 2 localiser MR images are performed (multi log and vertical long axis views). A voxel grid is then placed over the heart in maximal systole with the maximum amount of myocardium in each voxel. A Shim field is also applied over the ventricle to ensure optimal magnetic field uniformity [80].

In a human heart, ^{31}P spectrum, (Figure 1.13) a large PCr peak is typically seen at 0ppm followed by three peaks corresponding to γ-ATP (-2.7ppm), α-ATP (-7.8ppm) and β-ATP (-16.3ppm). Peaks for 2, 3 diphosphogycerate (DPG) and inorganic phosphate (Pi) can also be obtained [80]. 2,3 DPG is particularly useful in order to determine the proportion of the ATP peak contributed to by the ventricular blood within the voxel (see previous equation).
Quantification of each peak is performed by applying best fit curves and then measuring the area under the curve.

The PCr/ATP ratio is considered the best measure of energy metabolism in the cardiac myocytes. A number of studies have now been performed investigating cardiac spectroscopy and the majority of these have determined a normal value for PCr/ATP ratio of 1.83 +/- 0.12 [80].

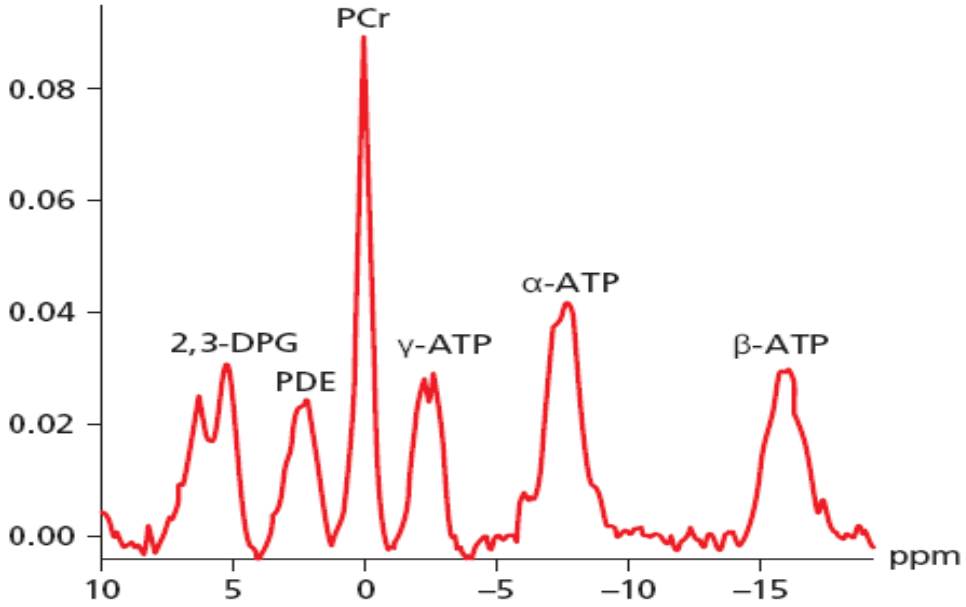

Figure 1.13 **An Example of a Cardiac ^{31}P Spectrum**

MR Spectrum "is a plot of the MR signal intensity as a function of MR frequency, typically measured in parts per million (ppm) relative to a resonant frequency of a reference compound." [83]

1.13 MR Spectroscopy in Clinical Practice

1.13.1 Left Ventricular Hypertrophy and Heart Failure

Chronic heart failure is consistently associated with a reduced PCr/ATP ratio in animals and humans regardless of the underlying pathology [84-86]. This relationship has been shown in some studies to be proportional to the degree of heart failure [87]. Other cardiac pathologies with lower than normal PCr/ATP ratios include ischaemic and idiopathic dilated cardiomyopathy [82] and possibly left ventricular hypertrophy [88]. We know that for many patients who develop left ventricular hypertrophy, unless treated, it progresses causing reduced contractility and symptoms of heart failure. It has been hypothesised that an alteration in high energy phosphate metabolism is involved in this loss of function and contractility. A study in 2006 was performed to compare control patients (with normal left ventricular mass index (LVMI)), patients with LVH and LVH plus chronic heart failure (CHF). A reduction in PCr/ATP ratio by 30% was demonstrated in both the LVH, and LVH and CHF groups compared to controls. However, no significant difference was noted between the two LVH groups [88]. Others have also demonstrated a difference between LVH and LVH and CHF in the context of high energy phosphate metabolism but have used the definition of CK forward flux as a marker of this instead of PCr/ATP ratios [88, 89]. These findings confirm the initial findings in animal studies [84, 85]. One of the reasons for this change in metabolism could be the reduction in the enzyme creatine kinase in LVH [85, 88].

Left ventricular hypertrophy (LVH) can be pathological or physiological. In athletes left ventricular hypertrophy is a physiological adaptation where contractility is preserved despite the increase in size. Investigation into high energy phosphate metabolism in this group revealed no difference between athletes and controls without LVH in terms of their high energy phosphate metabolism [90]. These findings, along with the fact that the systolic and diastolic function of the athletes was within the normal range, suggests that it is the functional capacity of the ventricle rather than the size per se, that causes a change in energy metabolism.

1.13.2 Uraemic Cardiomyopathy

Uraemia is associated with left ventricular hypertrophy, as part of a triad called "Uraemic Cardiomyopathy". Hypertension, arterial calcification and fluid overload are associated with LVH but LVH has repeatedly been shown to be an independent risk factor for both cardiovascular morbidity and mortality [11, 91, 92].

Limited information is available about the effect of uraemia on high energy phosphate metabolism but in one study, uraemia was also associated with a reduction in PCr/ATP ratio. However the same study also demonstrated that this was not an irreversible process. In fact following a kidney transplant the PCr/ATP ratio returned to that of normal patients [87].

1.14 Transforming Growth Factor Beta

Transforming growth factor beta (TGF-β) forms part of the transforming growth factor superfamily of cytokines. Other members of this family include activins, inhibins and bone morphogenetic proteins (BMP). Cytokines are defined as signalling molecules that are used in cellular communication and are vital for cell growth, repair and death. TGF-β in particular is involved with cell cycling, tissue repair and when over-expressed it can induce fibrosis. It is for these reasons that it has become a focus of scientific research over the past 30 years and raises the hope of a possible therapeutic target to prevent fibrosis and aid wound healing.

TGF-β was first identified over 25 years ago when it was isolated from platelets by Assoian et Al [93]. It is now known that the first discovered isoform was TGF-β_1. However, TGF-β exists in 3 isoforms in mammals; TGF-β_1, TGF-β_2 and TGF-β_3;all with similar biological actions. The isoforms are 60-80% homologous and are encoded by different genes [94]. All 3 isoforms are synthesised predominantly as homodimers although heterodimers of TGF-β_1 and TGF-β_2 has been identified in pigs [95].

TGF-β_2 was identified a few years after TGF-β_1, when it was isolated from porcine platelets [95], human glioblastoma cells [96] and bovine bone [97]. TGF-β_3 was characterised a year later in 1988 [98]. Two other isoforms (TGF-β_4 and TGF-β_5) have now been identified but have not yet been found in mammals [99]. On this basis they have been disregarded from further discussion in this chapter.

1.14.1 Biosynthesis

All three TGF-β isoforms are synthesised initially as a large protein pre-cursor molecule (390 amino acids in length). This consists of a secretory pro-protein (20-30 amino acids), latent associated peptide (LAP) and an active C-Terminus (112-114 amino acids) [100]. Figure 1.14 provides a schematic diagram of the pre-cursor molecule.

After production, the TGF pre-cursor molecule is processed in the golgi apparatus and the pro-protein removed. Now a biologically inactive form can be formed by the bonding of a TGF-β homodimer to a latency-associated peptide (LAP) homodimer [101] (Figure 1.15). The inactive form can either be secreted alone or with latent TGF-β binding protein. Latent TGF-β_1 cannot bind to TGF- β receptors; it requires activation via removal of the LAP homodimer. The mechanisms for this activation in vivo are not clear but in vitro temporary acidification or alkalinisation, extremes of temperature, or presence of certain cell types (e.g. activated osteoclasts, monocytes/macrophages) are required [102]. It has also been shown that TGF-β can reestablish latency by recombining with its LAP however the conditions and exact mechanisms for this are also ill-defined [103].

The active form is a homodimer of the TGF- β_1 C-terminals linked by 8 of the 9 cysteine residues forming disulphide bonds to produce the characteristic cysteine-knot structure of the TGF superfamily. While the 9th cysteine residues bond to ensure dimeric linkage between the two C-terminals in TGF- β_1 [100].

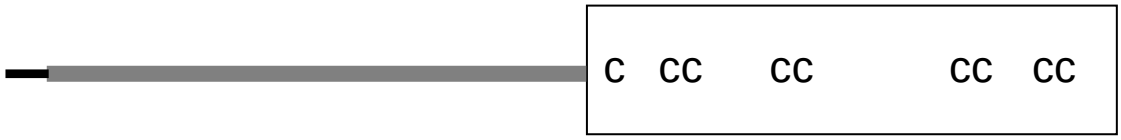

Figure 1.14 **A Schematic Diagram of a TGF-β Pre-cursor Molecule**

The thinner black line represents the secretory pro-protein molecule that is cleaved in the golgi apparatus. The thicker grey line represents the latent associated protein (LAP) and the rectangles represent the C-terminals that later form the active component of TGF-β. The letters “C” within the rectangle represent the nine Cysteine residues present within the C-terminal.

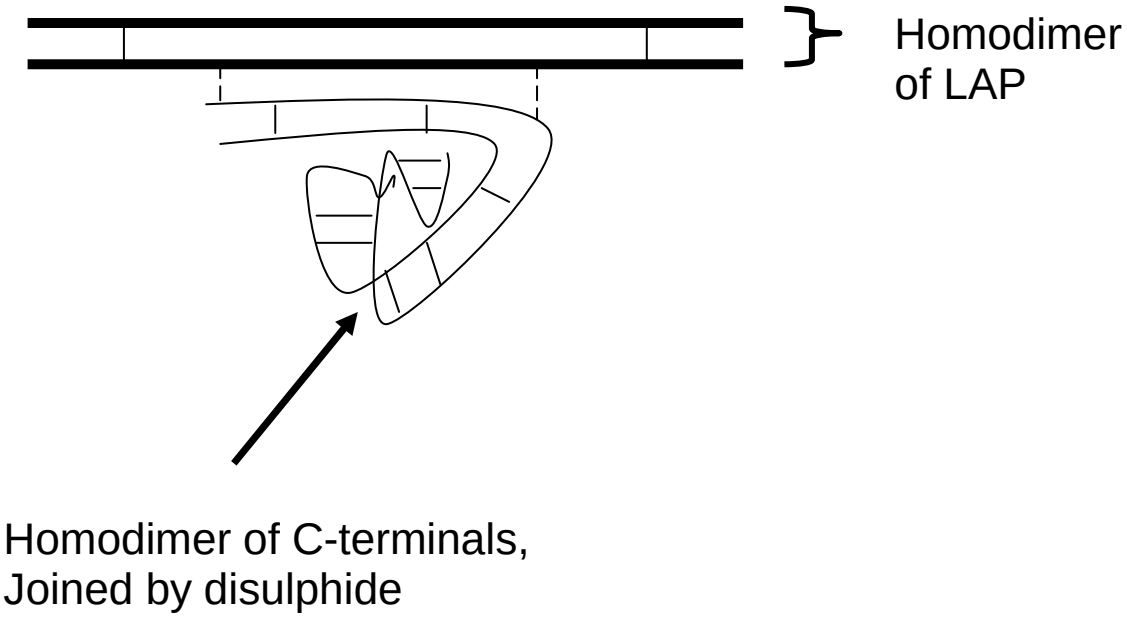

Figure 1.15 **A Schematic Representation of Latent TGF-β.**

This can either be secreted alone or in combination with latent TGF- β binding protein (LAP).

1.14.2 Expression of TGF-β_1

Most tissues within the body secrete and/or express one or more of the TGF-β isoforms. TGF-β_1 was first identified in platelets and it is here that the highest concentrations have been identified (especially in human placenta; 20mg/kg) [94]. In cardiac tissue; fibroblasts, myocytes, macrophages, lymphocytes and platelets have all been shown to release TGF-β_1 [104].

1.14.3 TGF-β Receptors

TGF-β_1 and TGF-β_2 have been found to bind to 3 cell surface receptors; Type I, II and III. Type I and II are transmembrane serine threonine kinases classified by weight (55 kDa and 70 kDa respectively). The Type III receptor is a much larger membrane anchored proteoglycan called betaglycan. Type III receptors have been shown to regulate the accessibility of TGF-β to the Type I and II receptors especially to TGF-β_2 [105, 106]. However Type III receptors are not essential for TGF-β regulation. This has been demonstrated using rat skeletal muscle myoblasts; TGF-β mediated increased extracellular matrix production in these cells despite the absence of Type III TGF-β receptors [107].

Type I and II TGF-β_1 receptors are both required for TGF-β_1 binding; occurring as heterotetrameric compounds that spans the cell membrane [108]. This is because once TGF-β_1 binds to the higher affinity Type 2 receptor; it activates the lower affinity type 1 receptor via phosphorylation. All the intracellular pathways that follow receptor activation have not been fully elucidated, but Smads have been implicated as the dominant pathway. SMADs

are intracellular proteins that act as transcription factors when activated by a member of the TGF-β superfamily. However there are many different SMADs and these have different roles in the transmission of signals from the TGF β superfamily receptor to the nucleus. Smad 2 and 3 form complexes with activated TGF-β receptor complex; are phosphorylated and then released. Once released, they complex with Smad4 and are transported to the nucleus via nucleoporins. Here they act to stimulate gene transcription either directly or in collaboration with other transcription factors [104, 106] (Figure 1.16). Smad 6 and 7 have been identified as inhibitors of this cascade and potentially form part of a negative feedback loop [109-111]. They compete with Smad 3/4 for the binding site of the TGF-β receptor 1 and increase its degradation [111]. TGF-β has also been found to increase Smad 7 transcription leading to the hypothesis that this forms part of a negative feedback loop [112].

Other intracellular pathways activated by TGF-β ligand receptor binding have been indentified but evidence for their exact roles in TGF-β's biological effects are inconclusive. Some of the non-Smad pathways investigated include; ERK1/2 (extracellular signal regulated kinase 1/2, JNK (c-Jun N-terminal kinase) and p38; all of which inhabit the mitogen-activated protein kinase family [106].

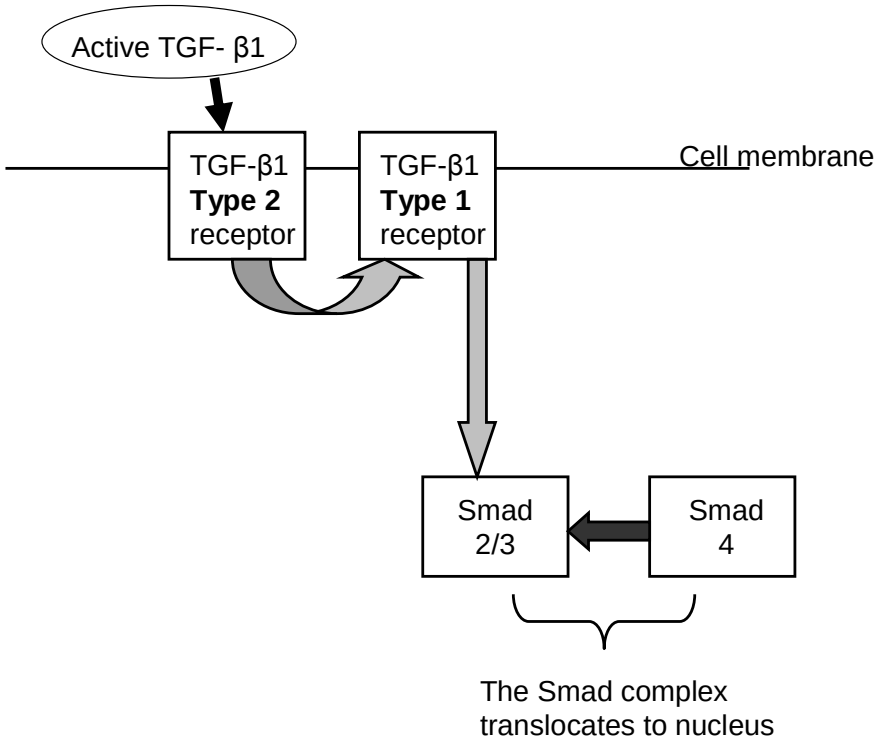

Figure 1.16 **A Schematic Diagram of TGF-β_1 Binding and the Intracellular Smad Pathways that follow.**

Key: The grey arrows represent phosphorylation

The black arrows represent binding.

1.14.4 TGF-β and Fibrosis

TGF-β has been shown to up-regulate many elements of the extracellular matrix that are essential for wound healing. Some of these include collagen (types I and III), fibronectin [113], osteopontin, chondroitin and tenascin [114]. In fact TGF-β_1 is probably one of the most potent stimuli for collagen production being shown to be more potent than platelet derived growth factor, insulin derived growth factor and basic fibroblast growth factor [115]. Under normal circumstances TGF- β_1 production is terminated once tissue healing is complete. However, during fibrosis it is thought that this negative feedback mechanism is altered or damaged allowing over expression of TGF- β_1. The negative feedback pathway has not been fully elucidated as yet but Plasminogen activator -1 (PA-1) (an important inhibitor of extracellular matrix formation) is up-regulated by TGF-β_1 [116]. Also TGF-β_1 has been shown to self regulate its own mRNA expression and protein synthesis demonstrating another possible negative feedback mechanism [108].

A TGF-β_1 knockout mouse has been developed but unfortunately the animals developed generalised inflammation and wasting, and died at about 3 weeks of age [117]. Therefore they were unsuitable for the study of adult rat pathology. Later on an alternative animal model, with over expression of TGF-β_1 in cardiac tissue, was developed (by gene transfer). In these mice, over expression of TGF-β_1 was found to cause cardiac hypertrophy and fibrosis [118]. Other similar animal models have demonstrated a link between over-expression of TGF-β_1 and fibrosis in other organs e.g. kidneys and lung [119, 120]. Evidence to

implicate over-expression of TGF- β_1 as a cause of fibrosis extend beyond the findings described above. Researchers found that an increase in TGF-β_1 levels proceeded extracellular matrix production and fibrosis, and that high levels of TGF-β_1 were found in areas of fibrosis [121, 122]. Mice injected with recombinant TGF-β_1 developed scarring and fibrosis of their hearts, lungs, kidneys, bones, pancreas, thymus and at the injection site [123]. This provides more evidence that TGF- β_1 is a stimulus for multi-organ fibrosis.

1.14.5 The Renin Angiotensin System (RAS) and TGF-β

Angiotensin II is the most studied RAS hormone in the context of TGF-β production and release in the heart. Recent research has discovered that Angiotensin II is a potent stimulator of TGF- β_1 release from rat cardiac fibroblasts [124]. However little is known about the regulation of TGF-β_1 release although prolonged angiotensin II infusion and local angiotensin II production post-infarction have been shown to up-regulate TGF-β_1 levels in rats [125, 126].

Recently research has been conducted examining the effect of aldosterone with respect to TGF- β_1 in humans with chronic kidney disease. This demonstrated a reduction in urinary TGF- β_1 and proteinuria following spironalactone administration. They concluded that spironalactone may have a role in preventing TGF- β_1 mediated renal fibrosis [127]. Further research is required to prove a link between aldosterone, TGF- β_1 and cardiac fibrosis in humans however.

1.15 Aims and Hypothesis

The aims of this project were:

- To examine the relationship between aldosterone and left ventricular hypertrophy in humans
- To determine the long term prognosis of patients with renal dysfunction and a raised renin/aldosterone level
- To examine the association between aldosterone, sodium, TGF-β_1 and cardiac fibrosis in rat ventricle tissue slices.

The hypotheses include:

- High aldosterone levels predispose to left ventricular hypertrophy in the presence of uraemia
- In the presence of renal dysfunction, a raised renin/aldosterone level reduces survival rates
- In the presence of a high sodium level, aldosterone associates with increased TGF-β_1 gene expression, causing increased TGF-β_1 levels and subsequently cardiac fibrosis

Chapter 2: Generic Methods

2.1 Introduction

Three studies are included within this project:

1) **West of Scotland Kidney Disease Study** – A follow-up survival analysis of patients enrolled in a study in the late 1990s, to investigate cardiac disease in patients with chronic renal failure. Any relationship between the renin-angiotensin system and survival/LVH were then examined.
2) **Aldosterone Study** – A side-line project using data from patients enrolled in a PhD cross-sectional prospective study. This project examined the relationship between aldosterone and left ventricular hypertrophy in the presence of uraemia.
3) **Rat Heart Slice Study** – This study included work up of a new technique (within the department) to incubate slices of rat ventricle for subsequent analysis. Following this, the slices were used to examine the relationship between aldosterone, salt and cardiac fibrosis/TGF-β_1 expression.

2.2 Clinical Studies

All patients were recruited from the Western Infirmary Hospital in Glasgow. Ethical and Research and Development approval for the Aldosterone Study was gained by Dr Rajan Patel as part of his PhD project.

Ethics approval for the West of Scotland Kidney Disease (WKD) study was gained at the time of study in the 1990s from the Hospital Ethics Committee [128].

Exclusion criteria for both clinical studies included:

- Those under the age of 18 years old
- Prisoners
- Those unable to give informed consent (e.g. learning difficulties, severe dementia)
- Pregnancy

Specific exclusion criteria for Magnetic Resonance Imaging included:

- Presence of metallic, mechanical or magnetic implants
- Patients unable to lie flat for the duration of the scan
- Claustrophobia preventing insertion in to the scanner
- Abdominal girth larger than the internal diameter of the scanner

Routine investigations preformed at initial research booking visit included:

- Venepuncture – This was performed for routine haematology (full blood count and HbA1c) and biochemistry (urea and electrolytes, calcium, phosphate, albumin, C-reactive protein, glucose, troponin I, parathyroid hormone and lipid profile). Any additional blood was aliquoted, centrifuged and stored at -80ºc within 20mins of venepuncture. This was thawed as

required, for additional specialised investigations, as per the study protocol.

- Renal function was calculated from the serum creatinine using the Cockcroft-Gault formula in the West of Scotland Kidney Disease study and MDRD6 formula in the Aldosterone study.
- Blood pressure – An average of three readings were taken after 10 minutes of rest (seated for the WKD study and supine for the Aldosterone study)

2.3 Echocardiography

Echocardiography was performed by an experienced echocardiographer using an Acuson 128 Siemens machine. Images and data collected were then analysed by a single experienced observer. All dialysis patients were scanned 24 hours after dialysis to ensure comparability and standardization of fluid status. Left ventricular (LV) dimensions and mass were calculated from two-dimensional M-mode images using the American Society of Echocardiography recommendations [129].

The LV mass calculation used was that validated by Devereux and Reichek [130]: LV mass = $1.04 \times [(IVST_d + PWT_d + LVID_d)^3 - LVID_d^3] - 13.6g$. Where $IVST_d$ is the interventricular septal thickness in diastole, PWT_d is the posterior wall thickness in diastole and $LVID_d$ is the left ventricular internal diameter in diastole.

Left ventricular mass index (LVMI) was then determined by indexing the LV mass to body surface area (BSA). Dubois formula for body surface area: BSA = 0.20247 x height(m)$^{0.725}$ x weight(kg)$^{0.425}$ [131]. Based on this calculation we could then determine which patients had LV hypertrophy (LVH). In men LVH was defined as a LVMI of greater than 131g/m^2 and in women as greater than 100g/m^2 [132]. The geometry of the LVH was also calculated and depended on the relative wall thickness (RWT) as classified by the American Society of Echocardiography criteria: RWT = [(2 x PWT_d) / $LVID_d$]. Where PWT_d is the posterior wall thickness in diastole and $LVID_d$ is the left ventricular internal diameter in diastole.

In the presence of LVH, if the RWT was greater than 0.45cm then it was classified as concentric hypertrophy, and if it was less than 0.45cm then it was eccentric hypertrophy.

2.4 Cardiac Magnetic Resonance (CMR)

All CMR images were taken using a 1.5 Tesla Siemens Sonata MRI scanner for the Aldosterone study. Patients were asked to fill in a safety questionnaire prior to entry into the scan room and to remove any metallic objects from their possession.

CMR was performed on a post dialysis day for those on dialysis to ensure standardisation for the same reasons as for echocardiography[2].

2.4.1 Patient Positioning

Patients were positioned head first and supine on the scanner table. A receiver coil was then placed on their anterior chest and strapped in position (to prevent movement during the scan). ECG leads were placed on the patient's chest to allow R wave recognition, enabling ECG-gating throughout. Instructions were given for breath holds (during image acquisition) to reduce respiratory motion artefact.

2.4.2 Image Acquisition

All images were acquired using Siemens technology steady-state free procession (TrueFISP) imaging and were ECG-gated.

Imaging parameters were standardised:

Repetition Time	3.14ms
Echo time	1.6ms
Flip angle	60^{o}c
Voxel size	2.2x1.3x8.0mm
Field of view	340mm

2.4.3 CMR protocol

1. Initially a multi-slice, ECG–gated, localiser image was taken in expiration.
2. Using the localiser image with the best view of the ventricles, a vertical long axis (VLA) image was planned. This was done by lining up the apex of the left ventricle with the mid point of the mitral valve.

3. Next the VLA image was used to plan a horizontal long axis (HLA) view. To do this, a line was drawn through the apex and the midpoint of the mitral valve.
4. From the HLA image, 3 short axis (SA) views were obtained. The 3 slices were planned by drawing a straight line across the atrio-ventricular groove separating the atria and ventricles.
5. Cine images were then acquired in the HLA, VLA, and left ventricular outflow tract orientation using these 3 SA views acquired above.
6. As before the HLA (4-chamber) cine image was used to plan the short axis slices. These were planned as previously described. Once the first SA cine image was acquired further slices (each 8mm deep with a 2mm gap) were performed in the same axis at 10mm intervals towards the apex until the whole ventricle had been covered. (Figure 2.1)

2.5 Image Analysis

A single, experienced, non-blinded, observer (Dr Rajan Patel) analysed all CMR images.

2.5.1 Mass and Function

Epicardial and endocardial borders of the left ventricle, in end systole and diastole, were traced manually from the short axis images. Calculations were then performed using Argus Siemens Software to determine left ventricular mass, left ventricular volumes and ejection fraction. Left ventricular mass and volumes

were indexed to the patient's body surface area. This was calculated using the Dubois formula as in echocardiography.

2.5.2 Definition of Left Ventricular Ejection Fraction (LVEF)

Left ventricular ejection fraction was calculated using the formula below:

$$\textbf{LVEF} = \frac{EDV - ESV}{EDV} \times 100$$

Where EDV is the end diastolic volume and ESV is the end systolic volume.

2.5.3 Definition of Other Left Ventricular Abnormalities

Left ventricular hypertrophy (LVH) is defined as a left ventricular mass index (LV mass/BSA: LVMI) of > 83.3g/m^2 in males and >66.8 g/m^2 in females. LV dilatation is defined as EDV/BSA > 111.7ml/m^2 in males or 99.3ml/m^2 in females or an ESV/BSA greater than 92.8ml in males or 70.3ml in females. These values have been determined from previously published LV dimension data in healthy volunteers and have been used in previous research at our unit [133, 134].

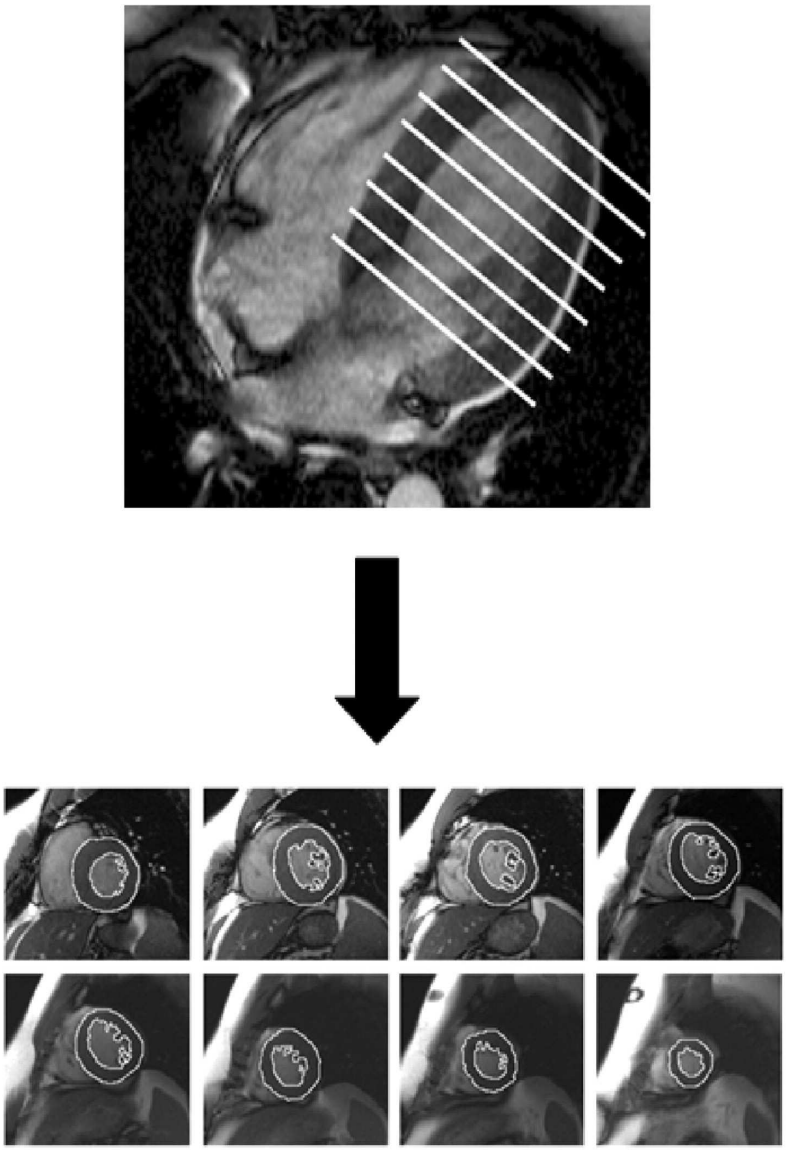

Figure 2.1 **Calculation of LVMI and Ejection Fraction from CMR Images.**

A CMR horizontal long axis view of the heart, with a schematic representation of the position of the short axis cine loop slices. At the inferior end of the arrow are the short axis views, with the epicardial and endocardial borders of the left ventricle delineated.

2.6 Radioimmunoassay for Aldosterone

Serum aldosterone was measured for the Aldosterone study using a (Coat-a-Count, Siemens, Los Angeles) radioimmunoassay. This procedure was closely supervised by a technician trained in the handling and disposal of radioactive substances (Mary Ingram, Glasgow University, BHF building). Serum stored at -80ºc was thawed and 200µl from each sample were alloquoted for assay.

2.6.1 Method

- Reconstitute each vial of ^{125}I Aldosterone (total counts at iodination 40,000cpm) with 110ml of distilled water. Let it stand for 10mins then gently invert to mix.
- Reconstitute the standard solutions; A with 6ml of distilled water and B-G with 3ml of distilled water. (Standar A=0ng/dl aldosterone, B =2.5ng/dl, C=5ng/dl, D=10ng/dl, E=20ng/dl, F=60ng/dl and G=120ng/dl)
- Label seven antibody coated 12x75mm polypropylene tubes “A-G”
- Into each tube, place 200microlitres of the appropriate standard solution
- Label another tube “total count”

- Pipette 1ml of ^{125}I aldosterone into each of the eight tubes and vortex briefly
- Add 200microlitres of the patients thawed serum to the remaining appropriately labeled 12x75 polypropylene antibody coated tubes
- Again, add 1ml of ^{125}I aldosterone to each tube containing patient serum and vortex briefly
- Store at room temperature for 18 hours
- After the 18 hours, remove any excess moisture in the tubes (except from the total count tube). This involves decanting the tubes thoroughly and then using a foam decanting rack to allow the tubes to drain for 2-3min. Then strike the tubes sharply on absorbent paper to shake off all residual doplets.
- Use an automated gamma counter (1470 WALLAC Wizard, GMI, Ramsay, Minnesota, USA) and count for 1minute. Calculate the standard curve, total count and aldosterone levels in the serum samples. Tthe results are in nanograms/decilitre (ng/dl) of aldosterone.
- Calculate, record and appropriately dispose of all solid and liquid radioactive waste to comply with current safety requirements.
- The quoted normal aldosterone values are 4-31ng/dl standing and 1-16 ng/dl recumbent for a normal sodium intake (6-25 µg/day).
- Samples with an aldosterone concentrations above the standard G concentration (i.e.120ng/dl) should be diluted and re-assayed to ensure accurate results or they should be reported as >120ng/dl

2.6.2 Intra-Assay Reproducibility

Reproducibility was demonstrated by repetition of the standard curve solutions within and between different assays, as well as calculation of the standard curve correlation co-efficient (R=1.0 in both of the two assays used). Serum samples with known concentrations of Aldosterone were also used.

Repeat assays of outlier results were performed at 0.5 and 0.25 times the original serum concentration as per the manufacturer's guidelines. The results are shown in Figure 2.2. Unfortunately despite dilution the Outlier 2 results were still >120ng/dl and therefore were likely to be subject to increased error (as such these results were therefore reported as >100ng/dl for the purpose of analysis).

2.7 ECG

As part of the Aldosterone Study a standard 12-lead ECG was taken during the hospital visit by Dr Rajan Patel. It was recorded at 25mm/s and 1mV/cm. During the recording the patient was at 45º and standard lead placement was adhered to. Analysis was also carried out by Dr Rajan Patel (un-blinded). QT dispersal was measured on 3 separate ECG recording and calculated using University of Glasgow, ECG interpretation algorithm (Burdick Atria 6100, US).

2.8 Exercise Tolerance Test

All the patients in the Aldosterone study underwent an exercise treadmill test according to a standard Bruce Protocol. A 12 lead ECG and blood pressure were recorded at rest prior to the test. The ECG recording was then continued throughout the test and the blood pressure was measured at specified intervals and at maximal exertion. The following measurements were used for interpretation: total exercise time achieved, maximal heart rate and systolic blood pressure, ST changes and symptoms limiting exercise. The test was halted if the patients experienced angina, breathlessness, fatigue, dizziness or if there were any of the following ECG changes; ST depression ≥3mm, ventricular tachycardia or fall in blood pressure ≥30 mmHg or a rise in systolic blood pressure ≥230mmHg. The test was considered inconclusive if the patient's heart rate failed to reach 85% of the predicted heart rate before the test was terminated. No medications were stopped prior to undergoing this treadmill test. This test was conducted and analysed by Dr Rajan Patel.

	Original Aldosterone result (ng/dl)	2nd Assay result at 0.25 concentration (ng/dl)	2nd Assay result at 0.5 concentration (ng/dl)
Outlier 1	152.9	65.2 (270.4)	141.2 (282.4)
Outlier 2	617.4	133.7 (534.8)	286.0 (572.0)

Figure 2.2 **Results table containing outlier readings of serum aldosterone concentration, obtained using the aldosterone radioimmunoassay (ng/dl)**

The result in brackets is the calculated original serum concentration of aldosterone in the sample.

2.9 Laboratory Animal Study

2.9.1 Animals

Six Male Wistar-Kyoto control (WKC) rats of 250g were used for the final experiment (however other rats were used initially to refine the technique). These rats were culled and the hearts dissected out, before being placed in calcium free buffer (CFB) solution on ice. The heart was then delivered to the tissue culture laboratory for further processing.

2.9.2 Tissue slices

(All tissue processing and media exchanges were performed in a tissue culture hood using sterile techniques).

Once the heart arrived in the tissue culture laboratory the heart and CFB solution were poured out into a sterile petri-dish and the dish was placed on ice. Initial experiments were performed by dissecting the atria and great vessels from the ventricles using forceps and a microtome blade. The ventricles were then cut into smaller longitudinal sections using the same technique. Unfortunately, this proved very challenging and it was difficult to ensure the slices were thin enough for culture.

In an attempt to improve the situation, the sections were fixed in 4% agarose. This was made by heating 4g agarose in 100ml of CFB solution in a microwave, then cooling the mixture to 37ºC. The roughly cut slices were then gently transferred onto microtome cassettes and the agarose mixture was poured over the top. These cassettes were then placed in the fridge for 30mins for the

agar to set before being cut on a microtome (thickest setting 30µm). Unfortunately the tissue was not rigid enough within the agar to obtain accurate clean slices and therefore another technique was needed.

Finally, a rodent heart slicer matrix was purchased (Zivic Instruments, Pittsburg, USA) that enabled sections of 500microns to be cut in the coronal plane. First a small volume of CFB solution was poured over the top of the matrix to prevent dehydration of the tissue. Then the matrix was placed on a bed of ice to cool it. The heart was then taken out of the CFB solution and placed in the matrix using sterile forceps. Prior to sectioning, razor blades (Zivic instruments, Pittsburg, USA) were then partially inserted into the slice channels, one at a time, such that the blade touched the heart (Figure 2.3). (To remove the atria and great vessels the blades were inserted below the atrio-ventricular groove.) Once all the channels were filled with blades, the blades were then pushed down into the matrix simultaneously. To obtain the slices, all the blades were removed simultaneously between the thumb and ring finger. Once out of the matrix, the uppermost blade was removed to reveal the first slice. The slice was then transposed to the culture well using forceps gently applied to the outermost aspect. This process was repeated until all the slices were removed from the blades.

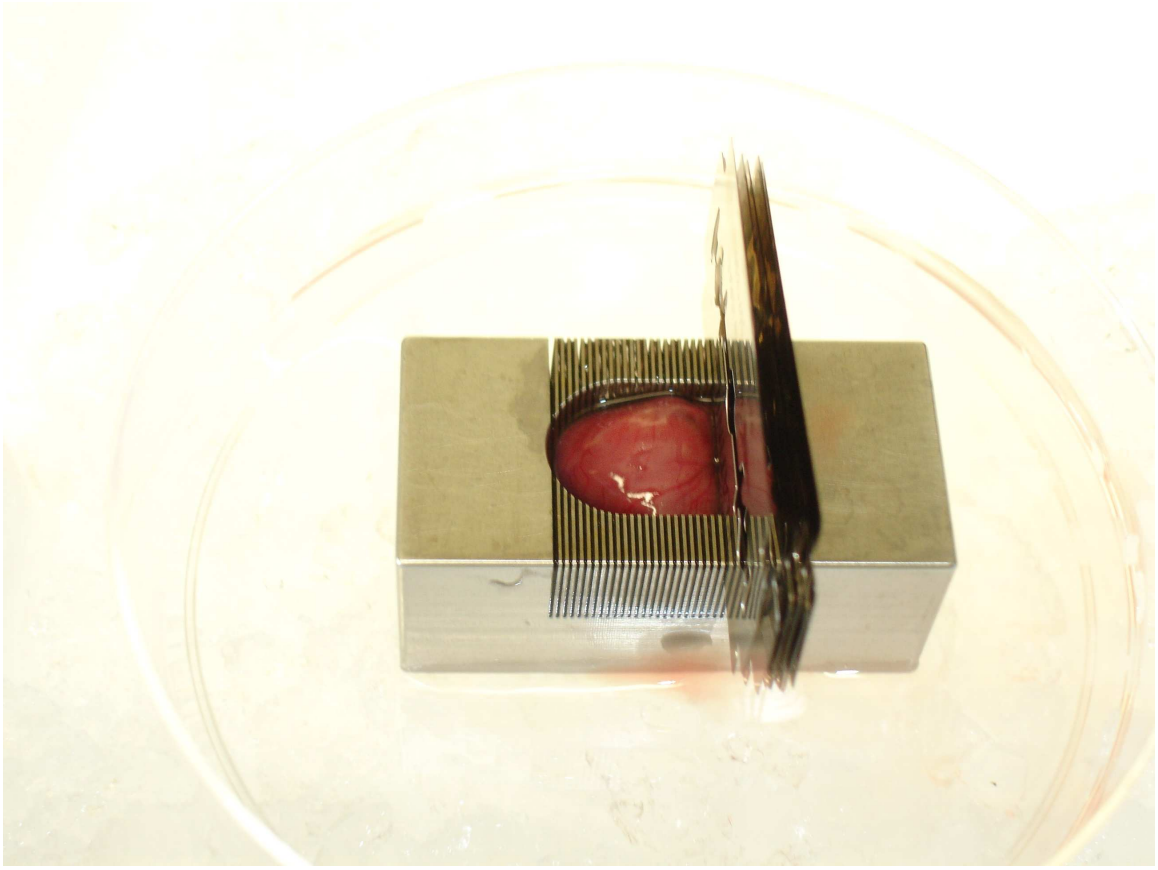

Figure 2.3 **A Rat Heart Photographed during Slicing, within the Heart Slicing Matrix.**

Razor blades are inserted into the slots that are 0.5mm apart.

Since the slices varied in diameter and thickness of the ventricular walls (depending on the level of the section within the ventricle) a weight was taken at the end of culture. Unfortunately this was wet tissue weight because the tissue was need for further processing and could therefore not be dried. The weight of the weigh boat was also taken after the slice was removed so that any fluid remaining on there was not included in the weight of the slice. That weight was then subtracted from the weight of the slice.

TGF beta-1, luminescence and MTT colorimeter measurements were referenced to these weights.

2.9.3 Tissue Culture

Calcium free buffer solution (CFB) was used initially for transfer of the heart from animal to tissue culture hood and while sectioning. Figure 2.4 shows the constituents and prepartation methods of the CFB solution.

The slices were placed in well of media (following sectioning) for incubation. The Media used for heart slice culture was taken from the protocol for cardiomyocyte culture developed by S.G. Baillie, University of Glasgow. The culture media was made using the protocol below:

1. Mix 400ml of DMEM (Invitrogen, Paisley, UK) with 100ml of Media199 (Invitrogen, Paisley ,UK)
2. Remove 75ml of above solution.
3. To the remaining 425ml, add 50ml heat inactivated horse serum and 25ml of heat inactivated fetal calf serum and 5ml of 1% Penicillin/Streptomycin mix.

	mM Strength	Weight(g) per 1 litre (1x solution)	Weight(g) per 500ml (10x solution)
NaCl	120	7.01	35.05
Hepes	20	4.77	28.85
KCl	5.4	0.40	2.0
$NaH_2 PO_4$	0.1	0.16	0.78
$Mg SO_4 7H_2O$	0.8	0.20	1.00
Glucose	5.5	0.99	4.95

Figure 2.4 **Calcium Free Buffer Solution Recipe**

Glucose was added on the day of the experiment.

NaOH was added (at 37˚c) to achieve pH 7.4

The solution was made up in Endotoxin free water and autoclaved prior to use.

During the first few experiments each well of a 6 well plate was filled with 3ml of media; 1.5ml outside and inside the cell culture inserts (0.4µm pore size semi-porous membrane, 30mm diameter, Millicell, Cork, Ireland). The heart slices were placed on top of the membrane inside the inserts. The slices were maintained for 48 hours at 37ºc and 95% air/5% CO_2. This section of the protocol was further developed after an initial trial to reduce the volume of media in each well and consequently increase the proportion of TGF-β produced compared to the volume in the media/serum. Alternative inserts were purchased (0.4µm pore size but 12mm diameter; Millicell, Cork, Ireland) to fit a 12 well plate. 0.4ml media was added to the inside of the insert and 0.6ml outside as per the manufacturer's instructions.

Fetal calf serum and horse serum potentially both contain TGF-β and other cytokines that could interfere with the interpretation of the TGF-β assay and development of fibrosis. Therefore preliminary experiments were carried out to determine if this was an essential component of the media for rat heart slice culture. Unfortunately the slices without the added serum were subjectively noted to be reducing in viability much more quickly than in those with added serum. Published successful rat heart slice culture experiments also reported the use of fetal calf serum in the media [135]. It was therefore deemed essential and the final results were adjusted to take into account the amount of TGF-β in the serum that was added to the media.

2.9.4 Aldosterone Treatment of Slices

A Stock solution of Aldosterone was made up at 10^{-3}moles/l in the media described above. Each rat provided 6 or more suitable slices for culture. In the first 4 rat hearts, 3 slices were cultured in media alone and 3 were cultured with media plus aldosterone 10^{-6}M. (Figure 2.5) Other concentrations of aldosterone (10^{-4}, 10^{-7}, 10^{-11} moles/l) were used for subsequent rat heart slice culture.

2.9.5 Sodium Concentration in the Media

First the sodium concentration of media 199 and DMEM were determined from the manufacturer's information.

Media 199 contained: 26.2mmol/l $NaHCO_3$

117.2mmol/l NaCl

1.01mmol/l NaH_2PO_4

Total Sodium concentration in Media 199 = 144.41mmol/l

DMEM contained: 44mmol/l $NaHCO_3$

109.5mmol/l NaCl

0.9mmol/l NaH_2PO_4

0.4mmol/l tyrosine

0.04mmol/l phenol red

0.99mmol/l pyruvic acid

Total Sodium Concentration in DMEM solution = 155.83mmol/l

In the culture media containing 1 part Media 199 to 4 parts DMEM the sodium concentration was calculated to be 153.54mmol/l. The media was diluted to a concentration of 143.34mmol/l and 133.14mmol/l by the addition of autoclaved, distilled water. These altered sodium concentrations were used, along with aldosterone at 10^{-6}M, in the experiments using the last two rat hearts. In these experiments the slices were cut in half so that for each heart; 3 half slices were treated with media alone; 3 halves with aldosterone 10^{-6}M, 3 halves with diluted media sodium and 3 halves with both aldosterone 10^{-6}M and diluted media sodium.

2.9.6 Obtaining Samples for Tissue Processing and TGFβ-1 Quantification

After 24 hours of culture, the 12 well plates were removed from the incubator. The supernatant from each well was aspirated and collected in labelled epindorfs. These were stored at -80˚c for subsequent analysis.

The media was replaced in each well and the plate was then incubated for a further 24 hours. At the end of the 48 hour incubation the supernatants from each well were again aspirated, collected and frozen in epindorfs. The slices were weighed (as previously described) and then cut in half using a razor blade. One half was fixed in 10% formaldehyde overnight at 4˚C and then (1x) PBS at 4˚C awaiting tissue processing (Shandon Excelsior, Thermo-scientific, USA). The other halves were placed in a reservoir of O.C.T. (a water soluble glycol and resin compound) and then snap frozen at -60˚C using the cryobar in the cryotome

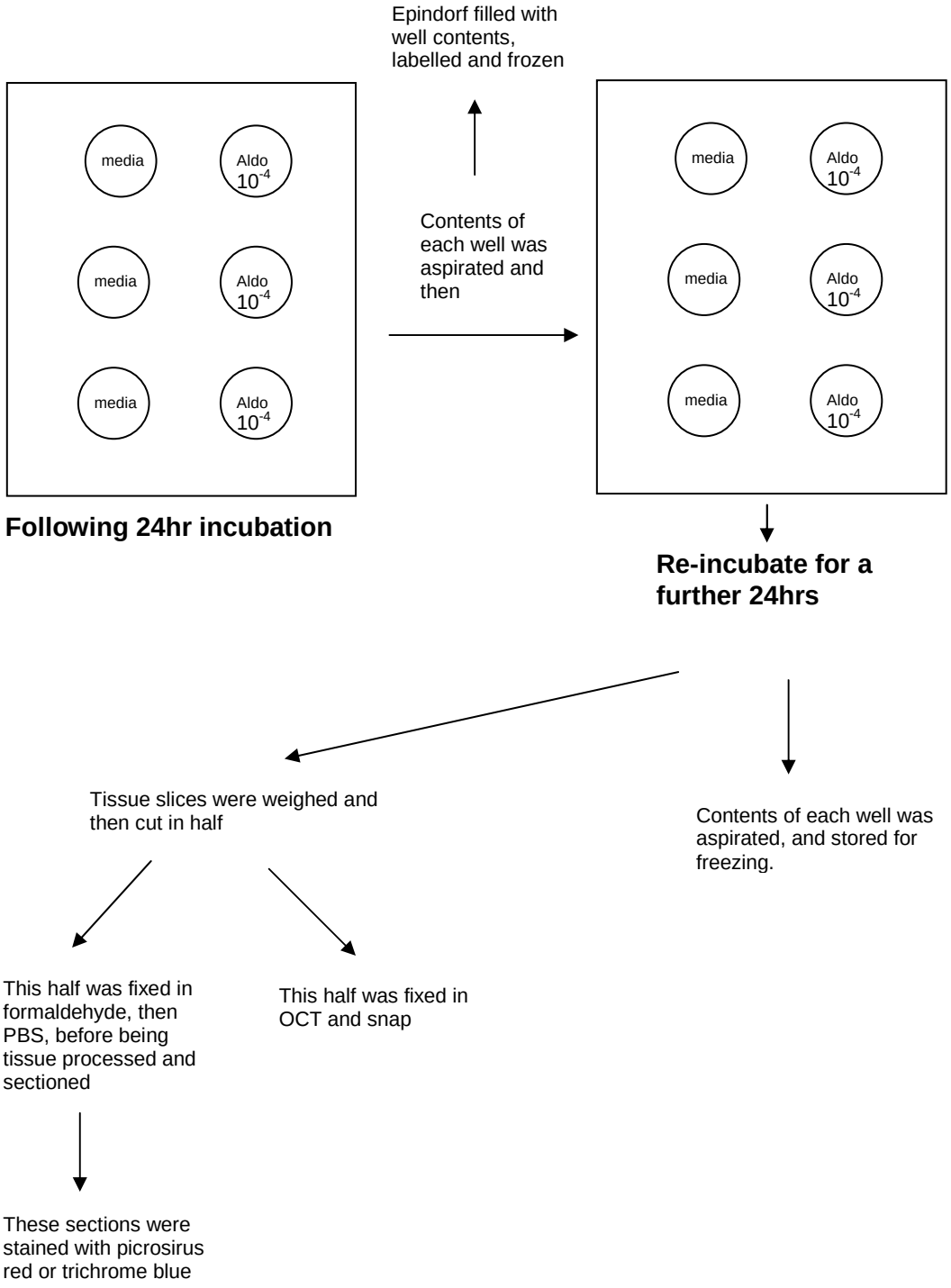

Figure 2.5 **Diagramatic Representation of the Experimental Steps used in the Rat Heart Tissue Culture Experiment.**

(Shandon Cryotome, Thermo Scientific, USA). The cryofrozen samples were then transferred to the -80°C freezer on dry ice for storage. (Figure 2.5)

2.9.7 Silination Method for Preparing Histology Slides

All slides used in this experiment were silinated prior to use to prevent slipping of the tissue section on the slide.

In a fumehood, Container 1 was filled with 7ml APES and diluted with 350ml Acetone. Container 2 was filled with 300ml acetone and Container 3 and 4 with distilled water. Glass Microscope Slides (76x26mm, Menzel-Glaser) were placed in a slide rack and immersed in the first container (APES/Acetone) for 5 seconds. It was then rinsed in acetone for a few seconds before being immersed in Container 3 for 5 mins and then Container 4 for 5 mins. The slides were then placed in an oven to dry at 42ºC overnight.

2.10 Paraffin Sectioning and Staining

Following PBS immersion the formaldehyde fixed heart slices were placed in cassettes and the cassettes labelled. These were then placed in the tissue processor overnight where they were put through a series of washes including formalin, alcohol, xylene and finally wax. Once the processing was complete, the cassettes were removed and placed in a 60ºC wax chamber until they were ready to imbed.

Imbedding involved filling a plastic container with hot wax and then placing a heart slice in the middle. The container was then transferred to a cold spot allowing the bottom layer of wax to set and the heart slice to be held firmly in

position. The cassette was then placed on top of the slice and wax before allowing the wax to set on a cold plate.

Once the wax had set the plastic container was removed and the block was ready to be sectioned on the microtome. The wax block was pared in and then the microtome was set to 5 microns. Sections were delicately cut from each heart slice, before transferring them to a water bath at 40ºC. (The water bath was used to remove any wrinkles in the wax and to wash off any debris on the sections.) The sections were then carefully placed on a silinated microscope slide. Two-three sections of each tissue slice were cut so that more than one stain could be used on each.

In order that the sections could dry and adhere to the slides, they were then placed in an oven at 60ºC for 3 hours and then 40ºC overnight. The following morning the slides were removed from the oven and stained, using the techniques described below.

2.10.1 Picrosirus Red Staining

This stain was used to stain collagen red within the slices, with a co-staining for nuclei using haematoxylin. Each slide was de-waxed and then hydrated with washes of the solutions described below (each for 7 minutes):

- Histoclear
- 100% Ethanol
- 95% Ethanol
- 70% Ethanol
- Distilled water

Next Weigerts haematoxylin (equal measures of Part A and B) was used to wash the slides for 8minutes, followed by a wash in running tap water for 10minutes.

Following this, the slides were stained with picrosirus red for one hour, washed in acidified water (0.86ml of HCL acid in 1 litre of distilled water) for 5 minutes, twice and then tap water for 5minutes, twice.

The slides were then vigorously shaken and blotted dry to remove any excess moisture. In order that the slides were dehydrated, 3 washes of reducing concentrations of ethanol were used for 7 minutes each:

- 70% Ethanol
- 95% Ethanol
- 100% Ethanol

Then histoclear was used for 1 minute, before mounting the cover slip on each slide with histomount. The slides were then viewed under a light microscope to assess the amount of fibrosis present.

2.10.2 Trichrome Staining

Trichrome stain was used to identify collagen within tissue. Three dyes were used; the first stain (Biebrich Scarlet 1%) binds to cytoplasm, muscle and collagen, the second (Phosphotungstic and Phosphomolybdic Acid) allows the collagen (but not the cytoplasm) to lose the Biebrich scarlet stain. The third (Aniline Blue) then stains the collagen blue. Each slide was de-waxed and then hydrated using a number of washes for 7 minutes each:

- Histoclear

- 100% Ethanol
- 95% Ethanol
- 70% Ethanol
- Distilled water

Next the Bouin's solution was heated to 56ºc in a waterbath. Once the slides had finished being de-waxed and rehydrated they were placed in the Bouin's solution for one hour.

Following this they were washed in running tap water for 10 minutes to remove the picric acid (contained within the Bouin's solution). Then they were placed in Weigert's working haematoxylin for 10 minutes before being rinsed again in distilled water. Next the slides were stained using Biebrich's Scarlet for 2 minutes. They were then rinsed in distilled water prior to staining in Phophotungstic/phosphomolybdic acid for 10 minutes. The next stain used was Aniline Blue which the slides were placed in for 5 minutes. They were then rinsed in distilled water, placed in Acetic acid (1%) for 3 minutes and rinsed again. The slides were then dehydrated using two 7 minute washes of 95% ethanol and two, 7 minute washes of 100% ethanol. Finally, the slides were placed in histoclear for 1 minute. The slides were then ready for mounting with coverslips; using histomount.

2.11 TGF Beta-1 Gene Expression - Polymerase Chain Reaction (PCR)

2.11.1 Primers

- **TGFβ-1 primer** (TGF 1) – 20 bases

Forward – 5'- TGA GTG GCT GTC TTT TGA CG -3'

Reverse – 5'- TTC TCT GTG GAG CTG AAG CA -3'

This was designed using the program Primer3 (http://www.embnet.sk/cgi-bin/primer3_www.cgi) and was made from the known sequenced DNA for rat TGF beta 1 (Genebank; accession number NM_021578). Product size – 182 base pairs

- **TGFβ-1 primer** (TGF 2) – 20 bases

Forward – 5'- TGC TTC AGC TCC ACA GAG AA -3'

Reverse – 5'- TGG TTG TAG AGG GCA AGG AC -3'

- **Glyceraldehyde 3-phosphate dehydrogenase** (GAPDH) – 20 bases

Forward – 5'- ATG GGA AGC TGG TCA TCA AC -3'

Reverse – 5'- GTG GTT CAC ACC CAT CAC AA -3'

The above 2 primers were designed by VH Bio, Gateshead, UK.

2.11.2 Obtaining RNA from Heart Tissue

Initially spare atrial tissue was used to optimise the PCR conditions. All the steps in this method were carried out at room temperature. First of all the tissue was minced roughly with a microtome blade and then sonicated. A tissue

homogeniser was used following sonication to further breakdown the tissue. Once broken down, 1ml of tri-reagent was added and repeated pipetting was used to lyse the cells. This mixture was then incubated for 5mins. Next 0.2ml of chloroform was added and the mixture was shaken vigorously for 15seconds. This was incubated for a further 2-3minutes. Following this the mixture was centrifuged at 12,000rpm for 15minutes and the aqueous phase transferred to a fresh epindorf tube. To precipitate the RNA, 0.5ml of propan-2-ol was added to the epindorf and incubated for 10mins. Further centrifugation was then required at 12,000rpm for 10mins to collect the RNA pellet from the aqueous solution. The supernatant was removed and the pellet washed with 1ml of 70% Ethanol. The contents of the epindorf were then vortexed and centrifuged at 7000 rpm for 5minutes.

The ethanol was then removed and the pellet left to dry. Once dry, 30µl of Rnase free water was added and heated to 55-60ºc for 5minutes to allow the RNA to dissolve. A nanodrop was used to quantify the RNA within the sample. If the solution contained more than 1ng/µl then the mixture was diluted down to 1µg/µl using R-nase free water.

2.11.3 First Strand cDNA synthesis

Moloney-Murine Leukaemia Virus Reverse transcriptase (M-MLV RT) kit was used (Invitrogen,Paisley, UK) for cDNA synthesis.

2µl of each gene specific primer (3 pairs) were used, along with 1µl of 10mM dNTP mix, 1µl RNA and 6µl R-nase free sterile water was added to an R-nase free epindorf. Total reaction volume was 20µl.

The mixture was then heated to 65ºc for 5minutes before quickly chilling with ice. The content of the tube was then briefly centrifuged before 4µl of 5x first strand buffer, 2µl of 0.1M dithiothreitol (DTT) and 1µl of RNase Out Recombinant Ribonuclease Inhibitor (40units/µl) were added.

This mixture was then mixed gently, prior to heating to 37ºc for 2 minutes. Next 1µl (200units) of M-MLV RT was added and mixed by gently pipetting up and down. Then the mixture was incubated at 37ºc for 50mins and then 70ºc for 15mins to halt the reaction.

2.11.4 PCR

Go-Taq Flexi DNA Polymerase kit was used initially (Promega, Madison, USA). Using sterile nuclease free PCR tubes the solutions detailed in the Figure 2.6, were added at room temperature. Once all the contents of the tube were added, the mixture was gently mixed by repeated pipetting and then briefly centrifuged. The tubes were then placed in the thermal cycler (PTC-100 programmable Thermal Controller, MJ Research Inc, USA). (Figure 2.7) Once thermal cycling had finished and the reaction was stored at 4ºC the cycler was switched off and the samples removed and stored in the fridge until the PCR gel was set up.

Component	Final Volume
5x Green Go-Taq buffer	5 µl
dNTP mix (10mM)	0.5 µl
Reverse Primer	0.75 µl
Forward Primer	0.75 µl
Go-Taq enzyme	0.75 µl
DNA	1 µl
Nuclease free water	16.25µl (this volume is varied to make up total volume)
Total volume	25 µl

Figure 2.6 **Ingredients for PCR of Rat Heart DNA**

Step	Temperature (ºC)	Time	Number of Cycles
Initial denaturation	94	5 mins	1
Denaturation	94	30 secs	30
Annealing	Variable (50-59)	45 secs	30
Extension	68	1 min	30
Soak	4	indefinitely	1

Figure 2.7 **Thermal Cycling steps for PCR**

2.11.5 Optimisation

To optimise the experiment DNA with and without Reverse Transcriptase was used. In addition $MgCl_2$ was added at differing concentrations (2.5mM, 5mM and 7.5mM), DMSO (1.25µl) and differing volumes/concentrations of DNA were used. The volume of nuclease free water was calculated in these reactions to make the final volume of 25 µl.

The annealing temperature was also varied to include 50ºC, 56ºC and 59ºC. The optimal conditions discovered were an annealing temperature of 59ºC and the addition of 2.5mM $MgCl_2$ and 1.25 µl DMSO to the reaction mixture.

2.11.6 Running a PCR Gel

The gel was made using 40ml (1x) TAE buffer and adding 0.8g agarose. The mixture was then heated in a microwave until fully dissolved. Ethidium Bromide 4µl was then added and mixed. Before the agar set, it was poured into a prepared gel tray, the larger bubbles were pushed to the bottom of the gel and a comb was inserted at the top end to form wells within the gel.

This was allowed 20-30minutes to set before the comb was gently removed and the gel placed into the electrophoresis bath (filled with just enough TAE buffer to cover the wells and gel).

To load the wells, 15µl of the reaction mix was pipetted into each well sequentially. However the first well was left for the 100kbp DNA ladder and loading dye (5 µl of each).

Once all the samples had been loaded onto the gel, an electrical current was run through the solution at 100volts.

Electrophoresis was stopped when the fastest moving dye had moved half way down the gel or the bands had separated out sufficiently. The gel was then viewed in UV light.

A photo of the gel was then taken (Fluor-S multi-imager, Bio-Rad, USA) to record the results.

2.11.7 Real-time PCR

- DyNAmo SYBR Green qPCR kit (Finnzymes, Espoo, Finland).
- PerfeCta SYBR Green Fastmix for iQ (Quanta Biosciences, California, USA).

Instructions for real-time PCR for this enzyme master mix are detailed in Figure 2.9. Using sterile nuclease free PCR tubes the constituents of Figure 2.8 were added at room temperature from the kits provided. The tubes were then placed in a thermal cycler using the steps indicated in Figure 2.9.

Component	Final Volume
Master mix (2x)	10 µl
Reverse Primer	0.75 µl
Forward Primer	0.75 µl
DNA	1 µl
Nuclease free water	7.5 µl (this volume is varied to make up the total volume)
Total volume	20 µl

Figure 2.8 **Ingredients for real time PCR of Rat Heart DNA**

Step	Temperature (ºC)	Time	Number of Cycles
Initial denaturation	95	15 mins	1
Denaturation	95	30 secs	35
Annealing	59	30 secs	35
Extension	72	15 secs	35
Soak	4	Indefinite	1

Figure 2.9 **Thermal Cycling Steps for real time PCR**

2.11.8 Optimisation of Realtime PCR

Differing concentrations of $MgCl_2$ (1.5M in buffer - 7.5M), DMSO (0-1µl/reaction) and DNA (1-5µl) were used.The experiments were repeated using mRNA obtained from Rat's Blood buffy coat because it was thought that white blood cells would contain a larger volume of TGF beta 1 mRNA. However none of these alterations to the protocol provided any benefit.

2.12 TGFβ-1 ELISA

(TGFβ-1 mouse/rat/porcine/canine, Quantikine, R&D systems, Minneapolis) Cell culture supernatant was used for TGFβ-1 quantification. First activation of latent TGFβ-1 to immunoreactive TGFβ-1 was achieved by acidification of the supernatant with Hydrochloric acid (1N) followed by neutralisation with HEPES (0.5M) /Sodium Bicarbonate (0.5M) solution. After this the samples were immediately assayed on the Elisa plate.

This protocol is taken from the manufacturers guidelines:

1. Cell culture supernatant samples were defrosted and all reagents brought up to room temp.
2. The TGFβ-1 control was reconstituted with 1.0ml of deionised water.
3. 25ml of wash buffer was added to 600ml of deionised water (to make 625ml)
4. 20ml of calibrator diluent RD5-53 was diluted in 60ml of deionised water (to make 80ml of 1x solution)

5. TGF standard was reconstituted with 2.0ml of calibrator diluent RD5-53 (1x). This was mixed and allowed to stand for a minimum of 5 minutes with gentle mixing prior to making dilutions
6. To 350µl of supernatant 70µl was added of 1N HCL and mixed well
7. Then incubated for 10mins at room temp
8. The reaction was then neutralised by adding 45.5µl of 1.2N NaOH / 0.5M HEPES
9. Preparation of the standard solutions:

   200µl of the calibrator diluent RD5-53 (1x) was pipetted into a polypropylene tube with 200µl of water in it, mixing well. 200µl of that reaction was then aspirated and transferred to the next tube with 200µl of water in it. This dilution of 1:1 was completed when 6 tubes were filled. The original calibrator solution (served as a zero standard) and the diluent RD5-53 as a high standard.
10. Next 50µl of Assay Diluent RD1-21 was added to each well
11. Then 50µl of Standard or activated sample was added and repeated in triplicate. The plate was then gently tapped for one minute.
12. This was incubated for 2hrs at room temp
13. Each well was aspirated and washed, repeating the process three times using wash buffer (400µl). Complete liquid removal after each step is important. After the last wash any remaining buffer was removed and the plate inverted before blotting it against clean tissues.

14. Next 100µl of TGF conjugate was added to each well, covered with an adhesive strip and incubated for 2 hrs at room temp.
15. Equal volumes of the colour reagents A+B were then mixed together and used within 15 minutes (protected from light).
16. Step 13 was then repeated
17. After the final wash cycle, 100µl of substrate solution was added to each well and then incubated for 30mins at room temp in the dark.
18. Then 100µl of stop solution was added to each well. One the every well had stop solution added the plate was gently tapped to ensure mixing.
19. The optical density of each well was then determined within 30 mins using microplate reader set at 450nm.
20. A standard curve was calculated from the readings for the different standard concentrations.
21. The concentration of each sample was calculated from the standard curve and then multiplied by the dilution factor 1.3. All concentrations were then referenced to the weight of the slices.

2.13 Determination of the Viability of the Incubated Ventricular Tissue Slices

2.13.1 MTT assay

3-(4, 5-dimethylthiazol-2-yl)-2, 5-diphenyl tetrazolium bromide was used as a biological marker to detect living cells. MTT is cleaved only by active mitochondrial dehydrogenase enzymes and has been shown in other studies to reliably predict cell viability [136].

Tissue slices in media were treated at 0 hrs, 24 hrs and 48hrs of incubation with 20µg/ml of MTT. After treatment with MTT, the slices were incubated for a further 4 hours at 37ºC and 5% CO_2 /95%air, prior to assaying.

Since the media contained phenol red, and this interfered with the wavelength recorded during the assaying process, it was removed after incubation was complete. It was replaced with 1ml of calcium free buffer solution and 1ml isopropanol. The solution was then vortexed for 2 minutes; shaken to ensure thorough mixing, and then left to stand for 10 minutes to allow the cleaved MTT to dissolve out of the slice. Once the 10minutes were up, 200µl of the solution was added to 3 wells of a 96 well plate. Another 3 wells were filled with 100µl of isopropanol and 100µl of CFB as a control.

A 1420 multilabel counter (Wallac, Victor^2, PerkinElmer Life Sciences, USA) was then used to detect wavelengths of 540nm. The absorbance readings were referenced to weight of the slice in an attempt to standardise the assay for

the size of the slice and therefore give a rough estimate of the number of cells assayed.

2.13.2 Cytotoxicity Luciferase Assay

Cytotox-Glo Cytotoxicity assay (Promega, Wisconsin, USA) was used to detect dead cell protease activity. Dead cells leak proteases which cleave luminogenic AAF-Glo substrate. Once cleaved, aminoluciferase is released, which results in luciferase-mediated production of photons [137]. A lysis reagent is then added to determine the photon production after 100% cytotoxicity and therefore the proportion of initial dead cells in relation to the number in the total sample.

The method described in technical information provided by promega was for cell lines and therefore needed to be adapted [137]. The un-adapted method is detailed below:

1. Warm all the assay components in a waterbath at 37ºC
2. Add 5ml of Assay buffer to AAF-Glo substrate bottle
3. To prepare the lysis reagent; 33µl of digitonin is added to another 5ml of Assay buffer. This is then mixed well.
4. Harvest adherent cells, wash in fresh medium and re-suspend in new medium (without phenol red indicator)
5. Count the number of viable cells using a haemocytometer and trypan blue
6. Dilute to desired cell density
7. Add 100µl of medium and cells at desired density to each well
8. Add 50µl of CytoTox-Glo assay reagent prepared earlier to each well

9. Incubate at room temperature for 15 minutes and then measure luminescence
10. To determine the luminescence if all the cells were lysed; 50µl of lysis reagent is then added to each well and incubated for a further 15 minutes at room temperature
11. Luminescence was then re-measured in the same samples

However since this experiment used tissue slices rather than cell lines we needed to determine the effectiveness of the assay in our samples. We tried adding collagenase to the slices, to break down the extracellular support thereby breaking the slice down to its constituent cells before adding the CytoTox-Glo reagent. The idea behind this was to see if this improved the sensitivity of the test and because then we would be able to determine the viable cell count in the wells. Slices were treated with 100µl of collagenase type 1 at 400units/ml and then pipetted up and down gently. A 10µl sample of this solution was taken and 10µl of trypan blue was added. A haemocytometer was used to detect the number of viable cells after collagenisation (i.e. the number that did not turn blue). 20µl of the rest of the solution was added to each well to be assayed. 80µl of PBS was added to make a total volume of 100µl. 50µl of CytoTox-Glo assay reagent was then added and incubated for 15minutes at room temperature. 50µl of lysis reagent was added to the same wells. Incubated again for 15 minutes and then luminescence read again. Results indicated no significant increase in the

signal after 100% lysis indicating that collagenisation probably caused considerable lysis in itself. This was also confirmed using the haemocytometer and trypan blue exclusion where most of the cells were non-viable prior to lysis reagent addition. Since there was insufficient time to further optimise collagenisation of the samples it was decided that we would use the previous method without collagenase addition for this experiment.

Without breaking down the slice in to its constituent cells, we were unable to count the number of viable cells prior to the first part of the assying process. It was decided that the slices would be assayed whole and then the result would be referenced to the weight of the slice.

First the slice was washed twice in PBS (to remove any proteases on the surface of the cells and to remove any remaining phenol red). Next, the slice was added to 500µl of PBS in an epindorf. 250µl of the Cytotox-Glo assay reagent was then added to the epindorf. This was incubated for 15minutes at room temperature before 150µl of the reaction was pipetted into 2 wells of a 96 well plate.

Then 150µl of lysis reagent was added to the slice and remaining solution and again the mixture was incubated for 15minutes at room temperature. At the end of the 15 minutes, 200 µl of reaction mixture was added to 3 new wells of the 96 well plate and luminescence read again. Luminescence was read using the 1420 multilabel counter (Wallac, Victor^2, PerkinElmer Life Sciences, U.S.A.) described in the MTT assay methods. The protocol was

changed though, to read luminescence and to read each well for 5 seconds, and then calculate the count per second.

Chapter 3: West of Scotland Kidney Disease Study

3.1 Introduction

Renal failure markedly increases the risk of cardiovascular disease and in particular sudden cardiac death. Alongside this, it has also been determined that cardiovascular disease in renal failure differs from that in the general population. The term uraemic cardiomyopathy incorporates three; often distinct, but sometimes overlapping pathologies that have been indentified in this group. These are left ventricular dilatation, left ventricular hypertrophy and left ventricular systolic dysfunction.

Rat studies have found that aldosterone causes left ventricular hypertrophy in the absence of hypertension. It also causes an increase in fibrosis by increasing for example myofibroblasts and collagen production.

The role of the RAS in human uraemic cardiomyopathy is not fully understood. However, data in the hypertensive population demonstrates an association between left ventricular mass index and serum aldosterone levels. Further evidence for this link comes from a study of patients with Conn's disease (hyperaldosteronism). These patients have been found to have a higher incidence of left ventricular hypertrophy than other hypertensive groups e.g. essential hypertensive and patients with cushings syndrome [138].

Left ventricular mass index has even been shown to regress with spironalactone treatment in early chronic kidney disease patients [139].

3.2 Aims

A study performed in the late 1990s investigated electrocardiographic abnormalities in uraemic cardiomyopathy [128]. Using this database of patients with known chronic kidney disease, dialysis treatment and renal transplant recipients; our aim was to determine the relationship, if any, between the renin-angiotensin system and left ventricular hypertrophy, survival or progression to renal replacement therapy. Confounding factors for determination of left ventricular mass index, rate of renal progression, survival, renin and aldosterone levels were also investigated.

3.3 Methods

3.3.1 Patients

Patients were recruited from the Western Infirmary Renal Unit in Glasgow between 1998-9. The study design was a cross-sectional study of non-diabetic renal disease patients. Patients were identified and then grouped depending on their renal function and renal status (i.e. transplant, currently undertaking dialysis or chronic kidney disease). The group of patients classified as “chronic kidney disease” included patients with near normal renal function to those who were pre-dialysis. Sub-groups of Chronic Kidney Disease (CKD) were then formed using

quartiles formed from the range of renal function (Quartile 1 having the best renal functions) :-

Quartile 1(Q1) - serum creatinine (Cr) less than120µmol/L

Quartile 2 (Q2) – serum Cr 120-200µmol/L

Quartile 3 (Q3) - serum Cr 200-400µmol/L

Quartile 4 (Q4) – serum Cr greater than 400µmol/L.

Patients within each group were mailed randomly to establish contact and then gain consent. Exclusion criteria included those listed in the chapter 2, in addition to the presence of known diabetic nephropathy, overt heart failure and coronary heart disease. By the end of this process 188 CKD (n=47 per quartile), 55 haemodialysis (HD) and 53 transplant (Tx) patients were recruited.

3.3.3 Measurements

On entry into this study all patients underwent echocardiography, clinic blood pressure, ECG and height and weight measurement. Venepuncture was then performed after 30minutes rest, to obtain blood for haemoglobin, routine biochemistry, aldosterone and plasma renin concentration analysis. Also, a questionnaire was completed to gather information about drug and past medical history. All investigations were completed over the course of one day and in dialysis patients this was done on a day after their regular dialysis session. Unfortunately the time of day that the venepuncture took place was not recorded.

In October 2008, I revisited this database and obtained follow-up data from the electronic renal patient record. I recorded survival data, recent and mid

follow-up creatinine and current renal status (i.e. transplanted, on dialysis). To determine renal progression the latest or last creatinine up to the 10/10/08 was recorded or the last creatinine prior to transplantation/dialysis if applicable. Glomerular filtration rate (GFR) was then calculated using the Cockcroft-Gault formula. In the event that no creatinine was available prior to transplantation or dialysis then an arbitrary figure of 5ml/min GFR was used. Progression rates were then determined prior to renal replacement therapy initiation, death, or the latest creatinine in the records.

Eight patients in the CKD group who started haemodialysis (HD) or who were transplanted (Tx) (7 and 1 respectively) within 1 month of the study starting were reclassified as HD or Tx respectively in the follow up analysis.

3.3.4 Statistical Methods

Parametric data was described using the mean (± standard deviation) and non-parametric using the median (± inter-quartile range). In order to compare outcomes between the six groups, a one-way analysis of variance (ANOVA) calculation was used with a Bonferroni correction. P-values are quoted in reference to the variance from the 1st or 2nd Quartile group of CKD patients.

Correlations between non-normally distributed data were analysed using the Spearman correlation co-efficient. All regression analysis was performed using linear regression with an “enter” method for inputting variables. Kaplan-Meier survival analysis was used to demonstrate any significant differences in survival.

All statistical analysis was performed using SPSS v15.0 (SPSS Inc., Chicago, IL, USA).

3.4 Results

In the CKD groups, follow-up renal status (i.e. dialysis, transplant, CKD) and mortality status was obtained from the electronic patient record. Status was available in all 179 patients however recent creatinine was only available in 167 patients.

In the dialysis (HD) group renal status was available for all patients and survival status was absent in only 2 patients.

Information on transplant patients' death status was missing in 12 patients, perhaps due to the fact that very soon after their transplant operation they are followed up in satellite clinics without access to our electronic database and also due to the increased geographical movement in this group.

The characteristics of each group are shown in Figure 3.1 and 3.2 below. Unfortunately due to the redistribution of 8 CKD patients to the HD and Tx groups (as described above) the distribution of patient numbers, sex and age demonstrated some significant differences. In particular the 4th Quartile of CKD had almost half the number of males than the 1st Quartile. Patients in the 2nd-4th Quartile were also significantly older than those in the 1st quartile. BMI was significantly lower in the patients on renal replacement therapy or transplanted. The distribution of treated systolic blood pressure was found to be similar in each group.

The diastolic blood pressure was also similar, except in the case of the Tx group who had a significantly lower reading. Haemoglobin was found to fall within the groups from Q1 where it was 14g/dl down to 10.9g/dl when they reached dialysis. PTH followed a similar trend but as expected it increased as the renal dysfunction increased. CRP also increased with renal dysfunction. PTH, CaxPO4 and CRP reduced in the transplant group compared with Q4 and the HD group. Another unsurprising result was the demonstration of significantly more patients in Q4 and the HD group who had a history of cardiovascular disease. (Figure 3.1)

Particularly significant were the differences found in ACEI,ARB and BB prescription; CKD patients being prescribed the majority of ACEI/ARBs (35.2% vs 6.5% HD and 18.5% Tx) and transplant patients the beta-blockers (53.7% vs 35.8% CKD and 19.4% HD). (Figure 3.2)

No statistical significant difference was found when comparing any group and the 1st Quartile in terms of aldosterone, total renin, ARR, renal progression/year and 24hr urinary creatinine. (Figure 3.3)

	Q1	Q2	Q3	Q4	HD	Tx
Number	47	46	47	39	62	54
% Male	61.0	58.7	40.4	30.8	59.7	57.4
Age (yrs)	40.7 [10.1]	49.4* [12.4]	49.1* [13.0]	56.9* [12.5]	46.1 [14.0]	41.9 [12.4]
BMI	27.1 [7.6]	25.7 [6.6]	26.0 [6.5]	24.8* [6.4]	23.0* [5.6]	24.4* [6.9]
% Diabetic	2.1	8.7	2.1	5.1	4.8	3.7
% CVD	4.3	0.0	12.8	23.1**	19.4**	13.0
SBP	150.0 [31.0]	140.0 [29.3]	144.0 [28.0]	148.0 [36.0]	148.5 [42.5]	138.0 [21.5]
DBP	84.0 [20.0]	81.0 [16.5]	89.0 [12.0]	78.0 [14.0]	88.5 [25.3]	80.0* [15.3]
Hb	14.1 [2.6]	13.4* [3.1]	11.4* [1.9]	11.1* [1.5]	10.9* [2.7]	12.2* [2.3]
CaxPO4	2.29 [0.68]	2.17 [0.49]	2.63 [0.70]	3.36 [1.00]	4.24* [1.43]	2.22* [0.75]
PTH	3.6 [2.7]	5.4 [4.3]	12.2 [16.2]	31.4* [23.6]	45.6* [50.8]	8.2 [10.7]
CRP	2.2 [2.2]	2.7 [3.3]	3.2 [4.7]	4.0 [4.6]	5.3 * [11.1]	1.9 [2.4]
Alb	43.0 [3.0]	42.0 [4.0]	42.0 [4.0]	41.0* [3.0]	41.0* [4.5]	41.0 [5.0]

Figure 3.1 **Group Characteristics in the West of Scotland Kidney Disease Study**

Key: BMI, body mass index (kg/m^2)
CVD, history of Cardiovascular disease
SBP, systolic blood pressure (mmHg)
DBP, diastolic blood pressure (mmHg)
Hb, haemoglobin (g/dl)
CaxPO4, Calcium and phosphate product (mmol/l)
PTH, parathyroid hormone (pmol/l)
CRP, C-reactive protein (mg/dl)
Q1-4, CKD quartiles 1-4;
Albumin (g/l).

- $p<0.05$ for comparisons with Quartile 1; **$p<0.05$ for comparisons with Quartile 2 (ANOVA with bonferroni correction).

- The interquartile range is quoted in paracentesis.

	Q1	Q2	Q3	Q4	HD	Tx
ACEI/ARB (%)	17 (36.2)	14 (30.4)	19 (40.4)	13 (33.3)	4 * (6.5)	10 (18.5)
BB (%)	9 (19.1)	14 (30.4)	22 (46.8)	19 (48.7)	12 (19.4)	29 * (53.7)
CCA (%)	10 (21.3)	13 (28.3)	13 (27.7)	25 * (64.1)	10 (16.1)	21 (38.9)
Diuretic (%)	5 (10.6)	8 (17.4)	15 (31.9)	19 * (48.7)	8 (12.9)	10 (18.5)

Figure 3.2 **Medication at the Time of Enrolment into the Study.**

Key: ACEI, Angiotensin converting enzyme inhibitor

ARB, Angiotensin II receptor blocker

BB, Beta-blocker

CCA, Calcuim channel antagonist

Diuretic, any diuretic (only 1 patient was taking an aldosterone antagonist).

Percentages are recorded in brackets. * p= <0.05 for comparisons with Quartile 1 (ANOVA with bonferroni correction).

	Q1	Q2	Q3	Q4	HD	Tx
Aldosterone	16.5 [17.7]	19.0 [19.5]	19.5 [39.0]	16.5 [29.8]	15.5 [21.0]	12.0 [4.5]
Renin	17.0 [20.5]	19.0 [34.0]	13.0 [31.0]	10.5 [39.0]	12.0 [33.0]	27.5 [38.0]
ARR	1.1 [2.7]	1.4 [2.1]	1.3 [5.0]	1.6 [3.8]	1.0 [5.0]	1.2 [1.4]
Rate of prog./yr	2.4 [4.4]	2.1 [3.6]	2.8 [3.9]	2.2 [3.1]	n/a	n/a
24hr Urine Prot	0.1 [0.3]	0.2 [1.4]	0.3 [1.3]	0.9 [1.5]	1.7 [4.7]	0.1 [0.1]

Figure 3.3 **Aldosterone and Renin results, Renal Progression Rates and Proteinuria.**

Key: -ARR, Aldosterone renin ratio

-Rate of prog/yr, rate of reduction in Cockcroft-gault GFR per year (ml/min/yr)

-24hr Urine Prot, 24hr urinary protein (g/24hr)

-n/a, not available.

Units: Aldosterone (ng/dl); plasma renin concentration (ng/l).

The interquartile range is quoted in paracentesis.

Renin results were found to be significantly different depending on the use of ACEI ($p<0.001$) and BB ($p=0.002$) in the CKD group. However, Aldosterone levels were not significantly different when comparing the use of any of the groups of medication recorded. When considering the ARR; beta-blockers use was found to be associated with a higher ARR ($p<0.001$).

Although no significant differences were identified between the groups in terms of the presence of LVH or a reduced ejection fraction, a lower proportion of patients in the Tx group had a reduced ejection fraction than the other 5 groups. This was despite the persisting high prevalence of left ventricular hypertrophy in this group. (Figure 3.4) No significant correlations were found between aldosterone, renin or ARR and LVMI in any groups. However a positive correlation was found between systolic blood pressure and LVMI ($R= 0.282$, $p=<0.001$) and between LVMI and rate of progression of renal dysfunction ($R= 0.224$, $p=0.005$) in all CKD patients.

3.4.1 Survival Data

As expected, mortality rates increased with decreasing creatinine clearance and in those patients on dialysis. Those patients, who were transplanted, were found to have improved survival rates compared to those on HD or Quartile 4 CKD. (Figure 3.5)

We attempted to determine risk factors for death in these groups of patients. Neither achievement of blood pressure goals nor the presence of LVH had any significant effects on mortality in these patients. Variables that did demonstrate a trend towards a significant difference in survival were a CRP of

>3.29mg/l in the 3rd and 4th quartile (p=0.26) and a 24hour urinary protein level of ≥1g/day (p=0.023). 1g/day was used as the cut-off level because this level of proteinuria has been shown to be associated with a higher rate of renal progression and cardiovascular disease. An ARR of greater than 1.31 (the median result) in the CKD population showed a trend towards an increased mortality rate although neither renin nor aldosterone levels demonstrated any significant effects.

3.4.2 Correlation with Rate of Renal Progression

No significant correlations were found between aldosterone, renin, ARR or CRP and the rate of renal progression in any groups. However 24 hour urinary protein and BMI were positively correlated with the rate of renal progression (R= 0.187, p=0.024 and R= 0.167, p=0.032 respectively).

Linear regression analysis demonstrated a significant predictive value with diastolic but not systolic blood pressure (R^2=0.018 p=0.046) for the rate of renal progression in the CKD group. None of the medication groups were found to predict renal progression rates including ACEI.

	Q1	Q2	Q3	Q4	HD	Tx
% LVH	86.67	81.82	93.33	87.50	94.74	96.23
% Patients with EF<55%	65.22	68.89	56.52	66.67	66.67	40.00

Figure 3.4 **Left ventricular hypertrophy or an Ejection fraction less than 55% Identified from Echocardiogram.**

Key: LVH, left ventricular hypertrophy

EF, Ejection fraction.

	Quartile of kidney function					
	1	**2**	**3**	**4**	**HD**	**Tx**
No. Dead	0	2	5	11	18	9
% Dead	0.0	4.3	10.6	28.2	29.0	16.7

Figure 3.5 **Table of 10 yr Survival for the West of Scotland Kidney Disease Study patients**

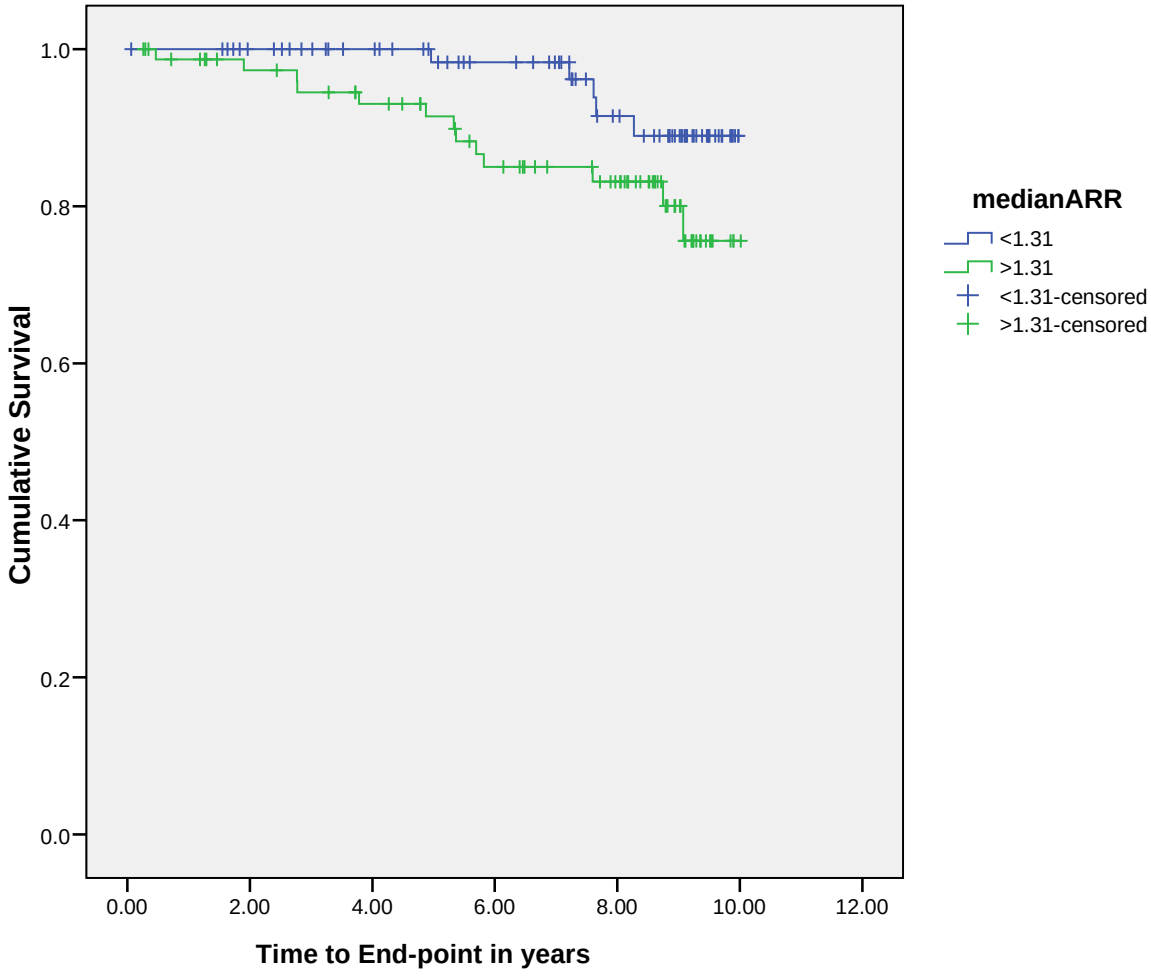

Figure 3.6 **A Kaplan-Meier Survival analysis of the CKD groups based on aldosterone renin ratio (ARR) compared to the median of 1.31ng/dl (p=0.056).**

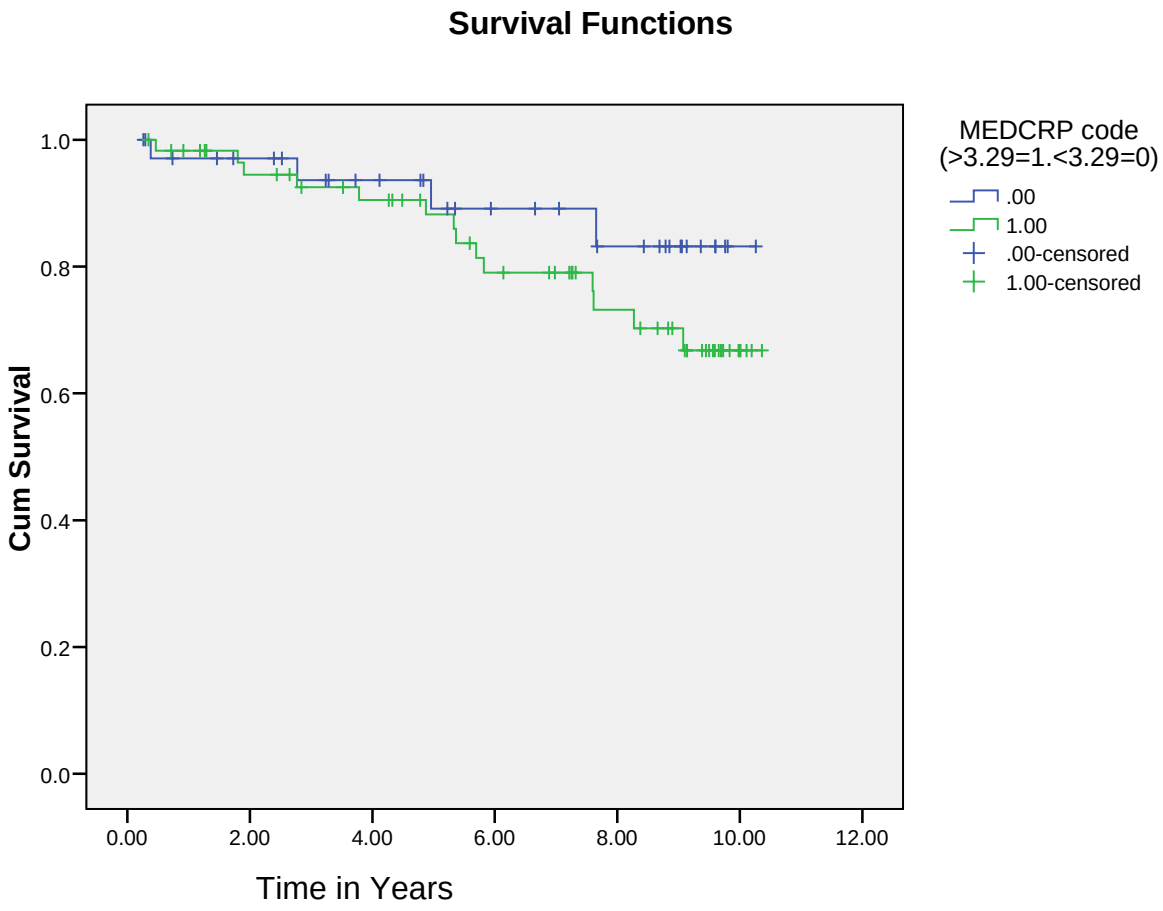

Figure 3.7 **A Kaplan-Meier Survival Curve comparing the mortality rates of patients in the 3rd and 4th Quartile in the context of a CRP greater than or less than the median value of 3.29 mg/l (p=0.26).**

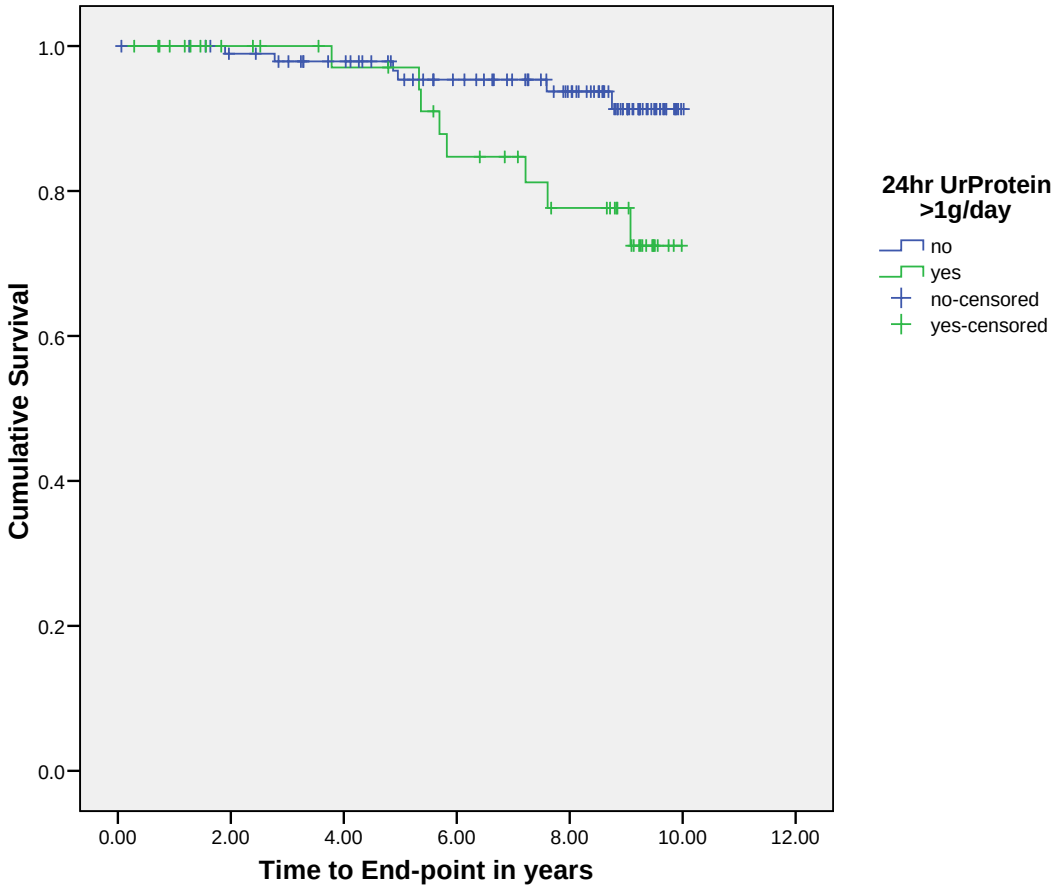

Figure 3.8 **A Kaplan-Meier Survival analysis of all the CKD quartiles based on 24hr Urinary Protein results of > or <1g/24hrs (p=0.023).**

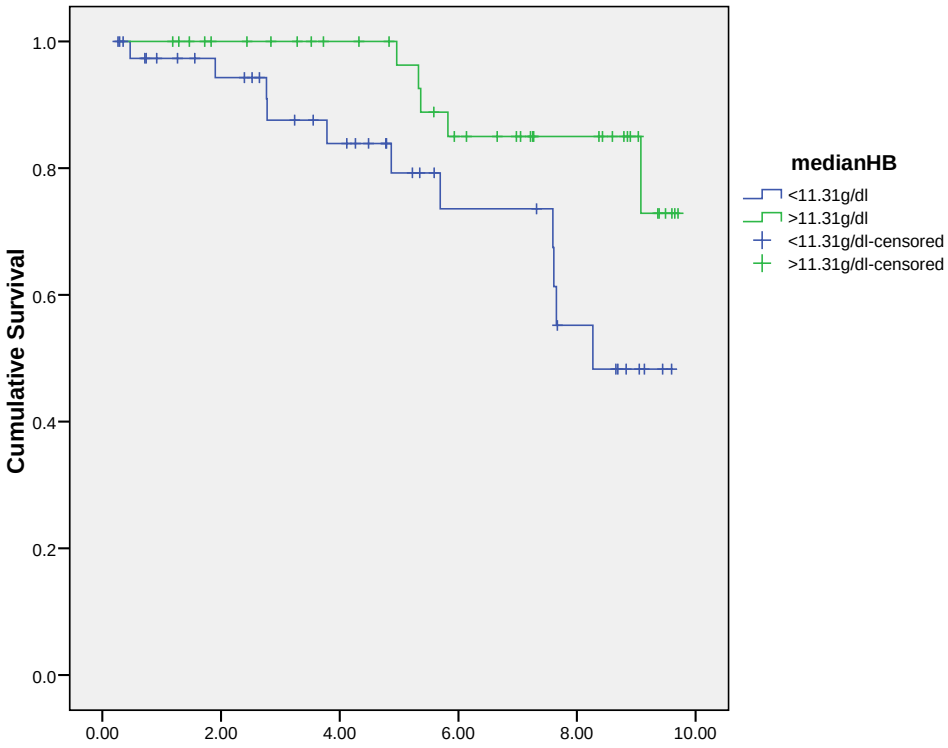

Figure 3.9 **A Kaplan-Meier analysis of CKD Quartiles 3 and 4 with respect to the median Haemoglobin level of 11.31g/dl (P=0.25).**

3.4.3 Electrolyte Levels, Blood Pressure and RAS

ARR was found to be significantly determined by Potassium (K^+) in CKD groups (R^2=0.06 p=0.001) however a potential cofounder was the prescription of Beta-blockers.

Given the mechanisms of aldosterone and renin control it was surprising that no significant determination of Aldosterone or Renin by Na^+, K^+ or systolic blood pressure levels were found.

3.5 Discussion

There has been great interest in the RAS, left ventricular hypertrophy and heart failure. Animal models in particular have demonstrated a link between the RAS, cardiac fibrosis and left ventricular hypertrophy. This interaction has been shown in most studies to be independent of blood pressure.

This dataset describes a selection of patients with a full range of renal dysfunction from very mild disease to end-stage renal failure, dialysis patients and kidney transplant recipients. At the onset and first analysis of this dataset the number of patients in each quartile of kidney function was equal at 47. However, on retrospective analysis, some of the patients in the 4th quartile were started on dialysis or transplanted within a month of being enrolled into the study. Those patients were therefore reclassified as dialysis patients or transplant patients respectively, from the start of this analysis. Unfortunately by doing this

the distribution of age, sex and BMI became statistically different between the different groups.

Since the blood sampling and analysis was performed before this research project, I had no involvement in the initial experimental planning, in particular, the aldosterone measurement. Since we know that aldosterone demonstrates diurnal variation and is affected by posture and salt intake it would, in hindsight, have been preferable to collect a 24hr urinary aldosterone and salt measurement. That way the average aldosterone level would be measured and the effect of the parameters above would have been minimized. No record was made of the time of day the blood sampling occurred so it might have been that some patients attended in the morning and some in the afternoon. These factors are thought to account, to some extent, for the lack of correlation between aldosterone and the other outcome factors measured.

Using the follow-up data, neither renin nor aldosterone was found to correlate with LVMI or influence survival rates in any group of renal dysfunction. However, LVMI, aldosterone and renin levels are also dependent to some extent of the medication patients are taking; in particular ACEI/ARB and BB. A significant proportion of patients especially CKD patients were on ACEI (35.2%) and BB (35.8%). ACEI are known to directly target the renin-angiotensin system and reduce aldosterone and whereas BB reduce renin directly. These findings were confirmed during analysis of this dataset. Age, sex nor BMI affected renin or aldosterone levels. Information about the length of time patients were taking the different medications was not recorded. This information would have been

useful since ACEI have been found in some studies to cause regression of LVH and tolerance to ACEI has been described with subsequent increases in aldosterone [140, 141].

Only 1 patient in this study was prescribed an aldosterone antagonist and no patients were prescribed a renin inhibitor at the time of study in the 1990s. If this study was to be repeated today the proportion of patients on aldosterone antagonists and renin inhibitors might well be significantly higher. These medications are also known to alter the hormone levels in the renin-angiotensin system and would further confound any results.

It is interesting to note that the proportion of dialysis patients on ACEI is significantly lower than CKD patients despite the fact that there is a higher incidence of left ventricular hypertrophy and dysfunction in dialysis patients. This is presumably due to the lack of evidence of mortality or cardiovascular risk benefit of ACEI in dialysis patients and the higher risk of hyperkalaemia in this group.

Previous studies have shown improved renal survival and slowing renal progression with ACEI especially in addition to ARBs. This was not a finding of this study. The reason for this is unclear. The duration of treatment was not classified at the time of study. Perhaps ACEI/ARBs are prescribed too late to slow progression or perhaps the doses of these medications are not high enough to affect renal progression. There is also no reliable way of checking compliance to these medications.

If this study was used as pilot data for a larger study (as proposed), some alterations to the study design or further study prior to starting are suggested. The effects of dialysis and transplantation on renin/aldosterone levels are not yet fully identified but would be worth studying. Quantification of the effect of ACEI/ARB/BB on renin and aldosterone levels at time points during treatment and during dialysis/ transplantation would also be useful. Another possibility is to only enroll patients who are not taking any of these medications although this would probably select out the more cardiovascular fit patients.

A measure of proteinuria and natruriesis would also be useful; proteinuria has been found to be a risk factor for cardiovascular mortality in this population (secondary outcome data) and salt intake has been linked, in animal studies at least, to cardiac fibrosis in the presence of aldosterone.

A relationship between inflammation and survival/cardiovascular disease in renal failure has been observed by other researchers. One of the measures of inflammation commonly quoted is CRP and this is one of the most clinically relevant and available measurements. Approximately 30-50% of dialysis patients have a raised CRP and the majority the have no identifiable cause [142]. The raised CRP has shown to be associated with increased mortality and cardiovascular disease [143, 144]. Our data also supported this link, when the CRP was greater than 3.29mg/dl.

3.6 Conclusion

No quartile of renal dysfunction studied, demonstrated any association between LVMI/survival rates and random aldosterone/renin levels. However the levels of aldosterone and renin were shown to be affected by ACEI/ARB/BB use. Further studies, where patients are not taking these medications and where an average 24hr aldosterone level is measured, are recommended before any association between the RAS and LVMI/survival can be ruled out.

Chapter 4: Aldosterone Study

4.1 Introduction

Aldosterone has been found to be a cause of cardiac fibrosis and left ventricular hypertrophy independent of blood pressure effects both in vitro and in vivo. Recent human study also found a positive correlation between aldosterone and left ventricular mass in patients with hypertension [145]. Left ventricular hypertrophy and the other forms of uraemic cardiomyopathy are well described in end stage renal failure. The recent finding of diffuse late gadolinium enhancement [133] in this group of patients (indicating cardiac fibrosis) also leads us to believe that aldosterone might play a role in it's pathogenesis. However the exact mechanisms for this remain unclear.

Our aim was to perform a cross-sectional prospective study to investigate the relationship between left ventricular hypertrophy (as assessed by cardiac magnetic resonance imaging) and aldosterone in dialysis and pre-dialysis patients.

4.2 Methods

4.2.1 Patients

82 patients were recruited from the Western Infirmary renal unit in Glasgow between 2007 and 2009. 35 pre-dialysis and 47 dialysis (including nine,

peritoneal dialysis) patients being considered for a renal transplantation were enrolled in total. These patients ranged in age from 22 to 78 yrs old.

We were unable to perform an MRI scan on 8 patients due to claustrophobia or ill health. These patients were excluded from further analysis. The other inclusion and exclusion criteria for this study can be found in the methods chapter.

4.2.2 Measurements

Each patient underwent a cardiac MRI scan, blood pressure, exercise tolerance test, ECG, venepuncture and height and weight measurement. All investigations were completed over the course of one day.

Venepuncture was performed prior to the MRI scan and samples were sent for routine biochemistry and haematology laboratory tests described previously. The remaining blood was centrifuged and frozen at -80ºC within 20mins of venesection. Serum brain natriuretic peptide (BNP) was measured using a one step radioimmunoassay (ShionoRIA, Shinogi, Japan) and serum aldosterone levels using the radioimmunoassay (Coat-a-count) described previously.

Patients were interviewed on the day of attendance to determine past medical history and current medication. Details were checked on the electronic patient record in areas of uncertainty.

4.2.3 CMR and Analysis

Cardiac MRI was performed using a 1.5 Tesla MRI Scanner (Siemens Sonata, Erlangan, Germany). In the dialysis patients this was performed on a post dialysis day to ensure standardisation across the group and to minimise the influence of fluid status on our results. Images were acquired as per the protocol described in the methods chapter.

The duration of the MRI scan was approx. 25 minutes for the mass and function images. However, these patients are part of an on-going study and therefore image acquisition was also performed for spectroscopy and flow mapping. The results of these latter two techniques are not included in this study.

4.2.4 Statistical Methods

One patient in the peritoneal dialysis group was found to have a very high aldosterone level of 614µg/dl even after repeating the radioimmunoassay. The reason for this result is unclear. The medication of this patient was reviewed but they were not on any medication known to have this effect. Since this extreme value was likely to skew the data, values above 120 were grouped together.

Parametric data (e.g. age, BMI, systolic blood pressure, SBP; diastolic blood pressure; DBP) was described using the mean and standard deviation. Where the data were non-parametric (e.g. LV measurements, aldosterone) the medians and inter-quartile ranges are quoted instead. The standard deviations or

inter-quartile range for a given value are recorded in square brackets in the following tables.

Interval data e.g. age, LVMI were compared between two groups of patients using the t-test or Mann-Whitney test as appropriate. Values in parentheses represent proportions.

Nominal data e.g. sex was compared between two groups of patients using the chi-squared test.

Correlations between non-normally distributed data were analysed using the Spearman correlation co-efficient.

All regression analysis was performed using linear regression with an "enter" method for inputting variables.

4.3 Results

4.3.1 Baseline Characteristics

A total of 82 patients were recruited in to the study initially however, after exclusions, 33 pre-dialysis and 41 dialysis patients were used for data collection and analysis.

Patient demographics, blood pressure, past medical and smoking history and current drug therapy (Angiotensin converting enzyme inhibitors, ACEI; Angiotensin II receptor blockers, ARB; Beta blockers, BB; Calcium channel antagonists, CCA) are summarised in Figure 4.1. Distribution of primary renal disease between groups is shown in Figure 4.2.

Sex, age, BMI and systolic blood pressure (SBP) were similarly distributed between the two groups. Current treatment with an ACEI or diuretics differed with a higher proportion of patients in the pre-dialysis groups on both of these medications.

We also compared the numbers of patients with a past medical history of macrovascular disease (excluding ischaemic heart disease) and found no significant difference between the two groups. There was a trend towards significance for ischaemic heart disease; with a higher proportion in dialysis patients.

The proportions of current smokers were not statistically different either. Patients were also analysed by their primary renal disease; no significant difference was found between the two groups for any of the categories of primary renal disease.

Aldosterone measurements in both groups were similar (p=0.883). The results are outlined in Figure 4.3.

4.3.2 Cardiac Dimensions and Function

Patients in both groups had a cardiac MRI scan to determine their LV mass and function. The results are recorded below in Figure 4.4; no significant differences were found between the two groups in any of the mass and function measurements taken. Also, no significant difference in the proportions of patients defined as having LVH, LV dilatation or a reduced EF when using the definitions in the methods chapter (Figure 4.5).

	Pre-dialysis	Dialysis	P-value
Number	33	41	
Age (yrs)	54.5 [13.2]	55.4 [12.7]	0.762
BMI (kg/m^2)	27.1 [4.7]	27.1 [4.8]	0.935
Male	23 (69.7)	31 (75.6)	0.572
SBP (mmHg)	148 [22]	145 [22]	0.556
DBP (mmHg)	82 [13]	88 [11]	**0.041**
Current Medication			
ACEI/ARB	21 (63.6)	13 (31.7)	**0.005**
BB	13 (39.4)	17 (41.4)	0.858
Diuretic	16 (48.5)	6 (14.6)	**0.002**
CCA	15 (45.5)	18 (43.9)	0.895
Past Medical History			
IHD	4 (12.1)	12 (29.3)	0.077
CVA	3 (9.1)	3 (7.3)	0.783
PVD	6 (18.2)	8 (19.5)	0.885
CHF	1 (3.0)	3 (7.3)	0.421
HTN	31 (93.9)	38 (92.7)	0.832
Smoking History			
Never	16 (48.5)	22 (53.7)	
Current	9 (27.3)	10 (24.4)	0.779
Ex- smoker	8 (24.2)	9 (22.0)	

Figure 4.1 **Patient Demographics in the Pre-dialysis and Dialysis group.**

Key: ACEI, Angiotensin converting enzyme inhibitor
ARB, Angiotensin II receptor blocker
BB, Beta blocker
CCA, Calcium channel antagonist
IHD, Ishaemic heart disease
CVA, Cerebrovascular disease
PVD, Peripheral vascular disease
CHF, Chronic heart failure
HTN, Hypertension.

The p-values in bold type indicate the p-values that have reached statistical significance.

Primary Renal Disease	Pre-dialysis	Dialysis	P-value
Diabetes	11 (33.3)	8 (19.5)	0.179
Glomerulonephritis	7 (21.2)	12 (29.3)	0.434
PCKD	1 (2.9)	4 (9.8)	0.255
Chr. Pyelonephritis	3 (8.6)	5 (12.2)	0.671
Renovascular	3 (8.6)	4 (9.8)	0.923
Unknown/other	8 (24.3)	8 (19.5)	0.626

Figure 4.2 **A Table detailing the number (proportion in brackets) of each group in terms of their primary renal disease.**

Key: PCKD - Polycystic kidney disease

Chr. - Chronic

	Pre-dialysis	Dialysis	P-value
Aldosterone (ng/dl)	17.8 [16.6]	19.7 [19.6]	0.617

Figure 4.3 **Aldosterone results**

	Pre-dialysis	Dialysis	P-value
Ejection Fraction (%)	64.4 [15.6]	66.0 [14.3]	0.728
EDV (ml)	120.9 [49.2]	112.6 [64.2]	0.572
ESV (ml)	44.9 [22.8]	40.5 [20.7]	0.242
LV mass (g)	154.0 [90.0]	190.4 [112.4]	0.341
LVMI (g/m^2)	85.7 [38.7]	96.0 [49.9]	0.364
EDV/BSA	64.2 [25.0]	57.4 [29.4]	0.358
ESV/BSA	21.9 [14.3]	19.6 [10.8]	0.190

Figure 4.4 LV mass and Function Measurements

Key: EDV, End-Diastolic Volume

ESV, End-Systolic Volume

LV Mass, Left Ventricular Mass

LVMI, Left Ventricular Mass Index

BSA, Body Surface Area

	Pre-dialysis	Dialysis	P-value
LVH	21 (63.6)	29 (70.7)	0.520
LV dilatation	1 (3.0)	3 (7.3)	0.421
Reduced EF	7 (21.2)	9 (22.0)	0.939

Figure 4.5 **Proportions of patients with MRI defined LVH, LV dilatation or Ejection Fraction <55%**

Key: LVH, Left Ventricular Hypertrophy

LV dilatation, Left Ventricular Dilatation

EF, Ejection Fraction

4.3.3 Correlations

No significant correlations were found between aldosterone or log aldosterone and age, BMI, SBP, DBP, Haemoglobin (Hb), C-reactive protein (CRP), Calcium (Ca), phosphate (phos), BNP, troponin, EF, EDV, ESV, LVMI, QT dispersal (QTD) or exercise time in the study population as a whole.

However, Aldosterone was found to be negatively associated with potassium (K) levels (correlation co-efficient -0.310, p= 0.009) (Figure 4.6).

LVMI positively correlated with phosphate (R-square = 0.256, p=0.033 respectively) (Figure 4.7).

Despite previous evidence suggesting an association of LVMI with BP and QTD we found no correlation between LVMI and these variables.

4.3.4 Regression Analysis

None of the variables studied determined the aldosterone levels found in these two groups of patients including ACEI, BB, K, SBP and DBP.

A regression analysis was also performed to determine the factors affecting LVMI; Phosphate levels were significant at a p-value of 0.028 however Aldosterone levels, ACEI nor BB use were not significant.

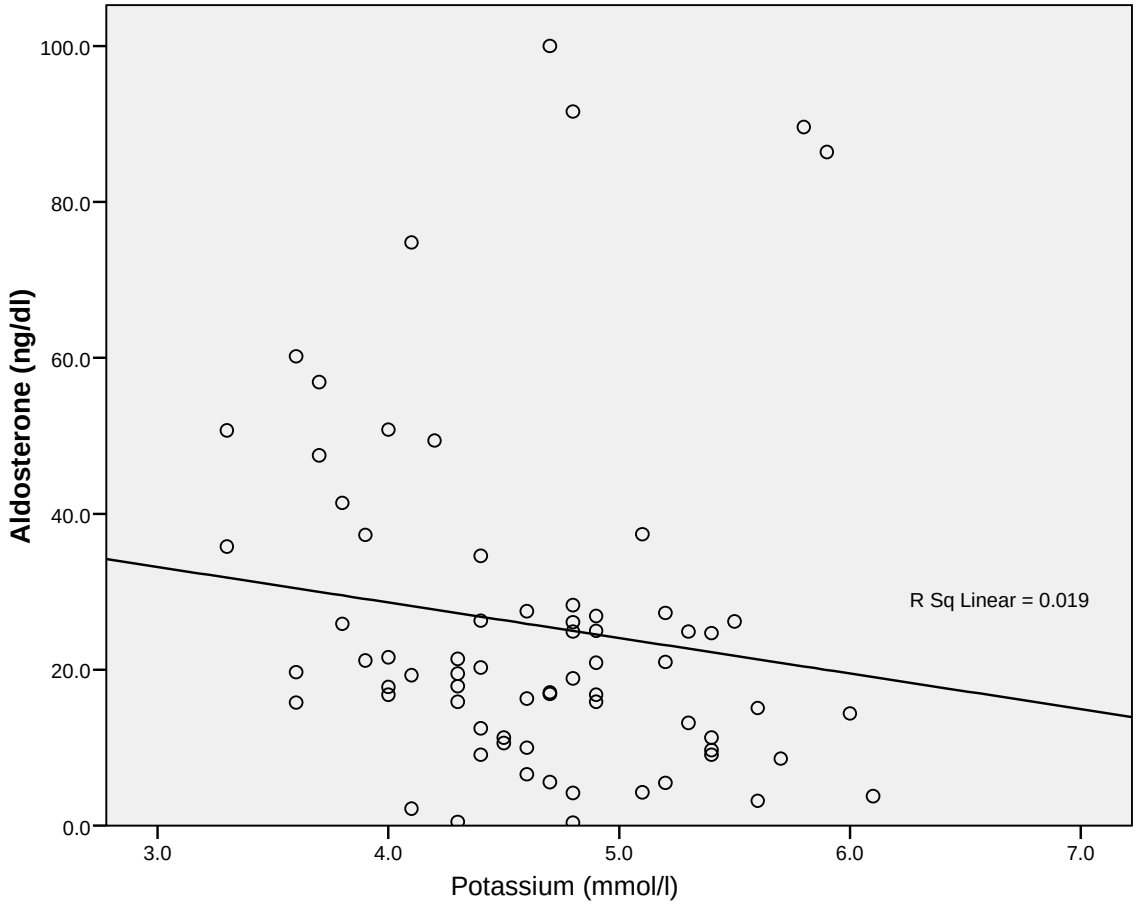

Figure 4.6 **A Graph of Serum Aldosterone plotted against Serum Potassium levels.**

A Regression line has been applied to the scatterplot.

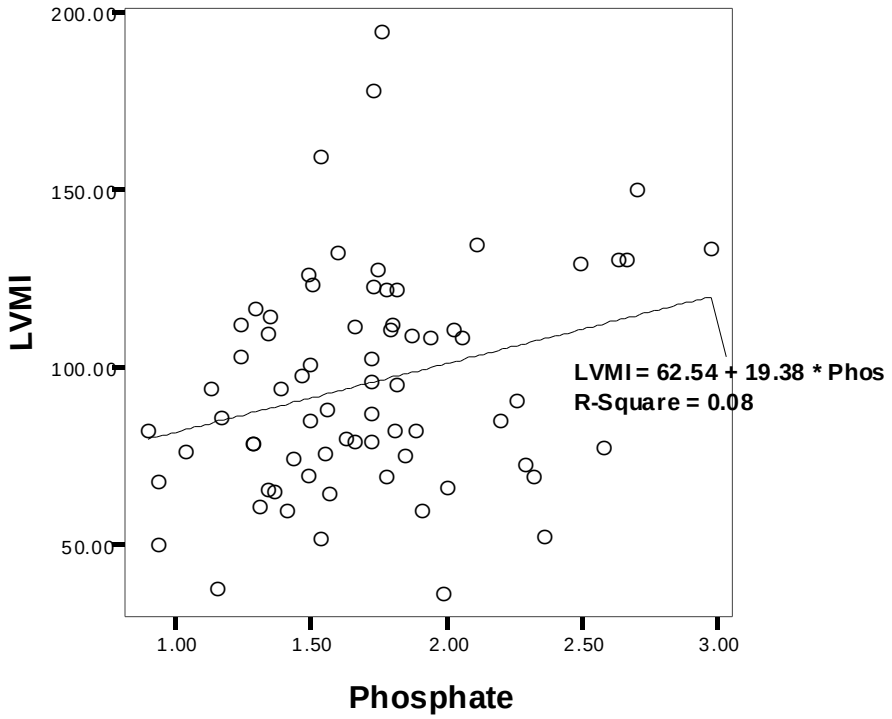

Figure 4.7 **A Scatter Graph of Phosphate level (mmol/l) against LVMI (g/m^2)**

4.4 Discussion

Previous evidence suggests a positive correlation between aldosterone (or the aldosterone:renin ratio) and left ventricular mass in hypertensive patients [146, 147]. This study found no significant relationship between aldosterone and left ventricular mass in the end-stage renal failure patients studied. There are many possible reasons for this. The fact that the aldosterone was taken as a one off serum sample could have been one of these reasons. Aldosterone is secreted in a diurnal pattern and is affected by posture. Therefore a 24hr aldosterone measurement e.g. 24hr urinary aldosterone measurement would have been preferable so an average reading could have been measured and these confounding factors minimized.

Another possible explanantion is the interaction between medication and aldosterone levels. In particular, beta-blockers reduce renin production and consequently reduce aldosterone production; whilst ACEI inhibit angiotensin II release and therefore aldosterone. Renin levels should also reduce through feedback mechanisms. BB and ACEI were prescribed in a substantial proportion of the pre-dialysis and dialysis patients (ACEI 63.6% vs 31.7% and BB 39.4% vs 41.4%) in this study. However in this analysis we found no evidence of a relationship between aldosterone and any medication recorded. In fact median aldosterone was 19.5pmol/dl in both those taking and not taking an ACEI.

Aldosterone escape has been described following 40 weeks ACEI treatment indicating a possible time and patient dependent effect on aldosterone production [141]. This is in-spite of the proven benefits of ACEI in hypertension

[148] and heart failure populations [149]. It seems likely given our results that a large proportion of patients on ACEI exhibited this escape phenomenon since the median aldosterone level in the ACEI treated group was higher than the normal range 1-31ng/dl [150]. However ACEI use was not associated with aldosterone levels in this patient group. It would have been usefult to have a record of the duration of treatment with an ACEI however this information was not collected at the time.

Aldosterone has been shown in animal and human studies to be associated with end-organ damage. However these effects have mainly been demonstrated in the presence of high salt intake. Serum sodium was not found to be related to aldosterone levels in this study however the aldosterone and sodium measurements were spot random measurements. In future studies we suggest determination of salt intake by 24hr urinary sodium measurement, to coincide with a 24hr aldosterone measurement, so that the results are not confounded by salt intake or postural/diurnal variations in aldosterone.

Aldosterone to Renin ratio has recently been recognised as the “best screening test for the diagnosis of primary aldosteronism” [151]. This is because it not only indicates the aldosterone level at that moment it also helps to identify any problems with feedback mechanisms or inappropriately high levels of aldosterone. Unfortunately renin measurement was not performed in this study but it would be something to consider including in future studies.

Rat studies have cited a possible paracrine effect of aldosterone within cardiac tissues although this issue is still controversial [152]. Therefore, the

deleterious effects of aldosterone reported in previous studies, might only be due in part to circulating aldosterone (produced in the adrenals). The remaining effects might due to an increase in aldosterone production in cardiac tissue itself. For example, evidence post-myocardial infarction has shown an increase in cardiac aldosterone levels compared to baseline [153]. Also mRNA of enzymes involved in aldosterone synthesis has been found in cardiac tissue indicating that de-novo synthesis is possible [152]. Human studies have failed to confirm this.

Dialysis patients are subject to extremes of fluid status and potassium during the course of their treatment. Therefore you might expect variations in aldosterone levels also. Unfortunately no data exists for the variability of aldosterone during ultrafiltration; dialysis or normal values for this subset of patients. In this study, we tried to standardise for fluid and potassium status by performing venepuncture and the MRI scan on a post-dialysis day. However we are aware that this probably didn't completely eliminate the effect of these two parameters on the readings we achieved.

In patients with normal renal function and consequently therefore, not on dialysis, we would expect aldosterone to be regulated to some degree by potassium. That is, when the potassium level falls this blocks further production of aldosterone. However, our results indicate a paradoxical relationship in this subset of patients i.e. as the potassium levels fell the aldosterone levels increased. From this result it could be suggested that the regulation of aldosterone release differs between end-stage renal failure patients and the

general population. Further investigations of the effects of dialysis on the renin-angiotensin- aldosterone system are needed to confirm or refute this hypothesis.

4.5 Conclusion

Aldosterone was not found to be associated with left ventricular mass index in this group of end-stage renal failure patients. Whether this is a true reflection of the interaction between aldosterone and the heart, in the context of renal failure, remains unclear. Further investigations are needed to determine the effect of renal replacement therapy, antihypertensive medication and salt intake on aldosterone's effects within the heart.

Chapter 5: Rat Heart Slice Study

5.1 Introduction

Aldosterone is associated, in animal and select human models, with cardiac fibrosis and left ventricular hypertrophy. Angiotensin II has been shown to increase TGF-β_1; consequently increasing extracellular matrix production and decreasing fibrin degradation; two mechanisms which underpin fibrosis and scar formation [154]. It has now been postulated that TGF-β_1 activation may be mediated by activation of aldosterone directly rather than angiotensin II's effect on aldosterone.

Previous researchers have used primary cell culture to perform such experiments but usually producing low yields from each animal after a relatively long process. Tissue slice culture could provide an alternative and was used widely in the 1940-60s.

Slice culture has the potential advantage of mimicking the interactions of different cells that would normally occur in the heart and maintaining the normal architecture. This method of culturing slices has been shown to be viable (using varied techniques e.g. immunohistochemistry, heart beating characteristics, gene expression, LDH release and oxygen consumption [155-157]).

Optimal slice thickness has also been evaluated; with a maximum thickness of 1mm quoted by W. Habeler et al [156] being cultured for up to 3 months. However the Walburg formula governing the diffusion of solutes into tissue slices indicates that the limiting slice thickness is 0.57mm [155]. This

corresponds with the findings of Pearson et al, of maximal oxygen consumption at 0.5-0.6mm thickness. Most reports have used 0.3-0.5mm thickness with success [155, 158, 159].

Other researchers have used primary rat renal mesangial cells and fibroblasts to investigate the effects of aldosterone on TGF-β_1 production and fibrosis in the kidney [160, 161]. However there are few studies investigating aldosterone's effects on TGF beta-1 production in the heart. The range of aldosterone concentrations in this study aimed to include a range likely to invoke the maximum response. No direct comparative studies have been published, therefore the results from the previously mentioned renal studies (max effects of 10^{-6} moles/l after 48hours [161]) were used as a reference. Physiological aldosterone concentrations (0.2 - 8 x 10^{-10}mol/l) (Coat-a-Count, Siemens, Los Angeles) were also included within our range.

5.2 Aims

The aim was to develop a rat heart tissue slice culture technique which could then be used for a pilot study into the effect of aldosterone and salt on the production and expression of TGF-β1 and the degree of cardiac fibrosis.

5.3 Materials and Methods

For the pilot study, six male Wistar-Kyoto control (WKC) rats of 250g aged between 12-14weeks were culled and their hearts removed for examination. The

heart was cut into coronal 0.5mm sections from the atrio-ventricular groove down the ventricles. Cutting the heart required the use of the rodent heart matrix described in the methods chapter and took place in the presence of cooled calcium free buffer solution.

Once the sections were cut, they were each placed in a well of a 12 well plate, on culture plate inserts. For each rat heart, 3 slices were used as controls (labelled “C”) and were placed in a well with 1ml of media only (1M 199:4 DMEM and 10% horse serum, 5% fetal bovine serum and 1ml of 1000units Penicillin /10mg/mlStreptomycin (Sigma-Aldrich, Dorset, UK)).

In order to investigate the effect of differing aldosterone concentrations, four rat heart were used. Three slices from each heart were placed in wells containing either 10^{-4}, 10^{-6},10^{-7} or10^{-11} M Aldosterone. Each of these set of three slices were controlled with 3 control slices from the same heart. The slices placed in aldosterone were labelled “A” (Figure 5.1)

To investigate the effect of sodium, 2 rat hearts were used. Three slices from each heart were placed in wells containing media diluted to a sodium concentration of 143.3mmol/l or 133.1mmol/l. These wells and the slices within them were given the code “N”. Each of the set of three “N” slices were controlled with 3 control slices/wells from the same heart.

It was also possible to investigate the effects of aldosterone 10^{-6}M in the presence of Na concentrations of 143.3mmol/l or 133.1mmol/. For this a further 3 slices were obtained from each of the rat hearts used for the Na set of the experiment. The media was diluted to the two sodium concentrations (detailed

above) and then aldosterone was added to a concentration of 10^{-6}M. These wells and the slices within them were given the code “NA” (Figure 5.1)

Any remaining slices, from the 6 rat hearts, were used to test viability. This was done using the MTT and CytoTox-Glo assays described in the Methods chapter. In essence the MTT assay was a colorimetric assay of the activity of mitochondrial enzymes within the cells of the heart slice. The Cyto-Tox Glo assay was a luminescence assay that emitted luminescence when it reacted with protease enzymes leaked from dead cells within the sample. This result was then compared to that of the luminescence emitted when all the cells in the sample were deliberately lysed. Viable cell luminescence (VCL) was then calculated:

VCL = Post-lysis luminescence – Pre-lysis Luminscence

All slices were incubated for 48 hours at 37ºC and 5% CO_2./95%air. After the first 24 hours all the media within the wells were removed and frozen at -80ºC for storage. The media was then replaced with the same concentration of media or aldosterone as at the start of the experiment.

At 48hrs, the slices were removed from the incubator and weighed (mean weight 29.8 mcg). The supernatant was removed for storage.

The slices were then cut in half. Half was formalin fixed overnight and the tissue processed for paraffin sectioning. The other half was snap frozen with nitrogen, fixed in O.C.T.

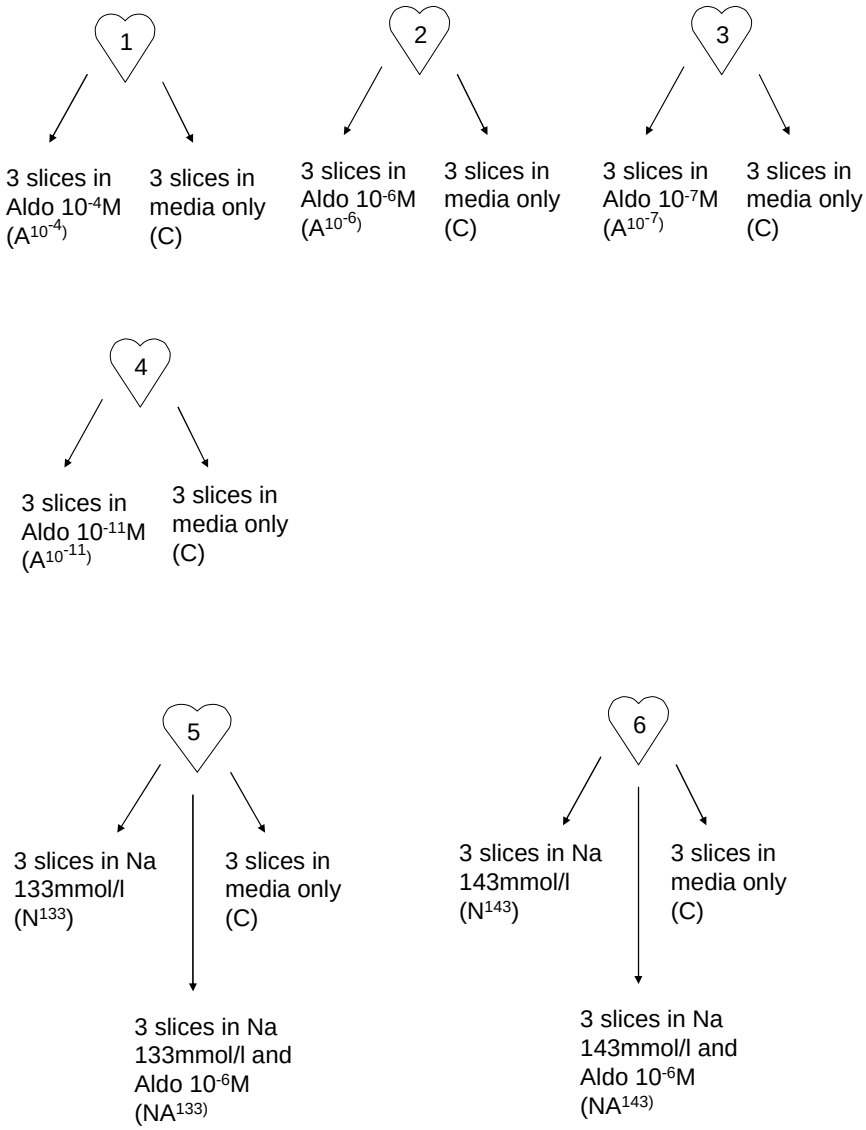

Figure 5.1 **Schematic Diagram of the Experimental Method.**
Each slice was incubated for 48hours

5.3.1 Staining for Fibrosis

Two to four, 5 micron sections were cut out of each of the wax embedded paraffin blocks prior to oven drying them onto a slide. One of the sections was stained with Picrosirus red and the other with Trichrome Blue to look for fibrosis.

5.3.2 TGF-β_1 Analysis

Preliminary reverse transcriptase polymerase chain reactions were undertaken to confirm TGF-β_1 gene expression in the rat heart (Figure 5.2). However, due to technical difficulties, real-time PCR was unable to quantify TGF-β_1 gene expression.

TGF-β_1 production by the tissue slices were analysed using a rodent TGF-β_1 Elisa kit (Quantikine, R&D systems, Minneapolis). Each of the frozen supernatant samples extracted at 24 and 48hours into the experiment were used for analysis. The samples were thawed once and the TGF-β_1 within each activated by acidification and then neutralisation (as per the manufacturer's guidelines).

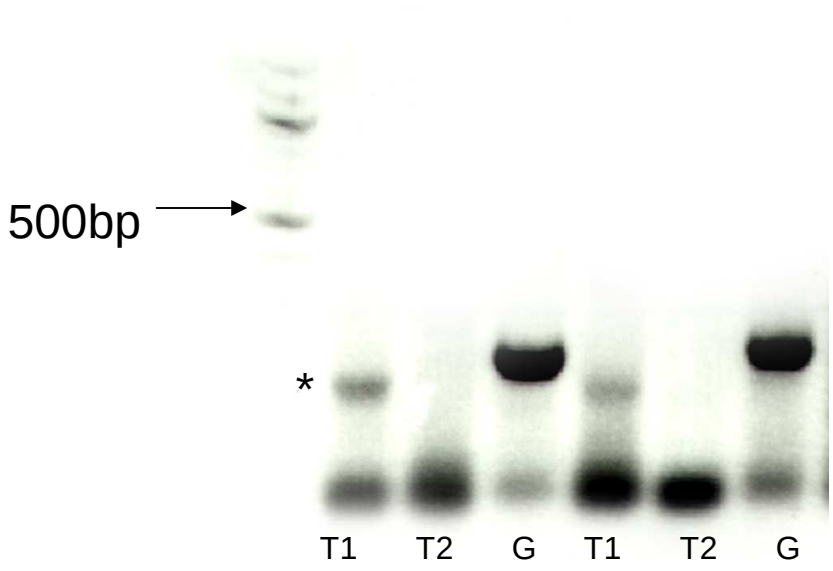

Figure 5.2 **PCR of Rat Atrial Tissue using GoTaq DNA Polymerase Enzyme with addition of $MgCl_2$ 0.25mM and 1.25µl of DMSO to the Mastermix**

Key: T1, TGF-β_1 primer 1

T2, TGF-β_1 primer 2

G, GAPDH primer.

* indicates the band produced by the amplification product of the TGF-β_1 primer 1 combining with the TGF-β_1 1 mRNA in the cardiac tissue.

A 100bp ladder was used to confirm the size of the amplification product and this is shown on the left handside.

5.4 Results

5.4.1 Viability of Tissue Slices

5.4.1.1 CytoTox-Glo Results

CytoTox Glo assay pre-lysis results represented the luminescence produced by the protease enzymes (released by dead cells) within the slice at the end of the 48hr incubation. The post-lysis results were recorded after a lysis reagent was added to the slice. The difference between these results was termed viable cell luminescence.

The results of this assay are shown in Figure 5.3, 5.4 and 5.5. These results show that there was a reduction in viable cell luminescence (VCL) over time even when corrected for the weight of the slice examined. The percentage reduction in VCL from the start of the experiment ranged from approximately 5 – 47% and was not affected by aldosterone or sodium concentrations.

5.4.1.2 MTT Assay Results

The MTT assay was a measure of the mitochondrial enzyme activity within living cells. The results are shown in figure 5.6 and 5.7. These results show that there was a reduction in absorbance detected over time. However the results suggest that there is partial improvement in mitochondrial activity between the 24^{th} hour and the 48^{th} hour of the experiment.

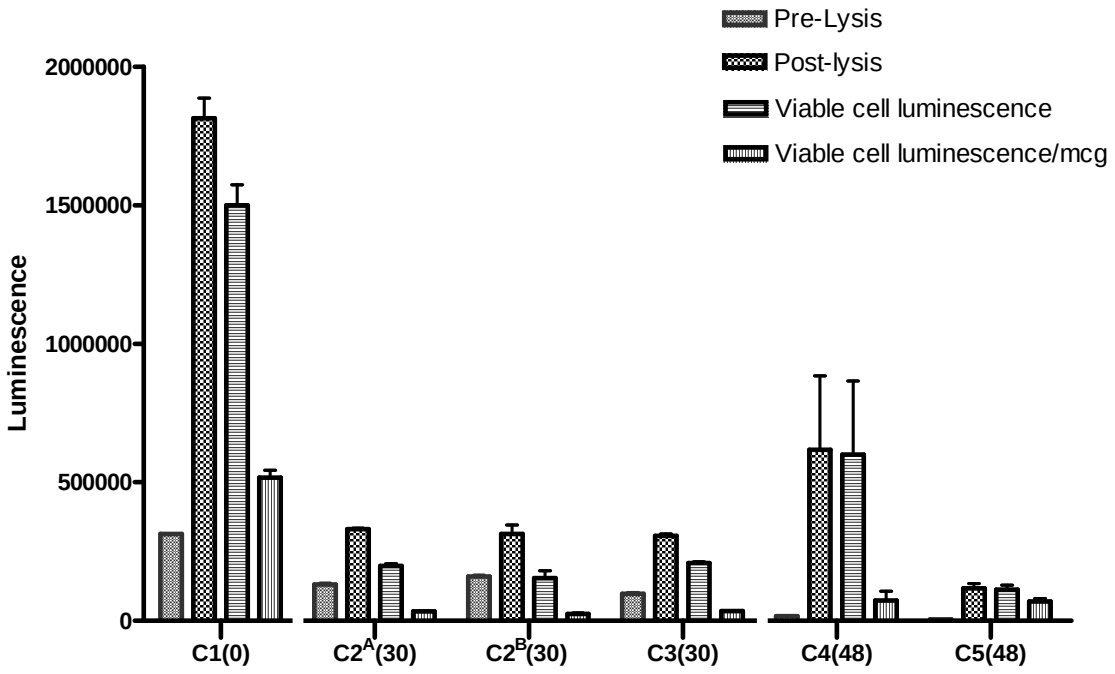

Figure 5.3 **CytoTox Glo Assay Results for Control Tissue Slices (C) at Specified Time Points During Incubation.**

This graph demonstrates a reduction in viable cell luminescence (an indicator of cell viability within the slices) over the 48hour incubation period. However it also shows that a proportion of cells remain viable even at the end of the 48hours.

Key: (n) - Number of hours of incubation prior to assaying
Suffix $^{A/B}$ – denotes that the two different results are from two halves of the same slice of tissue

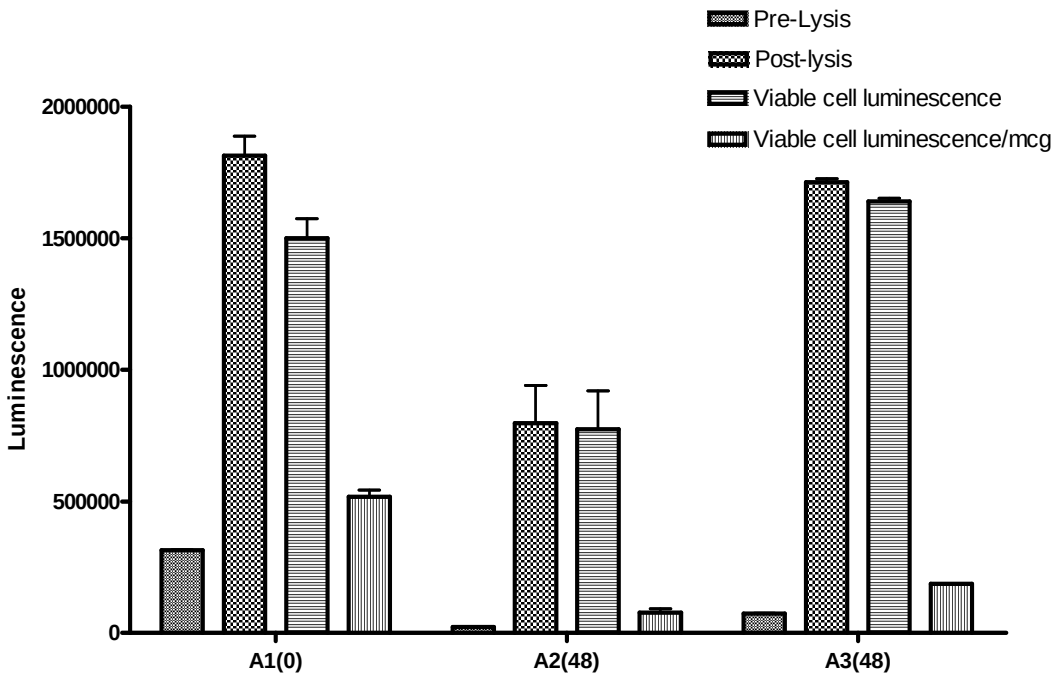

Figure 5.4 **CytoTox Glo Assay Results for Aldosterone 10^{-6}M Treated Slices (A) Over a 48hr Period**

This graph demonstrates a reduction in viable cell luminescence (an indicator of cell viability within the slices) over the 48hour incubation period in those slices treated with aldosterone 10^{-6}M. However these results are not significantly different to the decline in viability in control slices cultured for 48hrs.

Key: (n)- Number of hours of incubation prior to assaying

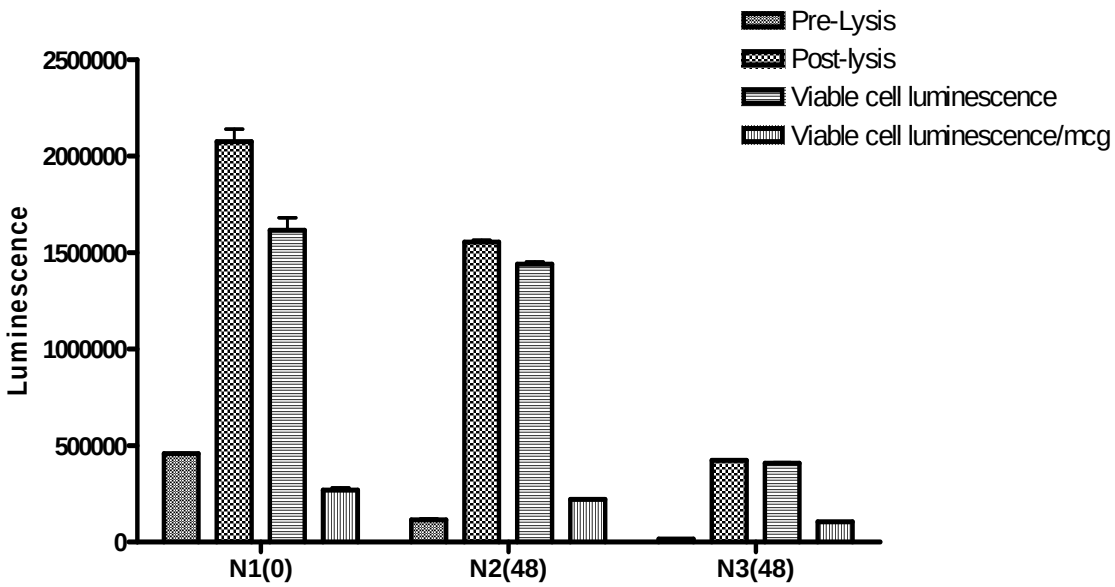

Figure 5.5 **Cyto-Tox Glo Assay Results for Tissue Slices Incubated in Diluted Media (i.e Na 133.3mmol/l)**

This graph demonstrates a reduction in viable cell luminescence (an indicator of cell viability within the slices) over the 48hour incubation period in those slices treated with aldosterone 10^{-6}M. However these results are not significantly different to the decline in viability in control slices cultured for 48hrs.

Key: (n)- Number of hours of incubation prior to assaying

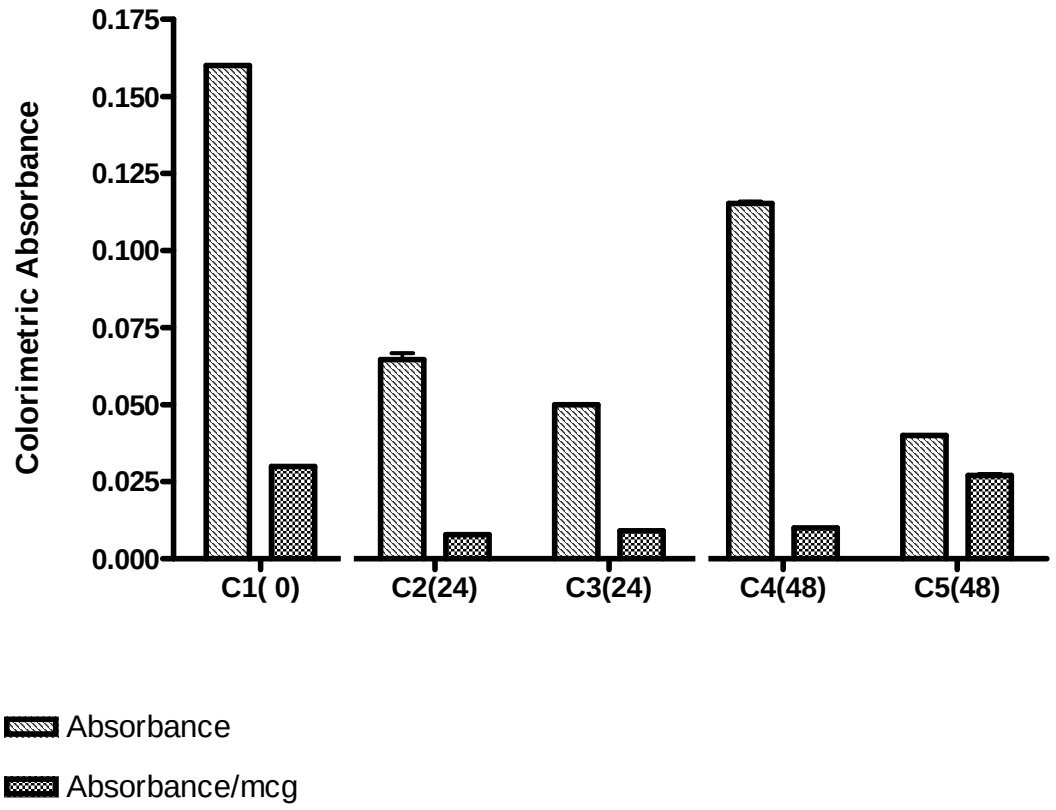

Figure 5.6 **The MTT Assay Viability Results for Control Samples (C).**

This graph demonstrates the mitochondrial activity levels within viable cells at the time of assaying. The results show that after an initial decline in enzymatic activity at 24hours this then improved after 48hours.

Key: (n)- Number of hours of incubation prior to assaying

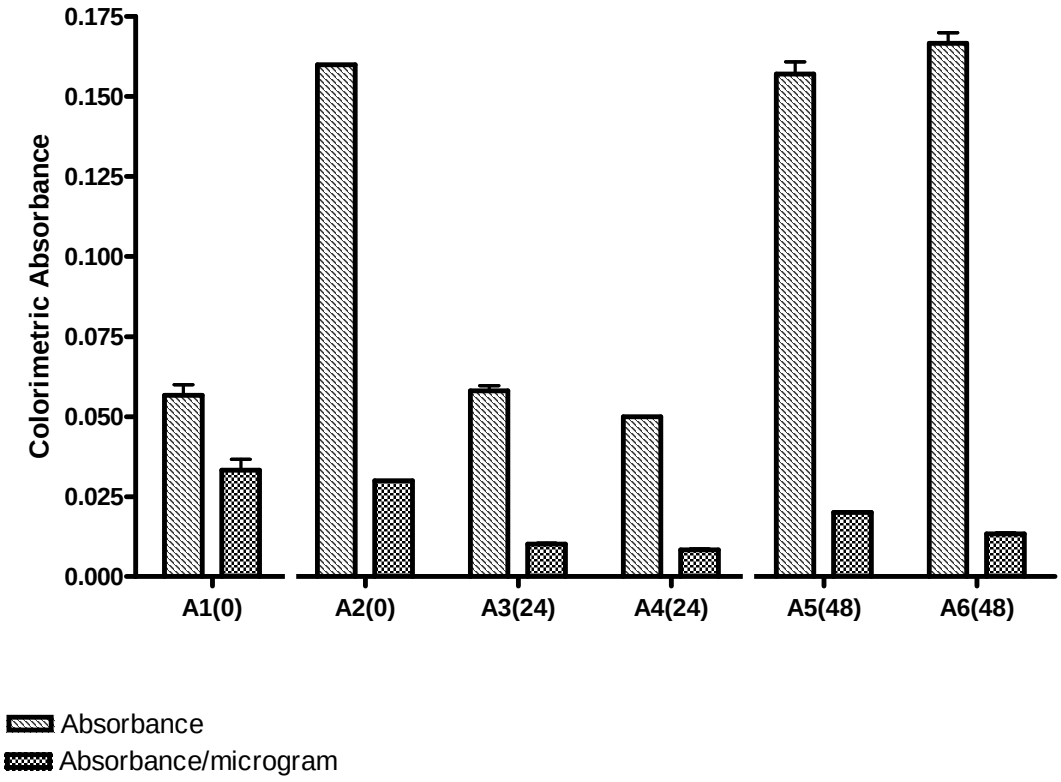

Figure 5.7 **MTT Viability Assay Results for Aldosterone 10^{-6}M Incubated Slices (A) Over 48hrs.**

This graph shows that the viable cell mitochondrial activity in slices treated with aldosterone 10^{-6}M follows the same pattern as that of control slices shown in the previous graph.

Key: (n)- Number of hours of incubation prior to assaying

5.4.2 *Fibrosis*

As expected perivascular staining was seen with both trichrome and picrosirus staining due to the collagen present in the vessel walls. There was no increase in perivascular or any other area of staining for either picro-sirus red or trichrome stain under any of the media conditions investigated or over time. Some typical examples of the histology staining are shown in Figures 5.8 for picro sirus red and Figures 5.9 for trichrome staining.

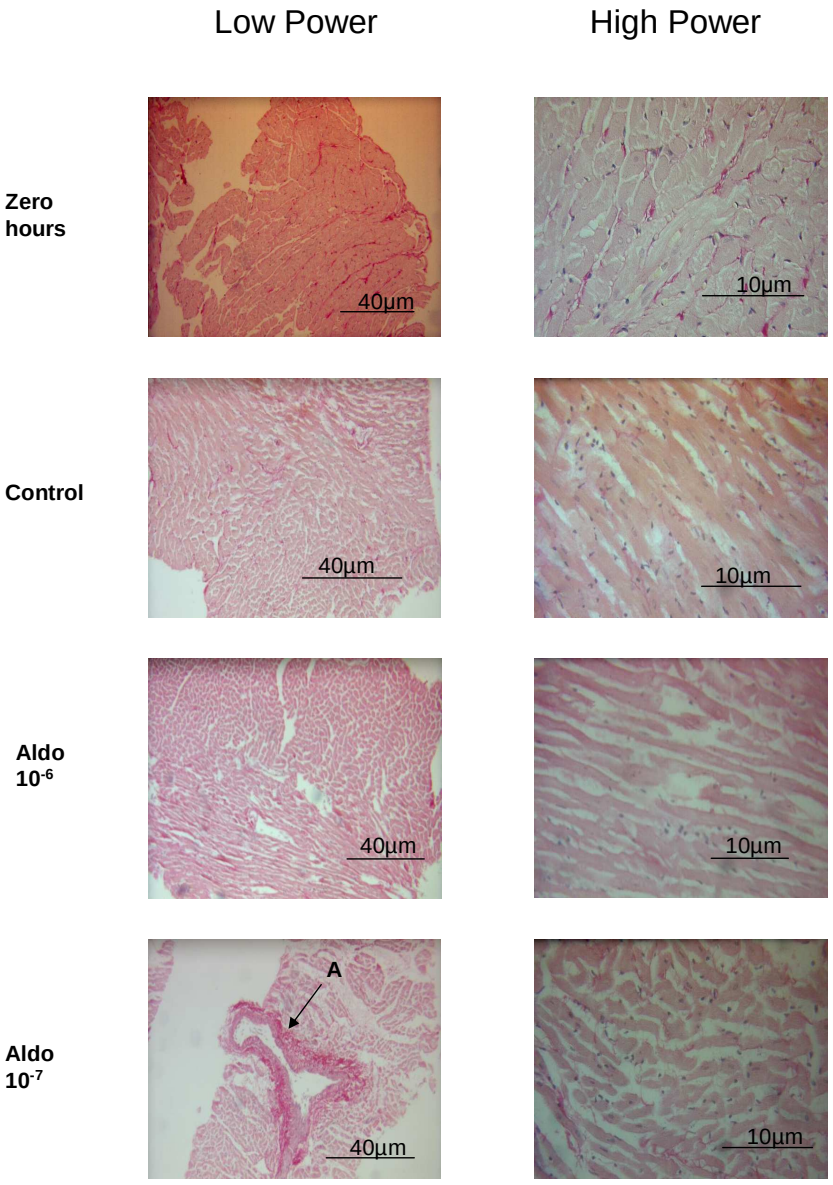

Figure 5.8 **Picro-Sirus Red Stained Sections of the Rat Heart Slices incubated in different aldosterone and sodium concentrations in the media.**

Apart from the first row of pictures the remaining pictures were taken of slices incubated for 48hours in the media. The zero hour labelled pictures were of heart slices prior to incubation.

Picrosirus stain was used to stain collagen pink.

The scale is shown on the bottom right corner of the image.

Key for all parts of Figure 5.8:

A – indicates the normal appearances of perivascular collagen staining with picrosirus red.
Control – heart slice incubated in media alone
Aldo 10^{-n} – heart slice incubated in the concentration of aldosterone shown in mol/l
Na 133/143 – heart slice incubated in the concentration of sodium stated e.g. 133mmol/l or 143mmol/l

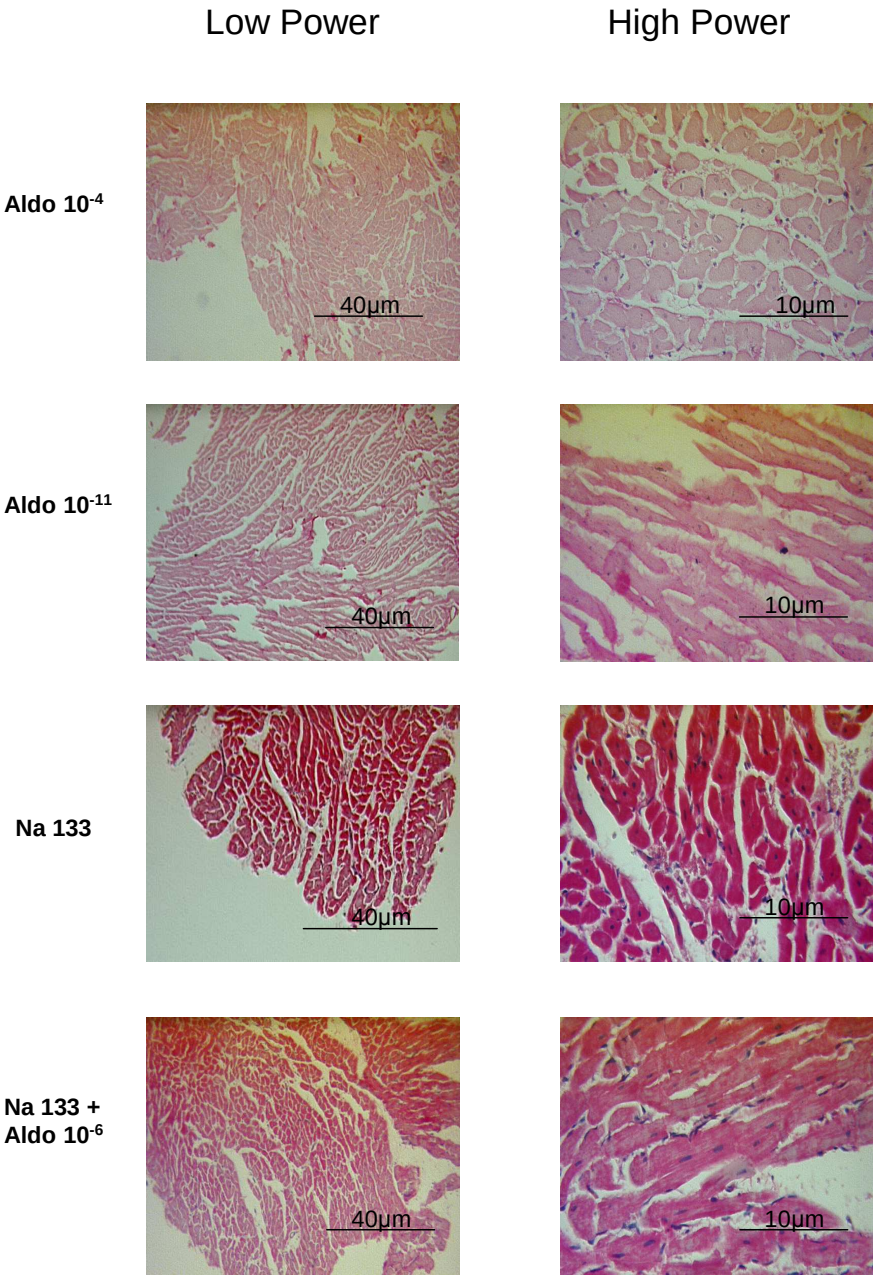

Figure 5.8 **Picro sirus red stained heart sections in different concentrations of aldosterone and sodium in the media**

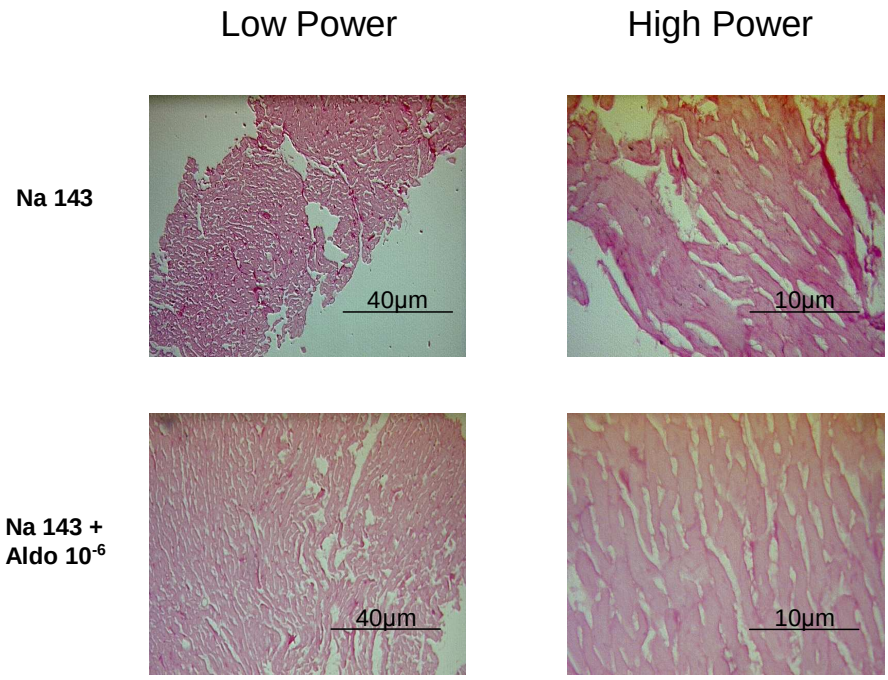

Figure 5.8 **Picro sirus red stained heart sections incubated in different concentrations of aldosterone and sodium in the media**

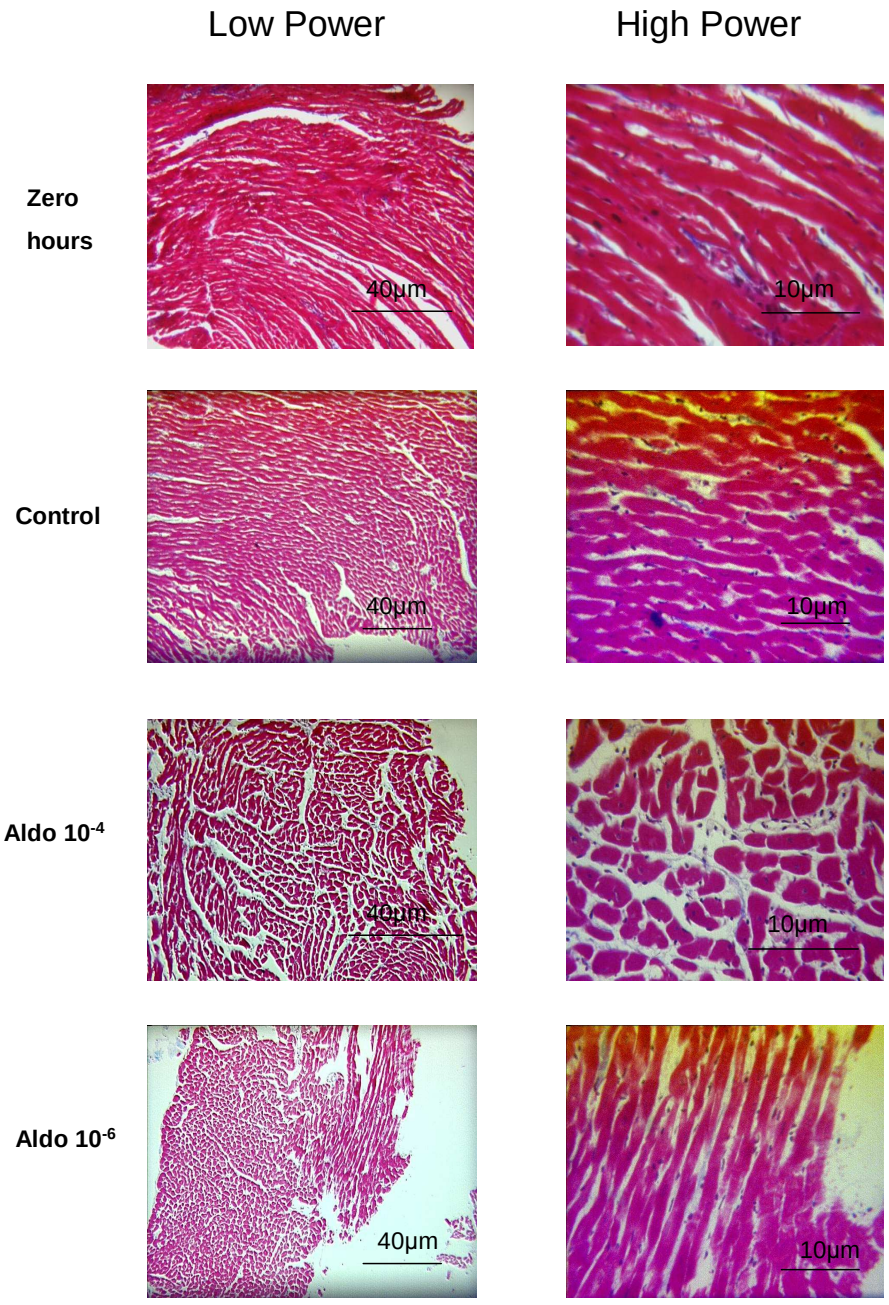

Figure 5.9 **Masson's Trichrome stained sections of Rat Heart Tissue in the different concentrations of aldosterone and sodium in the media.**

Apart from the first row of pictures the remaining pictures were taken of slices incubated for 48hours in the media. The zero hour labelled pictures were of heart slices prior to incubation.

Trichrome stain was used to stain collagen blue.

The scale is shown on the bottom right corner of the image.

Key for all parts of Figure 5.9:

A – indicates the normal appearances of perivascular collagen staining with picrosirus red.
Control – heart slice incubated in media alone
Aldo 10^{-n} – heart slice incubated in the concentration of aldosterone shown in mol/l
Na 133/143 – heart slice incubated in the concentration of sodium stated e.g. 133mmol/l or 143mmol/l

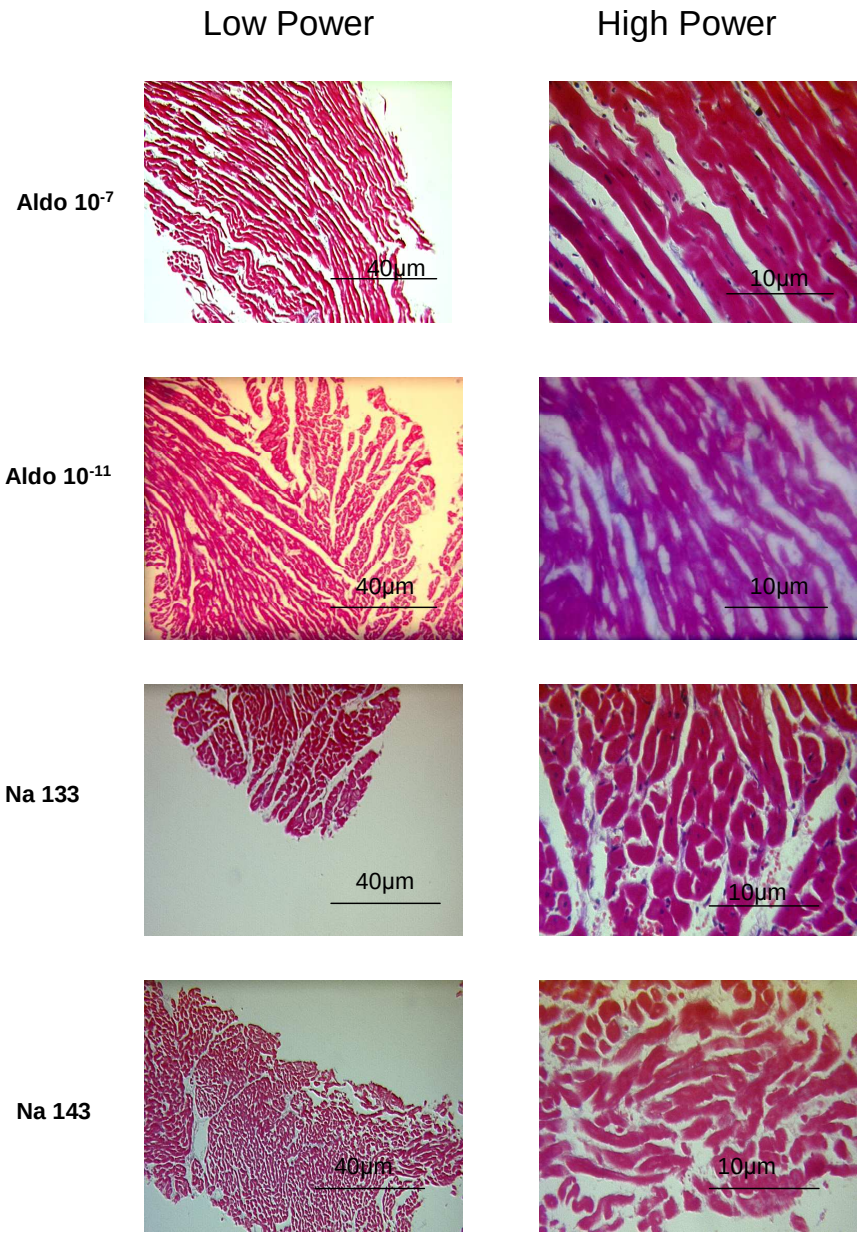

Figure 5.9 **Masson's Trichrome stained sections of Rat Heart Tissue**

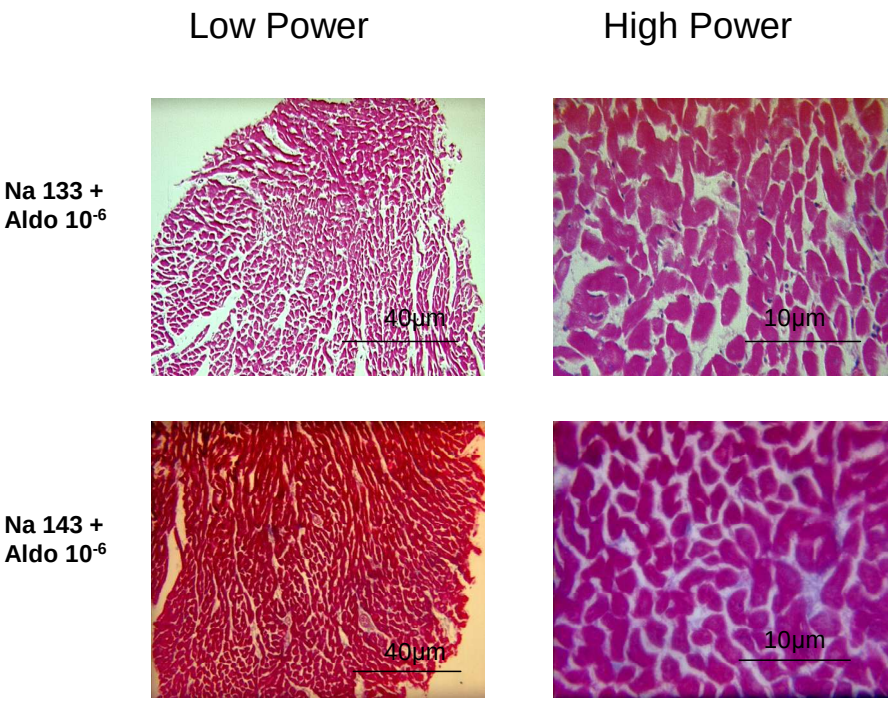

Figure 5.9 **Masson's Trichrome Stained Sections of rat heart sections**

5.4.3 TGF-β_1 Results

TGF-β_1 was found in significant amounts in the media after the addition of horse and calf serum (mean concentration = 1056.06pg/ml with a standard deviation of 148.88pg/ml). Unfortunately the serum was vital to the viability of the tissue slices and therefore could not be removed from the media prior to analysis. Elisa results demonstrated no significant change in TGF-β_1 concentration in any group from the baseline (i.e. the TGF-β_1 concentration in the media). All results were distributed within the variability of the ELISA kit, with only a relatively small difference in TGF-β_1 from the mean media concentration. These results are shown in Figures 5.10 and Figure 5.11.

Although PCR was not able to be optimised in time for completion of this project we were able to demonstrate that TGF-β_1 was being produced by the rat heart tissue. The results of the PCR are shown in methods section.

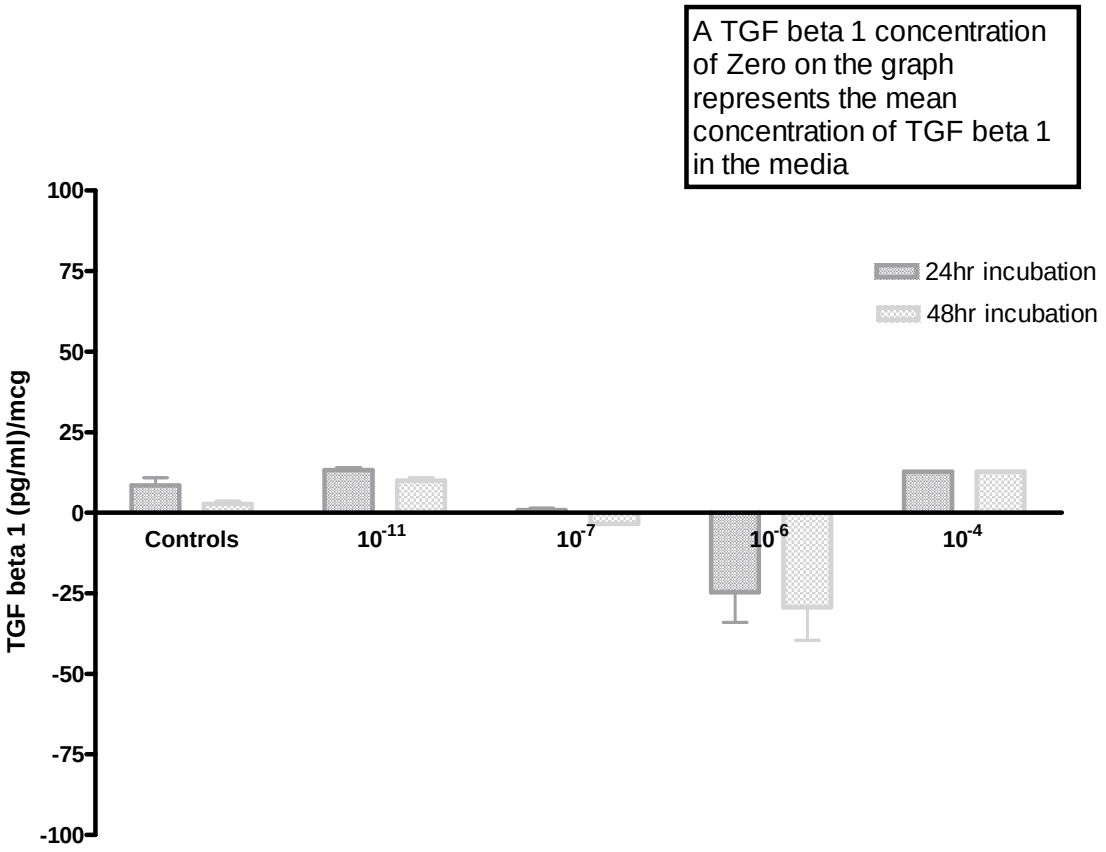

Figure 5.10 **TGF-β_1 Elisa Results for Control Slices and those Incubated with different concentrations of Aldosterone.**

The Elisa results in the table above are corrected for the media TGF- β_1 concentration and for the weight of the slices cultured (in mcg). However the mean media TGF- β_1 concentration is 1061pg/ml, standard deviation 148.8pg/ml. Therefore all of the above results are within the error of the Elisa assay.

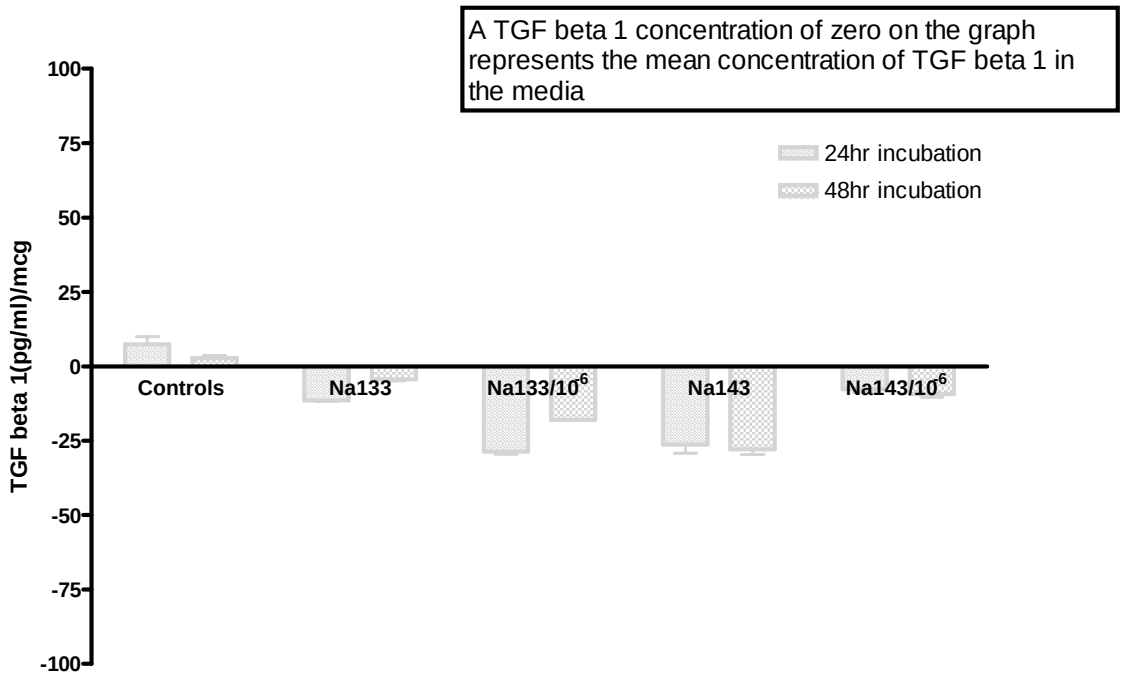

Figure 5.11 **TGF- β_1 Elisa Results for those slices incubated in Diluted Media (i.e. Na 133.1mmol/l or 143.3mmol/l)**

The Elisa results in the table above are corrected for the media TGF- β_1 concentration and for the weight of the slices cultured (in mcg). However the mean media concentration was 1061 pg/ml with a standard deviation of 148.8pg/ml. Therefore all of the above results are within the error of the Elisa assay.

5.5 Discussion

5.5.1 Limitations of the Study

Rat slice culture was an experimental technique attempted to try to mimic in-vivo tissue structure and cell to cell interactions. However as this was an experimental technique refinement was carried out prior to the investigation of the effect of aldosterone/salt on the heart slices.

The use of the rodent heart matrix allowed reassurance that the thickness of the ventricular slices remained relatively constant. However, the diameter of the slices varied depending on the distance from the atrio-ventricular groove, because the ventricle is narrower at the apex than the base. It is not known whether the diameter of the heart slice also influenced the diffusion of nutrients etc. to and from the media into the slice.

This study demonstrated no significant TGF-β_1 production or excretion by the heart tissue over 48 hours. However, if the amounts produced were very small then any production could have been overshadowed by the large amounts of TGF-β_1 in the serum containing media. Attempts were made to try the experiment without the use of horse and fetal calf serum however the viability of the slices meant this was not possible.

Within the TGF ELISA results there was variation in TGF-β_1 concentrations detected. However this variation occurred within the control slices and within the media (containing serum) itself suggesting that this variation was

within the range of sensitivity of the ELISA itself rather than a true variation in production.

It is also reasonable to suggest that the duration of culture was too short to detect any significant fibrosis or TGF-β_1 production. The duration of incubation was chosen for viability reasons and because other researchers had obtained results after 48 hours in renal cells.

The viability assessments used in this experiment were essentially untested on tissue slices and so adaptation of the techniques used for cell culture viability was needed to take account of this. Viability measurements were therefore difficult to interpret and optimise. It is reasonable to think that the diffusion of substrate into each cell would be affected by the surrounding cells and extracellular structures. Although the slices were a constant thickness and the results were referenced to the weight of the slice, these factors were not fully resolved within the time of this project.

5.5.2 Significance and Context of the Results

TGF-β_1 is a member of a super-family of cytokines called the transforming growth factor family; as such it is known to be involved in cell growth and repair. But the exact mechanisms and pathways for this are complex and incompletely understood.

Information about TGF-β_1's role in cardiac tissue is limited but expanding. For example, it is known to be produced in certain cells within the heart including myocytes, lymphocytes and fibroblasts. Involvement of the Smad pathway has been sited most often in the role of TGF-β in cardiac fibrosis. But the

concentrations of TGF produced are very small (2.22 ± 0.14ng/mg protein) and vary considerably over time and within the same species [126].

Angiotensin II is a proposed stimulus of release and over-expression of TGF-β_1 [162]. Chronic over expression of TGF-β_1 has been found to increase extracellular matrix production, cause cardiac fibrosis and subsequently lead to heart failure [154]. In the context of an acute ischaemic insult to the heart, TGF-β_1 is also up-regulated. Studies show that at the area of insult the levels of TGF- β_1 rise 3-4 fold [163]. It is for these reasons that TGF-β_1 has become the focus of research in an attempt to prevent cardiac fibrosis and subsequent heart failure.

In this experiment, we were interested in the potential role of aldosterone and sodium in the release of TGF-β_1 and any subsequent fibrosis that occurred. Aldosterone in the context of high salt intake in rats has been shown to be associated with left ventricular hypertrophy and cardiac fibrosis [67]. It has also been suggested that aldosterone, either directly or by induction of angiotensin II, stimulates TGF-β_1 production and release. Corroboration of these finding has occurred in translational human studies. These have shown that blockage of mineralocorticoid receptors with spironolactone can reduce morbidity and mortality in patients with moderate to severe heart failure [76]. More recently Eplenerone (a selective aldosterone blocker) has been licensed for use in the U.K. This has also been shown (in a randomised controlled trial) to reduce mortality and hospitalisation rates in patients following an acute myocardial infarction who subsequently develop heart failure [77].

Of the 3 forms of TGF-β it is thought that TGF-β_1 is most influential in the heart and this is where most research has centred so far. Perivascular and interstitial fibrosis were found to be the consequence of aldosterone and high salt intake over an 8 week period in the rats studied by Brilla and Weber in 1992 [67]. However, an increase in fibrosis was not seen on histological staining in either the aldosterone, high salt or aldosterone and high salt groups in our study. Some of the potential reasons for this are discussed in the limitations section. The 48hour duration of the experiment could have been too short for fibrosis to develop. Unfortunately it was not viable to increase the experiment duration much beyond 48hours.

At the time of designing this experiment, 48 hours was chosen for viability reasons and had been shown in other investigations to be long enough to elicit a response in TGF-β production (albeit in renal glomerula cells) [160]. It was also thought that a TGF-β_1 rise was likely to precede any fibrosis detected [104, 121]. However our research found no significant increase in TGF-β_1 production by the ventricular tissue over time or due to aldosterone (10^{-4} -10^{-11}M)/salt (133-153mmol/l) changes within the media.

The limitations of serum in the media are discussed in section 2.9.3 and therefore will not be repeated here. Other potential reasons not detecting a significant result include; TGF-β_2 or TGF-β_3 having more of a role within the heart than previously recognised; the time limit on the experiment was too short to invoke the TGF response or that the conditions within the experiment were not a

stimulus for a TGF-β_1 response at any time. The number of viable cells within the tissue slice would also have implications on TGF-β_1 release.

Tissue slice culture is a technique that enjoys the potential benefits of retention of in vivo architecture. The theoretical advantages of this include intact cell to cell interactions, spacial relationships between cell types and prevention of disruption of cytokine pathways and hormone responses. Researchers studying cardiac tissue have used many different techniques to maintain the slices in culture; some more successful than others. One of the most successful maintained the slices for 3 months [156]. Our study showed that the proportion of viable cells within the tissue slices dropped steeply over the first 24hours and then there was a trend towards a slight increase in the second 48hours.

However, the techniques used for assessing the viability need to be interpreted with caution. Validation of results within the tissue slices was difficult because most research/manufacturers instructions were directed towards primary cell culture rather that tissue slices. It is possible that the tissue slices were more viable than shown, and that the permeability of the cell wall for MTT or the release and maintenance of the dead cell proteases in the media were reduced after time in the media. It is also possible that the dead cell proteases were held within the structure of the tissue slice rather than being released in to the media and therefore were not present for assaying. The subjective impression of the slices was of reduced viability over the 48hours of incubation.

Potential reasons for the presumed reduction in viability could be due to the media used. The media chosen was that used by another group within the

University of Glasgow, to culture cardiac myocytes and therefore probably favoured viability of this group of cells over others. Also the rats we used were older than the embryonic tissue other researchers used. However those rats were chosen to demonstrate effects in adult rats, ensure enough tissue was obtained form each rat for control slices and viability slices to be taken and to keep the project within budget.

Heart tissue is highly oxygenated in the body by the rich blood supply. Some other researchers oxygenated the tissue during incubation which could provide additional benefits and improve viability if this project was to be repeated and improved in the future.

Further analysis of the media used, revealed a very high glucose concentration; 4500mg/l of D-glucose in DMEM and 1000mg/l of D-glucose in the Media 199. This equates to 55.6mmol/l in M199 and 250mmol/l in the DMEM. After dilution with the fetal calf, horse serum and pen/strep, the final glucose concentration was 177.7mmol/l. Since the human normal glucose range is approximately 4-11mmol/l this is a very high concentration and might account for some of the reduced viability demonstrated in the heart slices over time. However, most neat cell culture media have a glucose concentration between 1000-2000mg/dl.

5.6 Conclusions

Neither aldosterone nor changes in salt concentration within the media were shown to significantly affect TGF-β_1 production/release or the amount of

fibrosis within adult rat ventricular tissue slices over a 48hour incubation period. However, the limitations of this tissue slice culture technique were difficult to overcome in many cases. The viability of the slices was a particular issue, since this restricted the duration of the experiment and reduced the number of cells within the tissue that could have been producing the TGF-β_1 and collagen.

Chapter 6: Generic Discussion

The research, detailed in this thesis, aimed to address the title "Aldosterone and the Cardiovascular Complications of Chronic Kidney Disease". Aldosterone has held much promise as a potential target for treatment of heart failure, blood pressure and the cardiac complications seen in chronic renal failure (e.g. cardiac fibrosis and left ventricular hypertrophy). However the exact link between aldosterone and these pathologies is not yet fully understood.

Although evidence exists in animals and some patient groups (e.g. essential hypertensive patients), confirming a link between aldosterone and cardiac complications, the evidence in renal dysfunction is more limited.

A potential reason for this is the difficultly interpreting data in the context of renal replacement therapy, where there are marked fluctuations in fluid status/electrolyte balance, as well this many patients are prescribed medications that are known to affect the renin-angiotensin system e.g. ACE inhibitors (ACEI) and beta-blockers (BB). Greater than 30% of patients in the CKD quartiles of the WSKDS were prescribed an ACEI and 18.5% of those on dialysis. A high percentage of patients were also prescribed BB (>45% of CKD quartiles 3 and 4 and >50% of dialysis patients).

The normal values quoted for aldosterone and renin are also liable to interpretation errors. The normal values are based on patients with normal renal function and have not been verified in renal impairment. Given the swings of sodium and water concentration in the intravascular space, particularly of dialysis

patients, it would be reasonable to suggest that the normal value of these hormones would vary considerably. Furthermore Aldosterone and Renin are affected by posture, salt intake and aldosterone has a diurnal secretion pattern. Therefore, future investigators would be wise to measure 24hr urinary aldosterone and salt to allow for these confounding factors.

In the West of Scotland Kidney Disease Study, we showed that ACEI and BB had significant effect on renin levels. However, despite our expectations, neither ACEI nor BB significantly affected aldosterone levels in the patients studied.

No significant association was found between aldosterone and any cardiac complication in either of the clinical studies undertaken during this research. However, further research is needed to address the issues raised above, before we can exclude aldosterone as a factor in the development of uraemic cardiomyopathy.

Survival data in the WSKDS also failed to demonstrate a significant increase in the risk of death from raised serum aldosterone or renin levels (above the median) in the presence of renal dysfunction. However, the small number of patients enrolled in the study meant that the power of this study was not sufficient to demonstrate significance, particularly within the different renal function groups, and therefore research involving larger patient groups is suggested.

Very little research had been conducted on aldosterone's effect on cardiac fibrosis in rats, or on TGF-β_1 production/release at the time of experimental design. This posed challenges in terms of the range of aldosterone to use, the

duration of incubation and the amount of TGF-β_1 that we were trying to detect. Along with this, and more important to the hypothesis of this technique as an experimental model, was the viability of the slices over time. Again this was difficult to interpret in the context of tissue slices rather than cell culture; on which the viability tests had been validated. However, our results indicate that the cells within the slices did retain some viability at the end of the 48hr incubation but these results were very variable.

If more time was available for this research project I would have altered the media constituents to lower the intial sodium concentration. The initial sodium concentration used was >150mmol/l which is higher than normal in serum. It would have been more scientifically sound, to add sodium to the media instead of trying to dilute it as was the case in this experiment (thereby diluting more than just the sodium concentration). The effect of the glucose concentration in the media and its effect on osmolality is also a factor to worth reassessing in future experiments.

In conclusion, the human studies performed for this thesis provide useful information for future researchers investigating aldosterone/renin effects in renal patients. Unfortunately, the research was inconclusive and therefore further research is needed to confirm or refute the link between aldosterone and the cardiovascular complications of renal failure in humans. The results of the animal study were also inconclusive however important information was gained about this experimental technique and valuable lessons learned about potential modifications to improve the technique in the future.

References

1. Kundhal, K. and C.E. Lok, *Clinical epidemiology of cardiovascular disease in chronic kidney disease.* Nephron Clin Pract, 2005. **101**(2): p. c47-52.
2. Foley, R.N., P.S. Parfrey, and M.J. Sarnak, *Clinical epidemiology of cardiovascular disease in chronic renal disease.* Am J Kidney Dis, 1998. **32**(5 Suppl 3): p. S112-9.
3. Farrington, k., Hodsman, A., Steenkamp, R., Feest, T. Feehally, J (2006) *Chapter 4 : All patients receiving renal replacement therapy in the UK 2006*. UK Renal Registry
4. Norby, G.E., et al., *Effect of fluvastatin on cardiac outcomes in kidney transplant patients with systemic lupus erythematosus: a randomized placebo-controlled study.* Arthritis Rheum, 2009. **60**(4): p. 1060-4.
5. Zager, P.G., et al., *"U" curve association of blood pressure and mortality in hemodialysis patients. Medical Directors of Dialysis Clinic, Inc.* Kidney Int, 1998. **54**(2): p. 561-9.
6. Jungers, P., et al., *Incidence and risk factors of atherosclerotic cardiovascular accidents in predialysis chronic renal failure patients: a prospective study.* Nephrol Dial Transplant, 1997. **12**(12): p. 2597-602.
7. Cheung, A.K., et al., *Atherosclerotic cardiovascular disease risks in chronic hemodialysis patients.* Kidney Int, 2000. **58**(1): p. 353-62.
8. Savage, T., et al., *Calcified plaque is common in the carotid and femoral arteries of dialysis patients without clinical vascular disease.* Nephrol Dial Transplant, 1998. **13**(8): p. 2004-12.
9. Foley, R.N., Parfrey, P.S., Harnett, J.D., Kent G, *Clinical and echocardiographic disease in patient starting end stage renal replacement therapy.* Kidney Int, 1995. **47**: p. 186-192.
10. Silberberg, J.S., et al., *Impact of left ventricular hypertrophy on survival in end-stage renal disease.* Kidney Int, 1989. **36**(2): p. 286-90.
11. Levy, D., et al., *Prognostic implications of echocardiographically determined left ventricular mass in the Framingham Heart Study.* N Engl J Med, 1990. **322**(22): p. 1561-6.
12. Harnett, J.D., et al., *Risk factors for the development of left ventricular hypertrophy in a prospectively followed cohort of dialysis patients.* J Am Soc Nephrol, 1994. **4**(7): p. 1486-90.
13. Cannella, G., et al., *Regression of left ventricular hypertrophy in hypertensive dialyzed uremic patients on long-term antihypertensive therapy.* Kidney Int, 1993. **44**(4): p. 881-6.
14. Cruickshank, J.M., et al., *Reversibility of left ventricular hypertrophy by differing types of antihypertensive therapy.* J Hum Hypertens, 1992. **6**(2): p. 85-90.
15. Rambausek, M., et al., *Myocardial hypertrophy in rats with renal insufficiency.* Kidney Int, 1985. **28**(5): p. 775-82.

16. Ozasa, N., et al., *Relation among left ventricular mass, insulin resistance, and hemodynamic parameters in type 2 diabetes.* Hypertens Res, 2008. **31**(3): p. 425-32.
17. Herzog, C.A., J.M. Mangrum, and R. Passman, *Sudden cardiac death and dialysis patients.* Semin Dial, 2008. **21**(4): p. 300-7.
18. Herzog, C.A., et al., *Cause-specific mortality of dialysis patients after coronary revascularization: why don't dialysis patients have better survival after coronary intervention?* Nephrol Dial Transplant, 2008. **23**(8): p. 2629-33.
19. Tan, L.B., D. Schlosshan, and D. Barker, *Fiftieth anniversary of aldosterone: from discovery to cardiovascular therapy.* Int J Cardiol, 2004. **96**(3): p. 321-33.
20. Conn, J.W. and L.H. Louis, *Primary aldosteronism, a new clinical entity.* Ann Intern Med, 1956. **44**(1): p. 1-15.
21. *The Adrenal* in *The Oxford Texbook of Medicine*.
22. Wikipedia. *Aldosterone*. 2009 [cited; Available from: http://en.wikipedia.org/wiki/Aldosterone.
23. Wikipedia. *Cortisol*. 2009 [cited; Available from: http://en.wikipedia.org/wiki/Cortisol.
24. *Hormones of the Adrenal Cortex*.
25. Connell, J.M., et al., *A lifetime of aldosterone excess: long-term consequences of altered regulation of aldosterone production for cardiovascular function.* Endocr Rev, 2008. **29**(2): p. 133-54.
26. Freel, E.M. and J.M. Connell, *Mechanisms of hypertension: the expanding role of aldosterone.* J Am Soc Nephrol, 2004. **15**(8): p. 1993-2001.
27. Lehoux, J.G., et al., *Adrenocorticotropin regulation of steroidogenic acute regulatory protein.* Microsc Res Tech, 2003. **61**(3): p. 288-99.
28. Griffing, G.T., H. Pratt, and J.C. Melby, *Biphasic plasma aldosterone responses to four single-dose ACTH regimens.* J Clin Pharmacol, 1985. **25**(5): p. 387-9.
29. Bartter, F.C., L.E. Duncan, Jr., and G.W. Liddle, *Dual mechanism regulating adrenocortical function in man.* Am J Med, 1956. **21**(3): p. 380-6.
30. Tucci, J.R., et al., *ACTH stimulation of aldosterone secretion in normal subjects and in patients with chronic adrenocortical insufficiency.* J Clin Endocrinol Metab, 1967. **27**(4): p. 568-75.
31. Holland, O.B. and B. Carr, *Modulation of aldosterone synthase messenger ribonucleic acid levels by dietary sodium and potassium and by adrenocorticotropin.* Endocrinology, 1993. **132**(6): p. 2666-73.
32. Allen, R.G., et al., *Targeted ablation of pituitary pre-proopiomelanocortin cells by herpes simplex virus-1 thymidine kinase differentially regulates mRNAs encoding the adrenocorticotropin receptor and aldosterone synthase in the mouse adrenal gland.* Mol Endocrinol, 1995. **9**(8): p. 1005-16.
33. Williams, G.H. and R.G. Dluhy, *Aldosterone biosynthesis. Interrelationship of regulatory factors.* Am J Med, 1972. **53**(5): p. 595-605.

34. Library, O.U., *Steroidogenesis*. 2002.
35. Richards, A.M., et al., *Diurnal patterns of blood pressure, heart rate and vasoactive hormones in normal man.* Clin Exp Hypertens A, 1986. **8**(2): p. 153-66.
36. Venning, E.H., et al., *Influence of alterations in sodium intake on urinary aldosterone response to corticotropin in normal individuals and patients with essential hypertension.* Metabolism, 1962. **11**: p. 254-64.
37. Tremblay, A. and J.G. Lehoux, *Influence of captopril on adrenal cytochrome P-450s and adrenodoxin expression in high potassium or low sodium intake.* J Steroid Biochem Mol Biol, 1992. **41**(3-8): p. 799-808.
38. Pralong, W.F., et al., *Pyridine nucleotide redox state parallels production of aldosterone in potassium-stimulated adrenal glomerulosa cells.* Proc Natl Acad Sci U S A, 1992. **89**(1): p. 132-6.
39. Bird, I.M., et al., *Ca(2+)-regulated expression of steroid hydroxylases in H295R human adrenocortical cells.* Endocrinology, 1995. **136**(12): p. 5677-84.
40. Lotshaw, D.P., *Role of membrane depolarization and T-type Ca2+ channels in angiotensin II and K+ stimulated aldosterone secretion.* Mol Cell Endocrinol, 2001. **175**(1-2): p. 157-71.
41. Denner, K., et al., *Differential regulation of 11 beta-hydroxylase and aldosterone synthase in human adrenocortical H295R cells.* Mol Cell Endocrinol, 1996. **121**(1): p. 87-91.
42. Dluhy, R.G., et al., *Studies of the control of plasma aldosterone concentration in normal man. II. Effect of dietary potassium and acute potassium infusion.* J Clin Invest, 1972. **51**(8): p. 1950-7.
43. Condon, J.C., et al., *Calmodulin-dependent kinase I regulates adrenal cell expression of aldosterone synthase.* Endocrinology, 2002. **143**(9): p. 3651-7.
44. Pezzi, V., et al., *Ca(2+)-regulated expression of aldosterone synthase is mediated by calmodulin and calmodulin-dependent protein kinases.* Endocrinology, 1997. **138**(2): p. 835-8.
45. Ferrari, P. and Z. Krozowski, *Role of the 11beta-hydroxysteroid dehydrogenase type 2 in blood pressure regulation.* Kidney Int, 2000. **57**(4): p. 1374-81.
46. Marney, A.M. and N.J. Brown, *Aldosterone and end-organ damage.* Clin Sci (Lond), 2007. **113**(6): p. 267-78.
47. Rotin, D., V. Kanelis, and L. Schild, *Trafficking and cell surface stability of ENaC.* Am J Physiol Renal Physiol, 2001. **281**(3): p. F391-9.
48. Kemendy, A.E., T.R. Kleyman, and D.C. Eaton, *Aldosterone alters the open probability of amiloride-blockable sodium channels in A6 epithelia.* Am J Physiol, 1992. **263**(4 Pt 1): p. C825-37.
49. Verrey, F., J.P. Kraehenbuhl, and B.C. Rossier, *Aldosterone induces a rapid increase in the rate of Na,K-ATPase gene transcription in cultured kidney cells.* Mol Endocrinol, 1989. **3**(9): p. 1369-76.
50. Lee, I.H., et al., *Regulation of epithelial Na+ channels by aldosterone: role of Sgk1.* Clin Exp Pharmacol Physiol, 2008. **35**(2): p. 235-41.

51. Naray-Fejes-Toth, A., et al., *sgk is an aldosterone-induced kinase in the renal collecting duct. Effects on epithelial na+ channels.* J Biol Chem, 1999. **274**(24): p. 16973-8.
52. Debonneville, C., et al., *Phosphorylation of Nedd4-2 by Sgk1 regulates epithelial Na(+) channel cell surface expression.* Embo J, 2001. **20**(24): p. 7052-9.
53. Rotin, D., *Regulation of the epithelial sodium channel (ENaC) by accessory proteins.* Curr Opin Nephrol Hypertens, 2000. **9**(5): p. 529-34.
54. Hendron, E. and J.D. Stockand, *Activation of mitogen-activated protein kinase (mitogen-activated protein kinase/extracellular signal-regulated kinase) cascade by aldosterone.* Mol Biol Cell, 2002. **13**(9): p. 3042-54.
55. Stockand, J.D. and J.G. Meszaros, *Aldosterone stimulates proliferation of cardiac fibroblasts by activating Ki-RasA and MAPK1/2 signaling.* Am J Physiol Heart Circ Physiol, 2003. **284**(1): p. H176-84.
56. Jespersen, T., et al., *The corticosteroid hormone induced factor: a new modulator of KCNQ1 channels?* Biochem Biophys Res Commun, 2006. **341**(4): p. 979-88.
57. Spach, C. and D.H. Streeten, *Retardation of Sodium Exchange in Dog Erythrocytes by Physiological Concentrations of Aldosterone, in Vitro.* J Clin Invest, 1964. **43**: p. 217-27.
58. Haseroth, K., et al., *Rapid nongenomic effects of aldosterone in mineralocorticoid-receptor-knockout mice.* Biochem Biophys Res Commun, 1999. **266**(1): p. 257-61.
59. Wehling, M., et al., *Effect of aldosterone on sodium and potassium concentrations in human mononuclear leukocytes.* Am J Physiol, 1987. **252**(4 Pt 1): p. E505-8.
60. Boldyreff, B. and M. Wehling, *Non-genomic actions of aldosterone: mechanisms and consequences in kidney cells.* Nephrol Dial Transplant, 2003. **18**(9): p. 1693-5.
61. Michea, L., et al., *Eplerenone blocks nongenomic effects of aldosterone on the Na+/H+ exchanger, intracellular Ca2+ levels, and vasoconstriction in mesenteric resistance vessels.* Endocrinology, 2005. **146**(3): p. 973-80.
62. Sato A, S.T., *Aldosterone induced organ damage: plasma aldosterone level and inappropriate salt status.* Hypertension Res, 2004. **27**: p. 303-310.
63. Pimenta, E., et al., *Relation of dietary salt and aldosterone to urinary protein excretion in subjects with resistant hypertension.* Hypertension, 2008. **51**(2): p. 339-44.
64. Brilla CG, W.K., *Mineralocorticoid excess, dietary sodium and myocardial fibrosis.* J Lab Clin Med, 1992. **120**: p. 893-901.
65. Rocha R, R.A., Frierdich GE, Nachowiak DA, Kerec BK, *Aldosterone induces a vascular inflammatory phenotype in the rat heart.* Am J Physiol Heart Circ Physiol, 2002. **283**: p. H1802-H1810.
66. Brilla, C.G., L.S. Matsubara, and K.T. Weber, *Antifibrotic effects of spironolactone in preventing myocardial fibrosis in systemic arterial hypertension.* Am J Cardiol, 1993. **71**(3): p. 12A-16A.

67. Brilla, C.G. and K.T. Weber, *Mineralocorticoid excess, dietary sodium, and myocardial fibrosis.* J Lab Clin Med, 1992. **120**(6): p. 893-901.
68. Young, M., G. Head, and J. Funder, *Determinants of cardiac fibrosis in experimental hypermineralocorticoid states.* Am J Physiol, 1995. **269**(4 Pt 1): p. E657-62.
69. Weber, K.T., et al., *Pathologic hypertrophy with fibrosis: the structural basis for myocardial failure.* Blood Press, 1992. **1**(2): p. 75-85.
70. Paul M, K.R., Fernandez-Alfonso MS,Wagner D, *Cardiac gene expression of the compronents of the renin angiotensin system in human cardiomyopathy.* Journal of hypertension, 1994. **12**(Suppl 3).
71. Brilla, C.G., et al., *Collagen metabolism in cultured adult rat cardiac fibroblasts: response to angiotensin II and aldosterone.* J Mol Cell Cardiol, 1994. **26**(7): p. 809-20.
72. Nishiyama, A., et al., *Possible contributions of reactive oxygen species and mitogen-activated protein kinase to renal injury in aldosterone/salt-induced hypertensive rats.* Hypertension, 2004. **43**(4): p. 841-8.
73. Iglarz, M., et al., *Involvement of oxidative stress in the profibrotic action of aldosterone. Interaction wtih the renin-angiotension system.* Am J Hypertens, 2004. **17**(7): p. 597-603.
74. Gordon, R.D., et al., *High incidence of primary aldosteronism in 199 patients referred with hypertension.* Clin Exp Pharmacol Physiol, 1994. **21**(4): p. 315-8.
75. Swedberg, K., et al., *Hormones regulating cardiovascular function in patients with severe congestive heart failure and their relation to mortality. CONSENSUS Trial Study Group.* Circulation, 1990. **82**(5): p. 1730-6.
76. Pitt, B., et al., *The effect of spironolactone on morbidity and mortality in patients with severe heart failure. Randomized Aldactone Evaluation Study Investigators.* N Engl J Med, 1999. **341**(10): p. 709-17.
77. Pitt, B., et al., *Eplerenone, a selective aldosterone blocker, in patients with left ventricular dysfunction after myocardial infarction.* N Engl J Med, 2003. **348**(14): p. 1309-21.
78. Blink, E.J. (2006) *Basic MRI Physics*. **Volume**, 1-62
79. Westbrook, C., *MRI at a glance*. 1 ed. 2002, Oxford: Blackwell Science Ltd. 12-95.
80. Robert G. Weiss, R.K.-F.a.P.A.B., *Clinical Cardiac Magnetic resonance spectroscopy*, in *Cardiovascular Magnetic resonance*, W.J.M.a.D.J. Pennell, Editor. 2002, Churchill Livingstone: Philadelphia, US. p. 437-446.
81. Major, T.C., et al., *A Nonpeptide, Piperidine Renin Inhibitor Provides Renal and Cardiac Protection in Double-Transgenic Mice Expressing Human Renin and Angiotensinogen Genes.* Cardiovasc Drugs Ther, 2008.
82. Hardy CJ, W.R., Paul A. Bottomley and Gary Gerstenblith MD, *Altered myocardial high-energy phosphate metabolites in patients with dilated cardiomyopathy.* Am Heart J, 1991. **122**(3): p. 795-801.
83. Gaddam, K.K. and S. Oparil, *Renin inhibition: should it supplant ACE inhibitors and ARBS in high risk patients?* Curr Opin Nephrol Hypertens, 2008. **17**(5): p. 484-90.

84. Ingwall, J.S., et al., *The creatine kinase system in normal and diseased human myocardium.* N Engl J Med, 1985. **313**(17): p. 1050-4.
85. Ye, Y., et al., *High-energy phosphate metabolism and creatine kinase in failing hearts: a new porcine model.* Circulation, 2001. **103**(11): p. 1570-6.
86. Conway, M.A., et al., *Detection of low phosphocreatine to ATP ratio in failing hypertrophied human myocardium by 31P magnetic resonance spectroscopy.* Lancet, 1991. **338**(8773): p. 973-6.
87. Perseghin, G., et al., *Cross-sectional assessment of the effect of kidney and kidney-pancreas transplantation on resting left ventricular energy metabolism in type 1 diabetic-uremic patients: a phosphorous-31 magnetic resonance spectroscopy study.* J Am Coll Cardiol, 2005. **46**(6): p. 1085-92.
88. Smith, C.S., et al., *Altered creatine kinase adenosine triphosphate kinetics in failing hypertrophied human myocardium.* Circulation, 2006. **114**(11): p. 1151-8.
89. Bottomley, P.A., et al., *Four-angle saturation transfer (FAST) method for measuring creatine kinase reaction rates in vivo.* Magn Reson Med, 2002. **47**(5): p. 850-63.
90. Perseghin, G., et al., *Effect of the sporting discipline on the right and left ventricular morphology and function of elite male track runners: a magnetic resonance imaging and phosphorus 31 spectroscopy study.* Am Heart J, 2007. **154**(5): p. 937-42.
91. Kannel, W.B., et al., *Electrocardiographic left ventricular hypertrophy and risk of coronary heart disease. The Framingham study.* Ann Intern Med, 1970. **72**(6): p. 813-22.
92. Schillaci, G., et al., *Continuous relation between left ventricular mass and cardiovascular risk in essential hypertension.* Hypertension, 2000. **35**(2): p. 580-6.
93. Assoian, R.K., et al., *Transforming growth factor-beta in human platelets. Identification of a major storage site, purification, and characterization.* J Biol Chem, 1983. **258**(11): p. 7155-60.
94. Massague, J., *The transforming growth factor-beta family.* Annu Rev Cell Biol, 1990. **6**: p. 597-641.
95. Cheifetz, S., et al., *The transforming growth factor-beta system, a complex pattern of cross-reactive ligands and receptors.* Cell, 1987. **48**(3): p. 409-15.
96. Wrann, M., et al., *T cell suppressor factor from human glioblastoma cells is a 12.5-kd protein closely related to transforming growth factor-beta.* Embo J, 1987. **6**(6): p. 1633-6.
97. Seyedin, S.M., et al., *Purification and characterization of two cartilage-inducing factors from bovine demineralized bone.* Proc Natl Acad Sci U S A, 1985. **82**(8): p. 2267-71.
98. ten Dijke, P., et al., *Identification of another member of the transforming growth factor type beta gene family.* Proc Natl Acad Sci U S A, 1988. **85**(13): p. 4715-9.

99. Roberts, A.B., et al., *Multiple forms of TGF-beta: distinct promoters and differential expression.* Ciba Found Symp, 1991. **157**: p. 7-15; discussion 15-28.
100. Wikipedia. *Transforming growth factor beta*. [cited 2009 18th May]; Available from: http://en.wikipedia.org/wiki/TGF_beta.
101. UniProt. *Reviewed, UniProtKB/Swiss-Prot P01137 (TGFB1_HUMAN)*. 2009 [cited 2009 5th May]; Available from: http://www.uniprot.org/uniprot/P01137.
102. Miyazono, K. and C. Heldin, *Latent forms of TGF-beta: molecular structure and mechanisms of activation*, in *Clinical Applications of TGF-beta*. 1991, John Wiley and Sons Ltd: Chichester, UK. p. 81-89.
103. Wakefield, L.M., et al., *Recombinant TGF-beta 1 is synthesized as a two-component latent complex that shares some structural features with the native platelet latent TGF-beta 1 complex.* Growth Factors, 1989. **1**(3): p. 203-18.
104. Lijnen, P.J., V.V. Petrov, and R.H. Fagard, *Induction of cardiac fibrosis by transforming growth factor-beta(1).* Mol Genet Metab, 2000. **71**(1-2): p. 418-35.
105. Lodish, H., et al., *Molecular cell biology*. 3rd ed. 1995, New York: Scientific American Books. pg. 1161.
106. Klass, B.R., A.O. Grobbelaar, and K.J. Rolfe, *Transforming growth factor beta1 signalling, wound healing and repair: a multifunctional cytokine with clinical implications for wound repair, a delicate balance.* Postgrad Med J, 2009. **85**(999): p. 9-14.
107. Massague, J., J. Heino, and M. Laiho, *Mechanisms in TGF-beta action*, in *Clinical Applications of TGF-beta*. 1991, John Wiley and Sons Ltd: Chichester, UK. p. 51-59.
108. Van Obberghen-Schilling, E., et al., *Transforming growth factor beta 1 positively regulates its own expression in normal and transformed cells.* J Biol Chem, 1988. **263**(16): p. 7741-6.
109. Hayashi, H., et al., *The MAD-related protein Smad7 associates with the TGFbeta receptor and functions as an antagonist of TGFbeta signaling.* Cell, 1997. **89**(7): p. 1165-73.
110. Imamura, T., et al., *Smad6 inhibits signalling by the TGF-beta superfamily.* Nature, 1997. **389**(6651): p. 622-6.
111. Nakao, A., et al., *Identification of Smad7, a TGFbeta-inducible antagonist of TGF-beta signalling.* Nature, 1997. **389**(6651): p. 631-5.
112. von Gersdorff, G., et al., *Smad3 and Smad4 mediate transcriptional activation of the human Smad7 promoter by transforming growth factor beta.* J Biol Chem, 2000. **275**(15): p. 11320-6.
113. Ignotz, R.A. and J. Massague, *Transforming growth factor-beta stimulates the expression of fibronectin and collagen and their incorporation into the extracellular matrix.* J Biol Chem, 1986. **261**(9): p. 4337-45.
114. Massague, J., et al., *TGF-beta receptors and TGF-beta binding proteoglycans: recent progress in identifying their functional properties.* Ann N Y Acad Sci, 1990. **593**: p. 59-72.

115. Butt, R.P., G.J. Laurent, and J.E. Bishop, *Collagen production and replication by cardiac fibroblasts is enhanced in response to diverse classes of growth factors.* Eur J Cell Biol, 1995. **68**(3): p. 330-5.
116. Laiho, M., et al., *Enhanced production and extracellular deposition of the endothelial-type plasminogen activator inhibitor in cultured human lung fibroblasts by transforming growth factor-beta.* J Cell Biol, 1986. **103**(6 Pt 1): p. 2403-10.
117. Shull, M.M., et al., *Targeted disruption of the mouse transforming growth factor-beta 1 gene results in multifocal inflammatory disease.* Nature, 1992. **359**(6397): p. 693-9.
118. Rosenkranz, S., et al., *Alterations of beta-adrenergic signaling and cardiac hypertrophy in transgenic mice overexpressing TGF-beta(1).* Am J Physiol Heart Circ Physiol, 2002. **283**(3): p. H1253-62.
119. Kopp, J., V. Factor, and M. Mozes, *Transgenic mice with increased plasma levels of TGF-beta1 develop pregressive renal disease.* Laboratory Investigation, 1996. **74**: p. 991-1003.
120. Sime, P.J., et al., *Adenovector-mediated gene transfer of active transforming growth factor-beta1 induces prolonged severe fibrosis in rat lung.* J Clin Invest, 1997. **100**(4): p. 768-76.
121. Villarreal, F.J. and W.H. Dillmann, *Cardiac hypertrophy-induced changes in mRNA levels for TGF-beta 1, fibronectin, and collagen.* Am J Physiol, 1992. **262**(6 Pt 2): p. H1861-6.
122. Yoshioka, K., et al., *Transforming growth factor-beta protein and mRNA in glomeruli in normal and diseased human kidneys.* Lab Invest, 1993. **68**(2): p. 154-63.
123. Terrell, T.G., et al., *Pathology of recombinant human transforming growth factor-beta 1 in rats and rabbits.* Int Rev Exp Pathol, 1993. **34 Pt B**: p. 43-67.
124. Sadoshima, J. and S. Izumo, *Molecular characterization of angiotensin II--induced hypertrophy of cardiac myocytes and hyperplasia of cardiac fibroblasts. Critical role of the AT1 receptor subtype.* Circ Res, 1993. **73**(3): p. 413-23.
125. Zhao, W., et al., *Kidney fibrosis in hypertensive rats: role of oxidative stress.* Am J Nephrol, 2008. **28**(4): p. 548-54.
126. Sun, Y., et al., *Angiotensin II, transforming growth factor-beta1 and repair in the infarcted heart.* J Mol Cell Cardiol, 1998. **30**(8): p. 1559-69.
127. Guney, I., et al., *Antifibrotic effects of aldosterone receptor blocker (spironolactone) in patients with chronic kidney disease.* Ren Fail, 2009. **31**(9): p. 779-84.
128. Stewart, G.A., et al., *Electrocardiographic abnormalities and uremic cardiomyopathy.* Kidney Int, 2005. **67**(1): p. 217-26.
129. Sahn, D.J., et al., *Recommendations regarding quantitation in M-mode echocardiography: results of a survey of echocardiographic measurements.* Circulation, 1978. **58**(6): p. 1072-83.

130. Devereux, R.B., et al., *Echocardiographic assessment of left ventricular hypertrophy: comparison to necropsy findings.* Am J Cardiol, 1986. **57**(6): p. 450-8.
131. Dubois, D. and E. Dubois, *A formula to estimate the approximate surface area if height and weight be known.* Archive of Internal Medicine 1916. **17**: p. 863-71.
132. Levin, A., et al., *Prevalent left ventricular hypertrophy in the predialysis population: identifying opportunities for intervention.* Am J Kidney Dis, 1996. **27**(3): p. 347-54.
133. Mark, P.B., et al., *Redefinition of uremic cardiomyopathy by contrast-enhanced cardiac magnetic resonance imaging.* Kidney Int, 2006. **69**(10): p. 1839-45.
134. Alfakih, K., et al., *Normal human left and right ventricular dimensions for MRI as assessed by turbo gradient echo and steady-state free precession imaging sequences.* J Magn Reson Imaging, 2003. **17**(3): p. 323-9.
135. Parrish, A.R., et al., *Adult rat myocardial slices: A tool for studies of comparative cardiotoxicity.* Toxicol In Vitro, 1994. **8**(6): p. 1233-7.
136. Mosmann, T., *Rapid colorimetric assay for cellular growth and survival: application to proliferation and cytotoxicity assays.* J Immunol Methods, 1983. **65**(1-2): p. 55-63.
137. Promega. *CytoTox-Glo Cytotoxicity assay*. 2009 [cited 2009 29/05/09]; Available from: http://www.promega.com/tbs/tb359/tb359.pdf.
138. Tanabe, A., et al., *Left ventricular hypertrophy is more prominent in patients with primary aldosteronism than in patients with other types of secondary hypertension.* Hypertens Res, 1997. **20**(2): p. 85-90.
139. Edwards, N.C., et al., *Effect of spironolactone on left ventricular mass and aortic stiffness in early-stage chronic kidney disease: a randomized controlled trial.* J Am Coll Cardiol, 2009. **54**(6): p. 505-12.
140. Dahlof, B., K. Pennert, and L. Hansson, *Reversal of left ventricular hypertrophy in hypertensive patients. A metaanalysis of 109 treatment studies.* Am J Hypertens, 1992. **5**(2): p. 95-110.
141. Sato, A., et al., *Effectiveness of aldosterone blockade in patients with diabetic nephropathy.* Hypertension, 2003. **41**(1): p. 64-8.
142. Fine, A., *Relevance of C-reactive protein levels in peritoneal dialysis patients.* Kidney Int, 2002. **61**(2): p. 615-20.
143. Iseki, K., et al., *Serum C-reactive protein (CRP) and risk of death in chronic dialysis patients.* Nephrol Dial Transplant, 1999. **14**(8): p. 1956-60.
144. Albert, C.M., et al., *Prospective study of C-reactive protein, homocysteine, and plasma lipid levels as predictors of sudden cardiac death.* Circulation, 2002. **105**(22): p. 2595-9.
145. Milliez, P., et al., *Evidence for an increased rate of cardiovascular events in patients with primary aldosteronism.* J Am Coll Cardiol, 2005. **45**(8): p. 1243-8.
146. Duprez, D.A., et al., *Influence of arterial blood pressure and aldosterone on left ventricular hypertrophy in moderate essential hypertension.* Am J Cardiol, 1993. **71**(3): p. 17A-20A.

147. Muiesan, M.L., et al., *Inappropriate left ventricular mass in patients with primary aldosteronism.* Hypertension, 2008. **52**(3): p. 529-34.
148. Wing, L.M., et al., *A comparison of outcomes with angiotensin-converting--enzyme inhibitors and diuretics for hypertension in the elderly.* N Engl J Med, 2003. **348**(7): p. 583-92.
149. Garg, R. and S. Yusuf, *Overview of randomized trials of angiotensin-converting enzyme inhibitors on mortality and morbidity in patients with heart failure. Collaborative Group on ACE Inhibitor Trials.* Jama, 1995. **273**(18): p. 1450-6.
150. Shigematsu, K., et al., *Analysis of unilateral adrenal hyperplasia with primary aldosteronism from the aspect of messenger ribonucleic acid expression for steroidogenic enzymes: a comparative study with adrenal cortices adhering to aldosterone-producing adenoma.* Endocrinology, 2006. **147**(2): p. 999-1006.
151. Mazza, A., et al., *Endocrine arterial hypertension: diagnostic approach in clinical practice.* Minerva Endocrinol, 2008. **33**(2): p. 127-46.
152. Silvestre, J.S., et al., *Myocardial production of aldosterone and corticosterone in the rat. Physiological regulation.* J Biol Chem, 1998. **273**(9): p. 4883-91.
153. Silvestre, J.S., et al., *Activation of cardiac aldosterone production in rat myocardial infarction: effect of angiotensin II receptor blockade and role in cardiac fibrosis.* Circulation, 1999. **99**(20): p. 2694-701.
154. Gao, X., et al., *Angiotensin II increases collagen I expression via transforming growth factor-beta1 and extracellular signal-regulated kinase in cardiac fibroblasts.* Eur J Pharmacol, 2009. **606**(1-3): p. 115-20.
155. Fuhrman, G.J., F.A. Fuhrman, and J. Field, *Metabolism of rat heart slices, with special reference to effects of temperature and anoxia.* Am J Physiol, 1950. **163**(3): p. 642-7.
156. Habeler, W., et al., *An in vitro beating heart model for long-term assessment of experimental therapeutics.* Cardiovasc Res, 2009. **81**(2): p. 253-9.
157. Pillekamp, F., et al., *Establishment and characterization of a mouse embryonic heart slice preparation.* Cell Physiol Biochem, 2005. **16**(1-3): p. 127-32.
158. Burger, F. and F. Engelbrecht, *Metabolism of heart slices with special reference to the effect of hyperthermia.* South African Medical Journal, 1966(5th Feb): p. 124-126.
159. Parrish, A., et al., *Organ culture of rat myoscardial slices: An alternative in Vitro tool in organ-specific toxicology.* Toxicology mechanisms and methods, 1992. **2**(2): p. 101-111.
160. Huang, W., et al., *Aldosterone and TGF-beta1 synergistically increase PAI-1 and decrease matrix degradation in rat renal mesangial and fibroblast cells.* Am J Physiol Renal Physiol, 2008. **294**(6): p. F1287-95.
161. Han, J.S., et al., *Aldosterone-induced TGF-beta1 expression is regulated by mitogen-activated protein kinases and activator protein-1 in mesangial cells.* J Korean Med Sci, 2009. **24 Suppl**: p. S195-203.

162. Zhao, W., et al., *Oxidative stress mediates cardiac fibrosis by enhancing transforming growth factor-beta1 in hypertensive rats.* Mol Cell Biochem, 2008. **317**(1-2): p. 43-50.
163. Thompson, N.L., et al., *Transforming growth factor beta-1 in acute myocardial infarction in rats.* Growth Factors, 1988. **1**(1): p. 91-9.